University Kasdi Merbah - Ouargla
Faculty of Hydrocarbons and Energy
Renewable and earth and universe sciences
Department of Renewable Energy

Thesis

Master Academic

Field: Electrotecnique

Specialty: Renewable Energies in Electrotecnique

Presented by:

Mohammed houari Debbagh

Elhocine Mimouni

Theme

Energy Control of a Hybrid System Combining Wind and Solar Energy

Discussed publicly on:

09/06/2024

In front of a jury composed of:

Dr. Abada Z`hour	MCB	University Kasdi Merbah - Ouargla	President
Dr. Aboub Hania	MAB	University Kasdi Merbah - Ouargla	Examiner
Dr. Khentout Abd Elkader	MCA	University Kasdi Merbah - Ouargla	Director

Academic year: 2023/ 2024

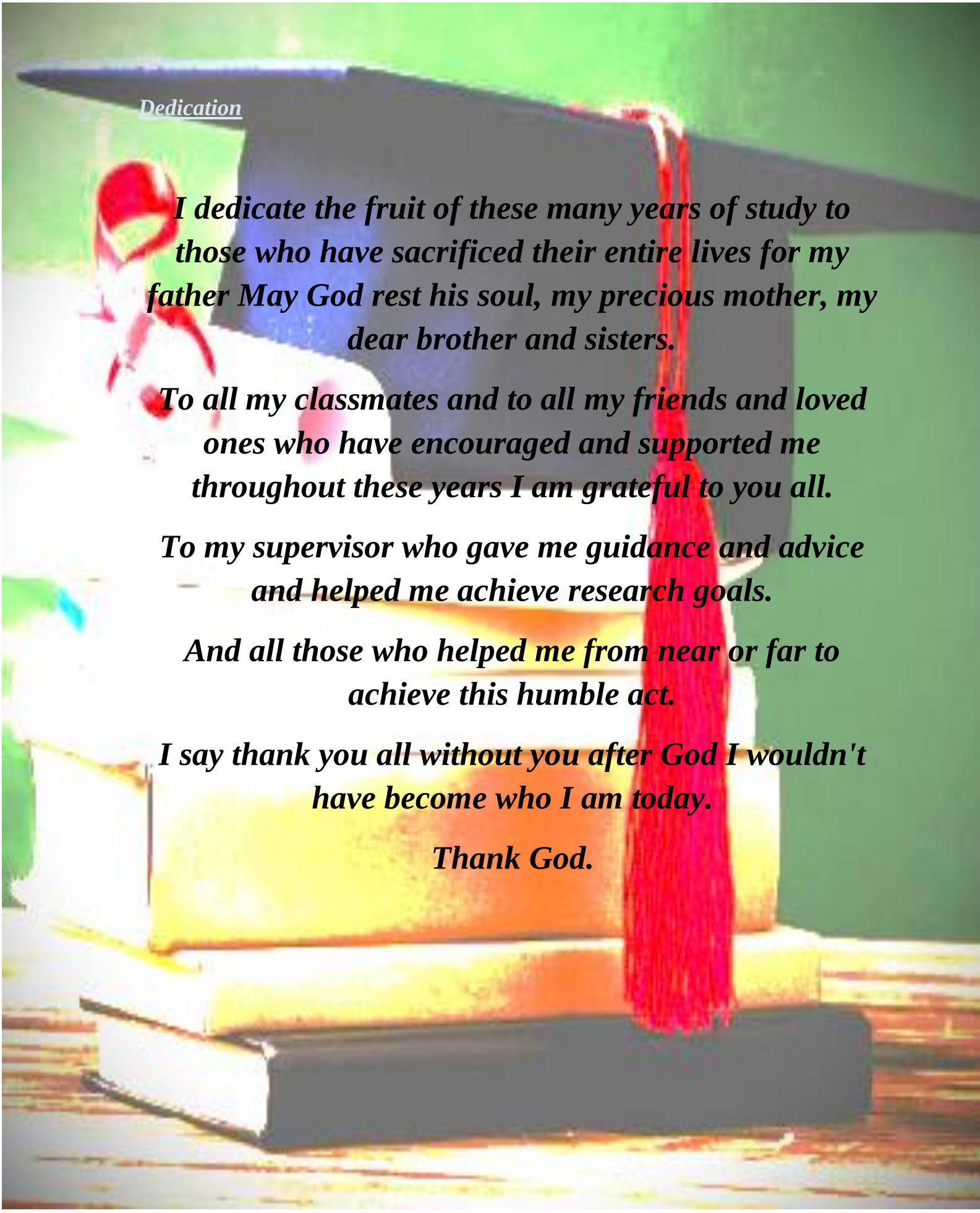

Dedication

I dedicate the fruit of these many years of study to those who have sacrificed their entire lives for my father May God rest his soul, my precious mother, my dear brother and sisters.

To all my classmates and to all my friends and loved ones who have encouraged and supported me throughout these years I am grateful to you all.

To my supervisor who gave me guidance and advice and helped me achieve research goals.

And all those who helped me from near or far to achieve this humble act.

I say thank you all without you after God I wouldn't have become who I am today.

Thank God.

HOUARI

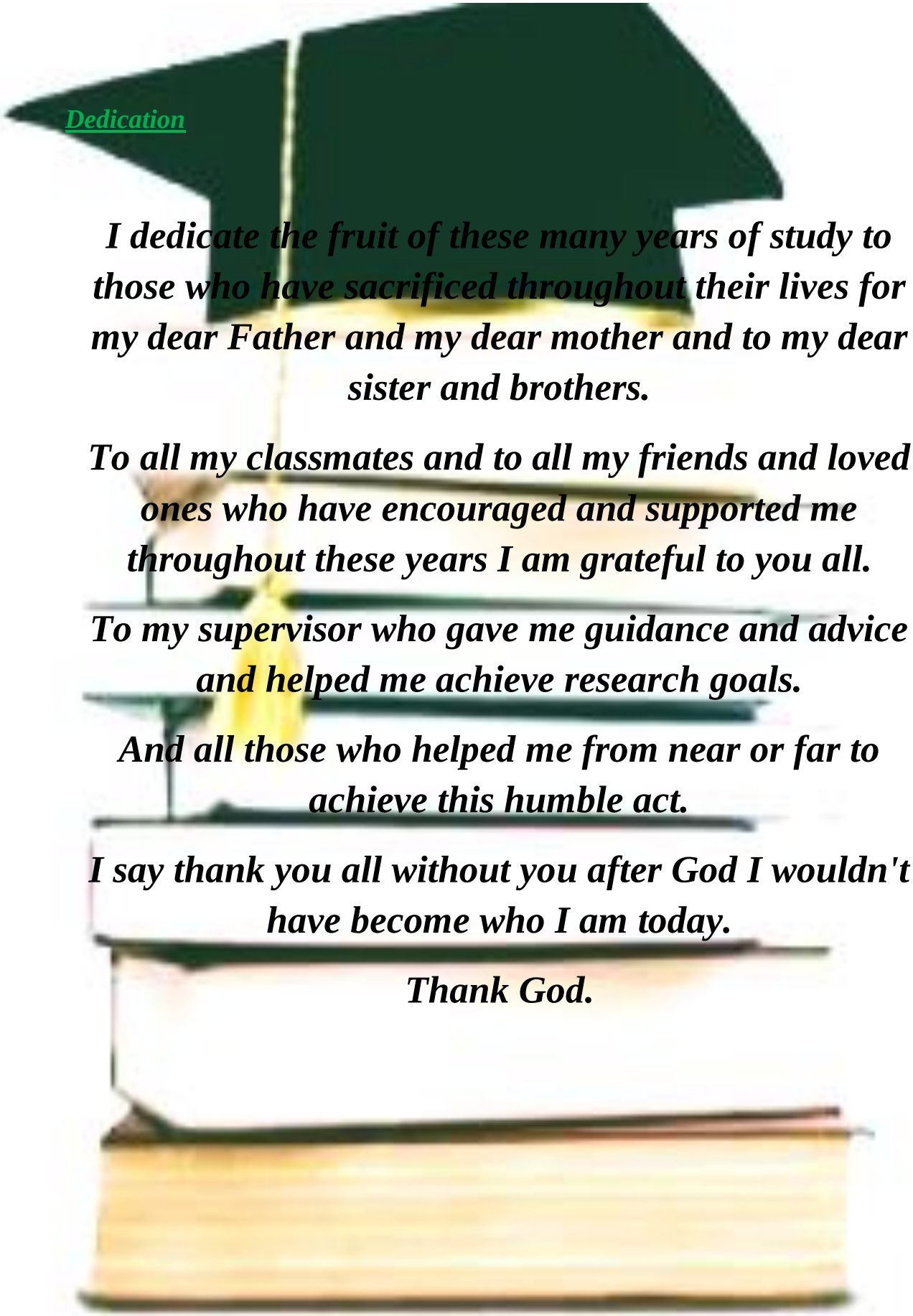

Dedication

I dedicate the fruit of these many years of study to those who have sacrificed throughout their lives for my dear Father and my dear mother and to my dear sister and brothers.

To all my classmates and to all my friends and loved ones who have encouraged and supported me throughout these years I am grateful to you all.

To my supervisor who gave me guidance and advice and helped me achieve research goals.

And all those who helped me from near or far to achieve this humble act.

I say thank you all without you after God I wouldn't have become who I am today.

Thank God.

ELHOCINE

Thanks

We would like to thank in the first place GOD the almighty and merciful who we

gave the strength and patience to accomplish this

Modest work.

Secondly, we would like to thank our promoter in charge of monitoring our work: **Dr. Khantout Abd Elkader**, For their encouragement, advice, and availability.

A big thank you to the jury members who agreed to review this work: **Dr. Abada Z`hour** who did me the honor of chairing the defense jury. **Dr. Aboub Hania**

to have agreed to review this work

We express our sincere thanks to the jury members for their interest in our research by agreeing to examine our work and enrich it with their proposals.

Finally, we would also like to thank our teachers from the Renewable Energy Department. Our friends and all the people who helped us near or far

to the realization of this work

HOUARI and HOCINE

Contents

Figure List

Tables list

Symbols List

Fi: represents the fitness value of individual i.

n: is the number of decision variables.

$\mathbf{w_j}$: is the weight associated with decision variable j.

$\mathbf{x_{ij}}$: is the value of decision variable j for individual i.

i: denotes particle's index.

t: is the current iteration's number.

f: is the objective function to be optimized (minimized).

x: is the position vector (or a potential solution).

N: is the total number of particles in the swarm.

$\mathbf{r_1}$ and $\mathbf{r_2}$**:** independent and identically distributed random numbers.

$\mathbf{C_1}$ and $\mathbf{C_2}$**:** are the cognition and social acceleration coefficients.

$\mathbf{X_{ij}}$, $\mathbf{V_{ij}}$: are position coordinates and velocity of the $\mathbf{i_{th}}$ agent in the $\mathbf{j_{th}}$ dimension.

$\boldsymbol{\tau_{ij}(t)}$**:** is the pheromone between **i** and **j** at time **t**.

$\boldsymbol{\eta_{ij}(t)}$**:** is the heuristic factor and **α** and **β** are the coefficients.

$\mathbf{J_k}$ **(i):** is the set consisting of the cities that ant **k** could select.

$\boldsymbol{A, A1}$ **:** surface of the wheel m^2

$\boldsymbol{A0}$ **:** the upstream surface (at the inlet of the current tube) m^2

$\boldsymbol{A2}$ **:** the surface downstream of the rotor m^2

$\boldsymbol{C, C1, C2}$ **:** weibull scale factor $m\ s^{-1}$

$\boldsymbol{k, k1, k2}$ **:** weibull shape factor.

$\boldsymbol{CP}$ **:** Coefficient de puissance.

Pthe: average theoretical power Kw

$\boldsymbol{Pabs}$ **:** the power absorbed by the rotor Kw

$\boldsymbol{PMax}$ **:** the maximum recoverable average power Kw

Pr: the average recoverable power per unit area A equal to 1 m^2 Kw

$\boldsymbol{Pu, Pu1, Pu2}$ **:** power output . Kw

Pn: nominal power.

$\boldsymbol{E}$ **:** average energy density recoverable over a year KW/m^2 Kw/m^2

$\boldsymbol{\eta}$ **:** Overall system performance.

$\boldsymbol{V0}$ **:** wind speed upstream of the rotor (initial) m/s

$\boldsymbol{V1}$ **:** wind speed in the plane of the rotor m/s

$\boldsymbol{V2}$ **:** wind speed downstream of the rotor m/s

$\overline{V}^3$**:** estimated wind speed with Weibull model $m\ s^{-1}$

$\boldsymbol{V^3}$ **:** average cubic wind speed estimated with Weibull model $m^3 s^{-3}$

$\boldsymbol{VD, VN}$ **:** start, nominal and stop speed $m\ s^{-1}$

$\boldsymbol{Vn1, Vn2}$ **:** rated speed $m\ s^{-1}$

$\boldsymbol{\rho}$ **:** air density kg/m^3

$\boldsymbol{\sigma}$ **:** Type of speed distribution m/s

$\boldsymbol{\sigma 2}$ **:** variance.

$\boldsymbol{RP}$ **:** Wind power factor.

$\boldsymbol{IV}$ **:** the index of change.

$\boldsymbol{Z1, Z2}$ **:** altitude m

$\boldsymbol{Z0}$ **:** soil roughness m

$\boldsymbol{Zg}$ **:** Geometric mean of altitude m

$\boldsymbol{Zr}$ **:** the reference height equal to 10m m

$\boldsymbol{\alpha e}$ **:** Exponent of the law of power.

n: Exponent of the law of power.

m: Scale factor extrapolation exponent.

$\boldsymbol{\alpha, \beta}$ **:** Constants without dimension.

A, B: coefficients for the proposed model.

f($\boldsymbol{V}$): frequency of occurrence of wind speeds.

f($\boldsymbol{V}$): Cumulative frequency of weibull distribution.

$\boldsymbol{ff0}$ **:** the frequency of calm winds.

$\boldsymbol{VPP}$ **:** most likely speed ms^{-1}

$\boldsymbol{VmaxE}$ **:** higher energy speed ms^{-1}

$\boldsymbol{r}$ **:** wind turbulence index.

$\boldsymbol{\varepsilon}$ **:** Dissipation rate of turbulent kinetic energy.

Introduction general

Introduction general

Renewable energy sources play a pivotal role in mitigating climate change and reducing our reliance on fossil fuels. Among these sources, solar and wind energy are two promising, strategic, and fast-growing sectors.

Since this study is being conducted in a desert region, specifically in the region of Ouargla in southern Algeria, solar and wind energy emerge as scientific solutions to meet the needs of areas far away from urban centers for electricity. Ouargla and its surroundings have many favorable conditions for wind and solar energy, as they contain vast open lands, somewhat acceptable winds, strong solar energy, and relatively flat terrain.

Setting up agricultural investments that depend on renewable energies to supply electricity is feasible. Therefore, we have prepared this memorandum to study the possibility of generating electricity through a hybrid system combining solar and wind energy. This memorandum is divided into four chapters:

- The first chapter, we talked about renewable energies in general, focusing on Algeria's potential in producing electricity using renewable energies.
- The second chapter covered hybrid systems and their optimization methods.
- As for the third chapter on assessing wind and solar energy potential with a case study, it was divided into theoretical and practical sections, including mathematical models for wind and solar energy and their application in the specific region.
- Finally, the fourth chapter discussed optimization of a hybrid system combining solar and wind energy using genetic algorithms, it is an application of one of the hybrid system optimization models.

Chapter I

Generalities about Renewable Energy

I.1. Introduction

Algeria, country rich in natural resources, faces energy challenges similar to those of the global community. With a diverse geology that includes vast oil and gas reserves, Algeria has traditionally relied on fossil fuels for electricity production. However, recognizing the importance of sustainability and energy security, the nation has been actively exploring non-conventional energy sources such as solar and wind power. In recent years, Algeria has made significant strides in increasing its electricity production capacity through renewable energy projects. Renewable energy refers to sources like solar, wind, hydroelectric, and geothermal power that are naturally replenished. By harnessing these resources, Algeria aims to reduce its dependence on fossil fuels and mitigate environmental impact while ensuring a stable energy supply for its population. The shift towards producing electricity with renewable energy not only aligns with global efforts to combat climate change but also positions Algeria as a leader in sustainable energy development.

I.2. Generalities about Renewable energy

I.2.1. Renewable energy

The definition of renewable energy according to the International Renewable Energy Agency (IRENA) includes all forms of energy derived from renewable sources in a sustainable manner, including bioenergy, geothermal energy, wind energy, solar energy, and ocean energy. Meanwhile, the International Energy Agency (IEA) defines renewable energy sources as coming from natural processes that are replenished at a faster rate than they are consumed.

I.2.2. Some definitions of Renewable Energy:

a. Energy production

Energy production refers to the process of converting various forms of resources into a usable form of energy. This may include the conversion of thermal energy into electricity (as in a thermal power plant), the exploitation of the kinetic energy of the wind (in a wind turbine), or the use of energy from the sun (via solar panels). The production of energy is essential to power our electricity and heat needs.

b. Energy consumption

Energy consumption refers to the final use of energy by being's humans and machines. This can encompass a wide variety of activities, such as lighting buildings, heating, air conditioning, transport, industrial production, etc. Their Energy consumption is measured in units such as kilowatt hours (kWh) for electricity or joules (J) for other forms of energy.

c. Energy reserves

Energy reserves refer to known and potentially accessible quantities of a given energy source. These may be proven reserves (which are ready to be exploited with current technologies), probable reserves (which are likely to be recovered under certain conditions), or possible reserves (which could be recovered with technologies future or different economic conditions). Energy reserves are crucial for assessing the sustainability and future availability of a given source.

d. Energy storage

Energy storage involves preserving a quantity of energy for use later. By extension, the expression also designates the storage of matter containing energy. Energy storage is at the heart of current challenges, whether it involves optimizing resources and energy or promoting access to them. It allows you to adjust “production” and “consumption” energy by limiting losses. Energy, stored when its availability is greater than the needs, can be returned at a time when demand is greater. In front of the intermittency or fluctuation of production of certain energies, for example renewable, this operation also makes it possible to meet constant demand.

I.2.3. Growth of renewable energy

Renewable energy is energy that comes from sources that do not deplete or can be replenished within a human's lifetime, such as solar, wind, hydro, bioenergy, and others. Renewable energy is important for reducing greenhouse gas emissions, improving air quality, and diversifying the energy mix.

2023 marks a step change for renewable power growth over the next five years. Renewable electricity capacity additions reached an estimated 507 GW in 2023, according to the data from the IEA [1], renewable energy use increased 3% in 2020 as demand for all other fuels declined. The primary driver was an almost 7% growth in electricity generation from renewable sources. Renewable energy accounted for one-seventh of the world's primary energy consumption in 2020 [2].

The IEA also projects that renewable electricity generation will expand by more than 8% in 2021, the fastest year-on-year growth since the 1970s [1]. Solar PV and wind are expected to contribute two-thirds of renewable growth, with China, the United States, the European Union, and India leading the way. By 2025, renewable' share of the global electricity generation mix is expected to rise from 29% to 35%, Asia will account for half of the world's electricity

consumption, and a third of global electricity consumption will be consumed in China, as shown in the (Fig I.1) [3].

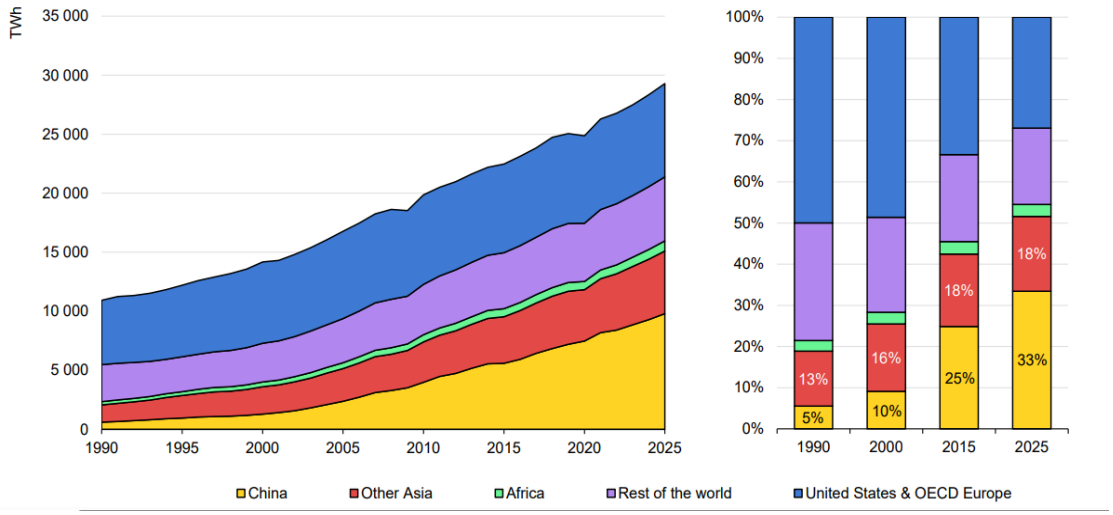

Figure I.1: Evolution of global electricity demand by region (left) and regional shares (right), 1990-2025 [4].

I.2.4. Electricity production by renewable energy

Electricity can be produced using renewable energy sources such as solar, wind, hydro, and geothermal power. These sources of energy are considered renewable because they are naturally replenished and do not deplete over time. Here is a brief overview of how electricity can be generated from each of these renewable energy sources:

I.2.4.1. Solar energy

Solar energy electricity production is the process of converting solar radiation into electricity using solar technologies. There are two main types of solar technologies: solar photovoltaic (PV) and solar thermal.

Solar PV uses solar cells to directly convert sunlight into electricity. Solar PV panels can be installed on rooftops, ground-mounted systems, or floating structures. Solar PV is the most widely used form of solar energy in the world [5].

Solar thermal uses solar collectors to absorb sunlight and transfer it as heat to a fluid, such as water or air. The heated fluid can then be used for space heating, water heating, or industrial processes. Solar thermal systems can also use concentrated solar power (CSP) to produce high-temperature steam that drives a turbine and generates electricity [6].

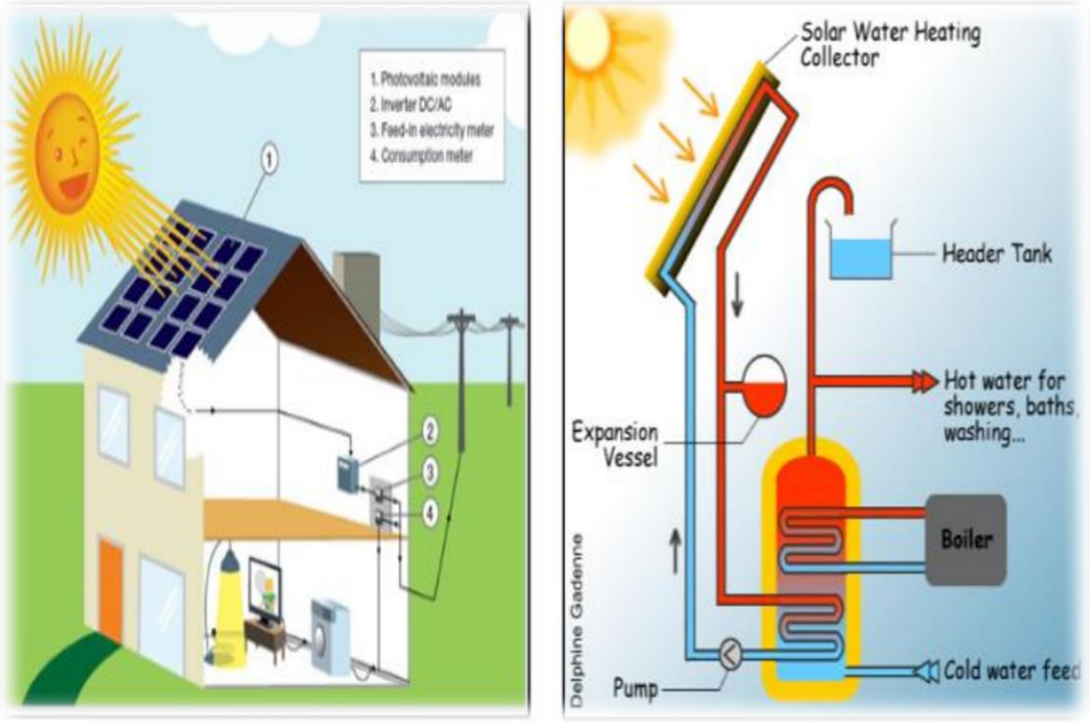

Figure I.2: Solar energy for the production of electricity and solar energy for heating system.

Table I.1: the main advantages and disadvantages of solar energy

The advantages	The disadvantages
• Solar energy provides autonomy in energy production and reduces dependence on fossil fuels and external sources.	• The quality and efficiency of solar panels in converting solar energy into electricity is varying and relatively low, reaching only 20%.
• Solar energy contributes to long-term money saving, reducing electricity bills and increasing the value of homes and real estate.	• The cost of purchasing and installing solar panels is initially high, and needs a lot of space to cover electrical needs.
• Solar energy provides local employment in the installation and maintenance of solar panels and associated equipment.	• Solar panels' ability to collect solar energy decreases depending on the geographical area. The more we move away from the equator towards the poles, the less solar energy is available.

I.2.4.2. Wind energy

Wind energy electricity production is the process of converting wind energy into electricity using wind turbines. Wind turbines are devices that capture the kinetic energy of the wind and transform it into rotational energy, which then drives a generator to produce electricity. Wind energy is a renewable and clean source of energy that does not emit greenhouse gases or cause pollution.

There are two main types of wind turbines: onshore and offshore. Onshore wind turbines are installed on land, usually in areas with high and consistent wind speeds. Offshore wind turbines are installed in the sea, where the wind is stronger and more stable. Offshore wind turbines are generally larger and more expensive than onshore ones, but they have higher capacity factors and less visual impact.

Figure I.3: On-shore wind turbines [7].

Table I.2: the main advantages and disadvantages of wind energy

The advantages	The disadvantages
• Wind energy is environmentally friendly, not producing any gas emissions or contaminants for air, water or soil.	• The quality and efficiency of wind turbines in converting wind power into electricity is varying and relatively low, reaching only 50%.
• Wind power is low operating cost, after covering the initial investment in wind turbine construction.	• The cost of purchasing and installing wind turbines is initially high, and needs a large area to cover electrical needs.
• Wind power provides local employment in the installation and maintenance of wind turbines and associated equipment.	• Wind turbines' ability to accumulate wind energy decreases depending on the geographical area. The more we move away from areas with strong winds, the less wind power is available.
• Wind energy receives government support in some countries, through grants, tax cuts and consumer encouragements.	• Wind turbines need periodic maintenance and continuous hygiene, to get rid of dust and plankton that reduce their effectiveness.

I.2.4.3. Biomass energy

Biomass energy electricity production is the process of converting biomass, which is organic material from plants and animals, into electricity using various technologies. Biomass can be burned directly, gasified, pyrolyzed, or converted into biofuels, and then used to generate electricity in power plants. Biomass energy is a renewable and clean source of energy that does not emit greenhouse gases or cause pollution.

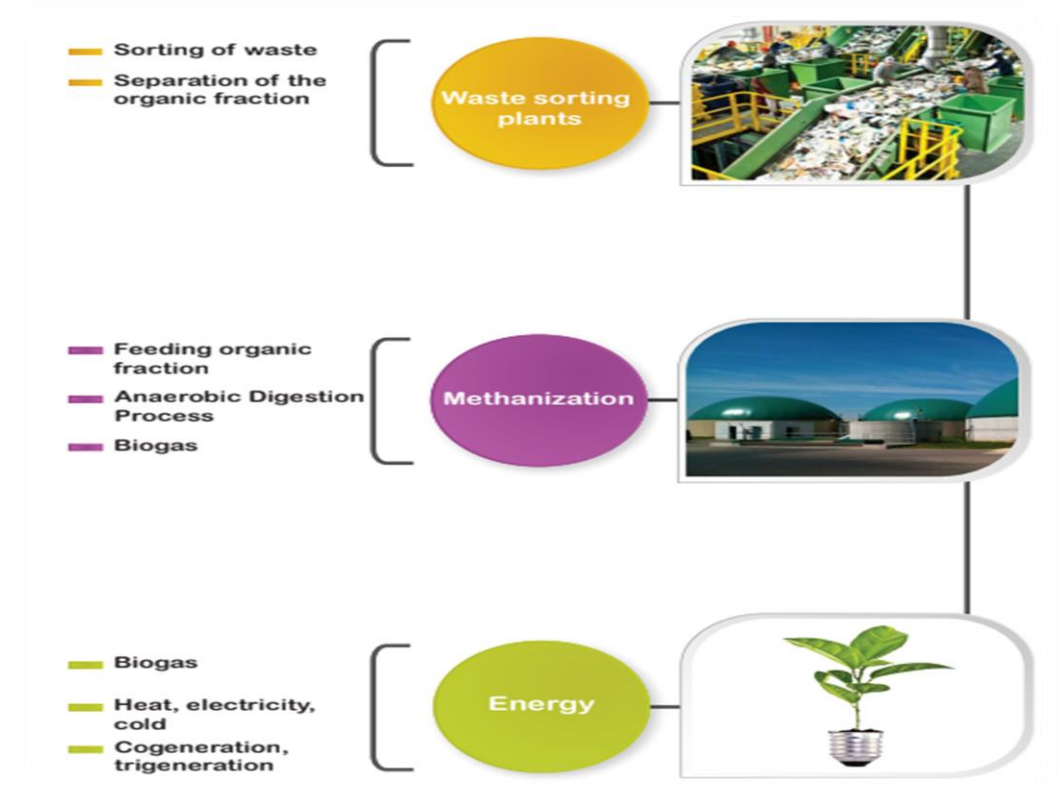

Figure I.4: Waste energy recovery chain (Methanization) [8].

Table I.3: the main advantages and disadvantages of biomass energy

The advantages	The disadvantages
• It is abundant and inexhaustible, as biomass is derived from the sun's energy through photosynthesis.	• It is intermittent, as it depends on the availability and quality of biomass feedstocks. Therefore, it needs to be combined with energy storage or other sources of energy to ensure reliability and stability.
• It is cost-effective, as the price of biomass technologies has decreased significantly over the years and the operation and maintenance costs are low.	• Biomass conversion requires significant land area due to low efficiency and varying biomass production by region.
• It is versatile, as it can be used for various applications and in different locations, including remote and off-grid areas.	• It faces technical, economic, and social barriers, such as the lack of adequate infrastructure, policies, regulations, incentives, and public awareness and acceptance.

I.2.4.4. Hydraulic energy

Hydraulic energy electricity production is the process of converting the energy of moving water into electricity using hydraulic turbines and generators. Hydraulic energy is a renewable and clean source of energy that does not emit greenhouse gases or cause pollution.

There are different types of hydraulic energy plants, such as:

- **Run-of-river plants:** These plants use the natural flow of a river to spin the turbines without storing water in a reservoir. They have a low environmental impact but depend on the river's water level and flow rate.
- **Storage plants:** These plants use a dam to create a reservoir of water that can be released when needed to generate electricity. They have a high environmental impact but can provide a reliable and flexible power supply.
- **Pumped-storage plants:** These plants use two reservoirs at different elevations and pump water from the lower one to the upper one during periods of low electricity demand. When there is high electricity demand, they release water from the upper reservoir to the lower one and generate electricity. They have a moderate environmental impact but can store excess energy and balance the grid.

Table I.4: the main advantages and disadvantages of hydraulic energy

The advantages	The disadvantages
• Hydraulic energy is environmentally friendly, does not produce any gas emissions or contaminants for air, water or soil.	• Hydraulic energy depends on the availability of water resources and is therefore affected by drought and climate change.
• Hydraulic power is considered to have a low economic cost, after covering the initial investment in the construction of dams and hydroelectric plants.	• The cost of purchasing and installing dams and hydroelectric plants is initially high, and needs a large area to cover electrical needs.
• Hydraulic power provides local employment in the installation and maintenance of dams, plants and associated equipment.	• Dams and hydroelectric plants adversely affect wildlife and water and cause ecosystem and biodiversity change.
• Hydraulic energy provides stable and reliable energy, less affected by weather or market fluctuations.	• Dams and hydroelectric plants need regular maintenance and continuous hygiene, to get rid of dust and plankton that reduce their effectiveness.

I.2.4.5. Geothermal energy

Geothermal energy electricity production is the process of converting the thermal energy stored in the Earth's crust into electricity using various technologies. Geothermal energy is a renewable and clean source of energy that does not emit greenhouse gases or cause pollution.

There are three main types of geothermal power plant technologies: dry steam, flash steam, and binary cycle. The type of conversion depends on the state and temperature of the subsurface fluid (steam or water) and the design of the power plant [9].

- **Dry steam plants:** use hydrothermal fluids that are already mostly steam, which is a rare natural occurrence. The steam is drawn directly to a turbine, which drives a generator that produces electricity.
- **Flash steam:** plants use geothermal reservoirs of water with temperatures greater than 182 °C. The hot water flows up through wells and some of it boils into steam as the pressure decreases. The steam is then separated from the water and used to power a turbine/generator. The leftover water and condensed steam are injected back into the reservoir.
- **Binary cycle:** plants use water at lower temperatures of about 107-182 °C. The water is passed through a heat exchanger, where it transfers its heat to a working fluid with a low boiling point, usually an organic compound. The working fluid is vaporized and used to turn a turbine/generator. The water and the working fluid are kept separated during the whole process.

Table I.5: the main advantages and disadvantages of geothermal energy.

The advantages	The disadvantages
• Terrestrial heat energy is a reliable and stable source of energy, not affected by weather or market fluctuations.	• The cost of purchasing and installing geothermal power plants is initially high, requiring open spaces and large-scale drilling.
• Terrestrial heat energy is an economic source of energy. It saves significant costs over the long term and receives government support in some countries.	• Geothermal power plants adversely affect the environment, potentially destabilizing the surface, earthquakes, water or chemical air pollution.
• Terrestrial heat energy is an available source of energy. It is present in the form of volcanoes, hot springs and heaters around the world.	• Geothermal power plants need periodic maintenance and continuous hygiene, to get rid of soils, plankton and solids that reduce their effectiveness.

I.2.4.6. Marine energy

Marine energy electricity production is the process of generating electricity from the natural movement and properties of water, such as waves, tides, currents, salinity, and temperature differences. Marine energy is a renewable and clean source of energy that can potentially meet a large portion of the world's electricity demand. According to the International Renewable Energy Agency (IRENA), marine energy has the potential to produce more than twice the world's current electricity consumption.

Different types of marine energy technologies can be used to produce electricity, such as:

- **Wave power converters:** These devices capture the energy from the surface waves of the ocean and convert it into electricity. Wave power converters can be floating, submerged, or attached to the shore or the seabed.
- **Tidal turbines:** These devices use the kinetic energy of the tidal currents to spin a rotor and generate electricity. Tidal turbines can be installed in coastal and estuarine areas where the tidal range is high and the water flow is predictable.
- **In-stream turbines:** These devices use the kinetic energy of the free-flowing water in rivers, lakes, and streams to generate electricity. In-stream turbines can be placed in fast-moving water without the need for dams or barrages.
- **Ocean current turbines:** These devices use the kinetic energy of large-scale ocean currents, such as the Gulf Stream or the Kuroshio Current, to generate electricity. Ocean current turbines can be deployed in deep water where the currents are strong and steady.
- **Ocean thermal energy converters:** These devices use the temperature difference between the warm surface water and the cold deep water of the ocean to produce electricity. Ocean thermal energy converters can be used in tropical regions where the temperature gradient is high.
- **Osmotic power:** This technology uses the salinity difference between fresh water and salt water to generate electricity. Osmotic power can be produced by using membranes that allow water to pass through but block salt ions, creating a pressure difference that can be used to drive a turbine.

Table I.6: the main advantages and disadvantages of marine energy

The advantages	The disadvantages
• Marine energy is a reliable and stable source of energy, not affected by weather or market fluctuations, and tidal and island power schedules are predictable.	• The cost of purchasing and installing offshore power plants is initially high, requiring open space and extensive drilling.
• Marine energy is an economic source of energy. It provides significant long-term costs and receives government support in some States.	• Marine power plants adversely affect the environment, potentially destabilizing the surface, earthquakes, water or chemical air pollution.
• Marine energy is an available source of energy, in the form of waves, tides, islands and currents throughout the world.	• Marine power plants need periodic maintenance and continuous hygiene, to get rid of soil, plankton and solids that reduce their effectiveness.

I.3. Energy situation in the world and Algeria

I.3.1. Energy in the world

The energy situation in the world is an important and complex topic, influenced by many factors such as economy, environment, politics and technology,

The demand for energy in the world is constantly increasing, especially in developing and emerging countries such as China India, and Brazil. According to the report of the International Energy Agency, the energy demand is expected to grow by 25% by 2040 [10].

Fossil fuels (oil, gas, and coal) still account for the largest share of energy sources in the world, but they face increasing challenges due to the depletion of reserves, the rise of prices, and the negative impacts on the environment and climate. They also face competition from alternative energy sources such as renewable energy, nuclear energy, and hydrogen [4].

Renewable energy (solar, wind, water, and biomass) has experienced rapid growth in recent years, thanks to the improvement of technology, the reduction of costs, and the increase of political and social support. According to the report of the World Energy Observatory, renewable energy currently accounts for 19% of electricity production in the world and is expected to reach 50% by 2035 [3].

Nuclear energy plays an important role in providing clean, stable, and low-carbon energy, but it faces challenges due to security and health concerns and the disposal of nuclear waste. It is also affected by competition from other energy sources and the public opposition. According

to the report of the International Energy Agency, nuclear energy currently accounts for 10% of electricity production in the world and is expected to decrease to 8% by 2040 [11].

Hydrogen is a potential energy source that can contribute to achieving carbon neutrality and enhancing energy security, especially in sectors that are difficult to electrify such as heavy transport, industry, and heating. But hydrogen faces obstacles due to the cost of production, transport, storage, and use, as well as the infrastructure, regulation, and social acceptance. According to the report of the International Energy Agency, hydrogen currently accounts for less than 1% of the final energy in the world and is expected to reach 7% by 2050.

I.3.2. Energy in Algeria

Algeria heavily relies on fossil fuels for energy, with oil and gas making up a significant portion of its exports. The country exports about 50% of its primary energy production, with electricity contributing minimally to total energy exports. Renewable energy sources have a negligible presence in Algeria's energy mix, while natural gas dominates electricity generation. Since 2006, oil and gas production in Algeria has been declining due to various factors like decreased production, reserve depletion, and low reserve renewal rates [12].

Algeria is working on renewable energy sources like solar, wind, and hydrogen. In 2013, they produced 154.6 million tons of oil equivalent, with a decrease in imports compared to the previous year. They used this production to meet domestic needs and for exports [13]. However, Algeria faces challenges like declining oil and gas prices globally, increasing domestic energy demand, and competition in the energy sector from other countries.

Algeria is aiming to diversify its energy sources, improve energy efficiency, and advance its energy industries. The government has laid out various plans like the National Action Plan for Energy Transition 2020-2030, the National Renewable Energy Plan 2015-2030, and the National Energy Efficiency Plan 2015-2030, among others. Algeria is also focusing on international cooperation in energy with partners like the European Union, OPEC, China, Russia, and African countries [14].

I.3.2.1. Geology of Algeria

The natural limits of Algeria are the Mediterranean Sea to the North (1200 km), Morocco to the West, Tunisia, and Libya in the East, Mauritania and Western Sahara in the South-West, and finally Mali and Niger in the South. The prime meridian (Greenwich) passes close to the city of Mostaganem. By its surface area (2,381,741 km2), Algeria is the largest country in Africa and the Arab world. The distances are very large, around 2000 kilometers from the

Mediterranean coast to the Hoggar massif region and 1800 km from Ain Amenas in the east to Tindouf in the west [15].

I.3.2.2. General morphology

Algeria includes four major areas from North to South:

The Tellian Atlas (or the Tell): Made up of steep reliefs and coastal plains, the richest are Mitidja in the center, Chelif in the West, and Seybouse in the East;

The highlands: The Saharan Atlas forms a long series of reliefs oriented NE-SW extending from the border of Moroccan to that of Tunisia;

The Sahara: which contains most of the hydrocarbon resources, is a desert made up of large expanses of dunes (Erg Oriental and Erg Occidental), stony plains (Regs) and dotted with oases, which are all urban centers like the cities of El Oued, Ghardaia and Djanet.

The Eglab massif to the West and the Hoggar massif to the East form, practically, the Southern limit of the Algerian Sahara.

I.3.2.3. Geological background

The history of the elderly's records is like the global development of tectonic plates being built in Algeria in multiple areas: The Alpine North Algeria, and in the south, the Saharan platform.

a) Alpine Algeria

Algeria's geological structure includes northern mountains formed during the Triassic period. The region comprises various structural and sedimentary groups, each with distinct oil targets. The Atlas Mountains feature water basins with deposits from Jurassic to Pliocene, focusing on Middle Cretaceous, Miocene, and Oligocene Eocene for oil. The Hodna Basin fills with deposits from Eocene to Miocene, targeting Eocene oil. The High Plateaus have limited sedimentary cover and focus on Lias oil. The Saharan Atlas Mountains formed from a rift filled with Triassic deposits, emphasizing Jurassic oil. The Shatt Mlghar Basin in Constantine has Cretaceous deposits and targets Cretaceous hydrocarbons [16].

b) The Saharan platform

The geological characteristics of different basins in the southern Algerian Alps are examined, focusing on their sedimentary covers, reservoirs, and the potential for hydrocarbon exploration. Specific basins like Tindouf-Reggane, Bashir, Ahnet-Timimoun, Moudir-Aghmor-Miya

Valley, and Sinqiliz Elizi Ghadamis are analyzed in terms of their locations, sedimentary cover thicknesses, and significant reservoirs. The discussion underscores the likelihood of discovering liquid and gaseous hydrocarbons in these regions, attributed to the presence of Bazlaouzic formations [12].

I.3.2.4. Unconventional energy sources

Algeria has great potential for solar, wind, hydro, geothermal, and bio-power energy generation. Renewable energies in Algeria occupy only a small part of the national electricity mix (0.8%) and the production is shared between the hydraulic sector generated in 2018 (389 GWh), or 0.7% of the total solar photovoltaic energy (11 GWh) and thermodynamic (58 GWh) at 0.1% of the binding balance [17].

Algeria aims to include 27% of renewable energy generation in its energy mix by 2030. The country is progressing slowly in terms of renewable energy development, as of 2021. Algeria is focusing on increasing solar generation by 2030 [18].

I.3.2.4.1. Solar potential

Algeria has a significant potential for solar energy due to its geographical location. The country receives annual sunshine exposure equivalent to 2,500 KWh/m. The daily solar energy potential varies from 4.6 kWh/m² in the north to 6.6 kWh/m² in the south, as shown in the (fig I.1) [19].

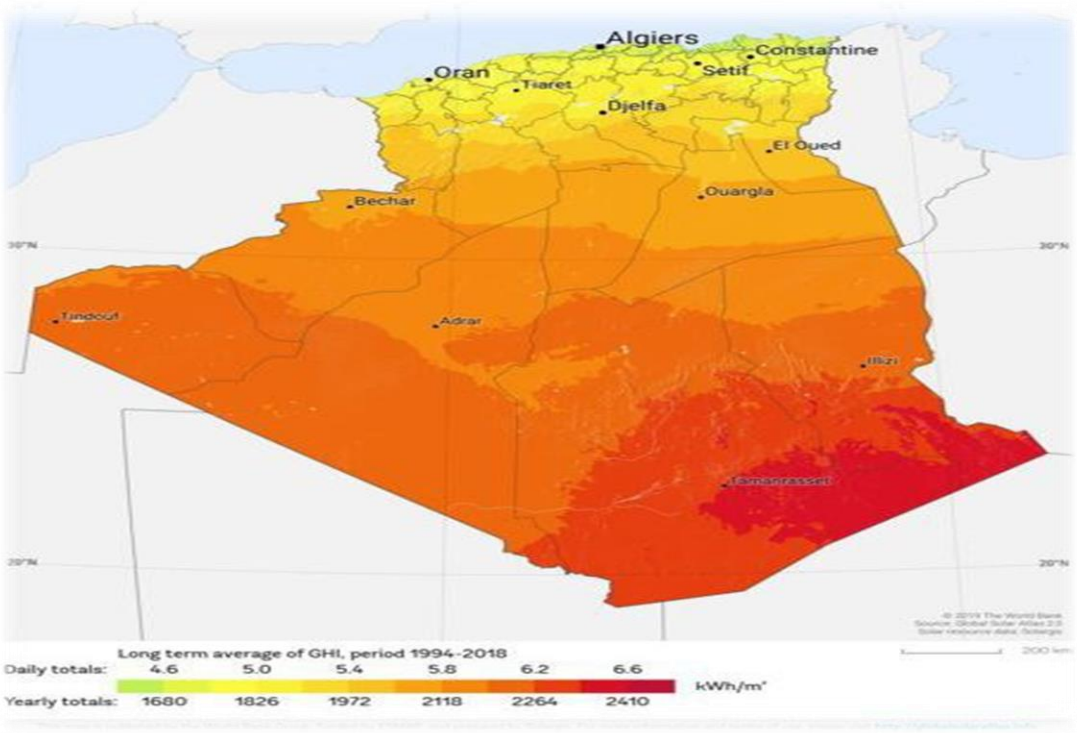

Figure I.5: Global irradiation in Algeria [20].

The Algerian government has set ambitious renewable energy targets. By 2030, the country aims to reach a clean energy capacity of 22,000 megawatts. It expects to generate most of its renewable power through solar photovoltaic technology, with a capacity of around 14,000 megawatts [21]

In addition, the government has planned substantial projects to increase infrastructural and financial investment and successfully shift to green energy sources. Some 60 solar photovoltaic plants, concentrated solar power plants, wind farms, and hybrid power plants are planned [21,22].

I.3.2.4.2. Wind potential

Algeria has a significant potential for wind energy. The country's wind energy potential is estimated to be about 35 TWh/year. Almost half of the country experiences significant wind speed [21,22].

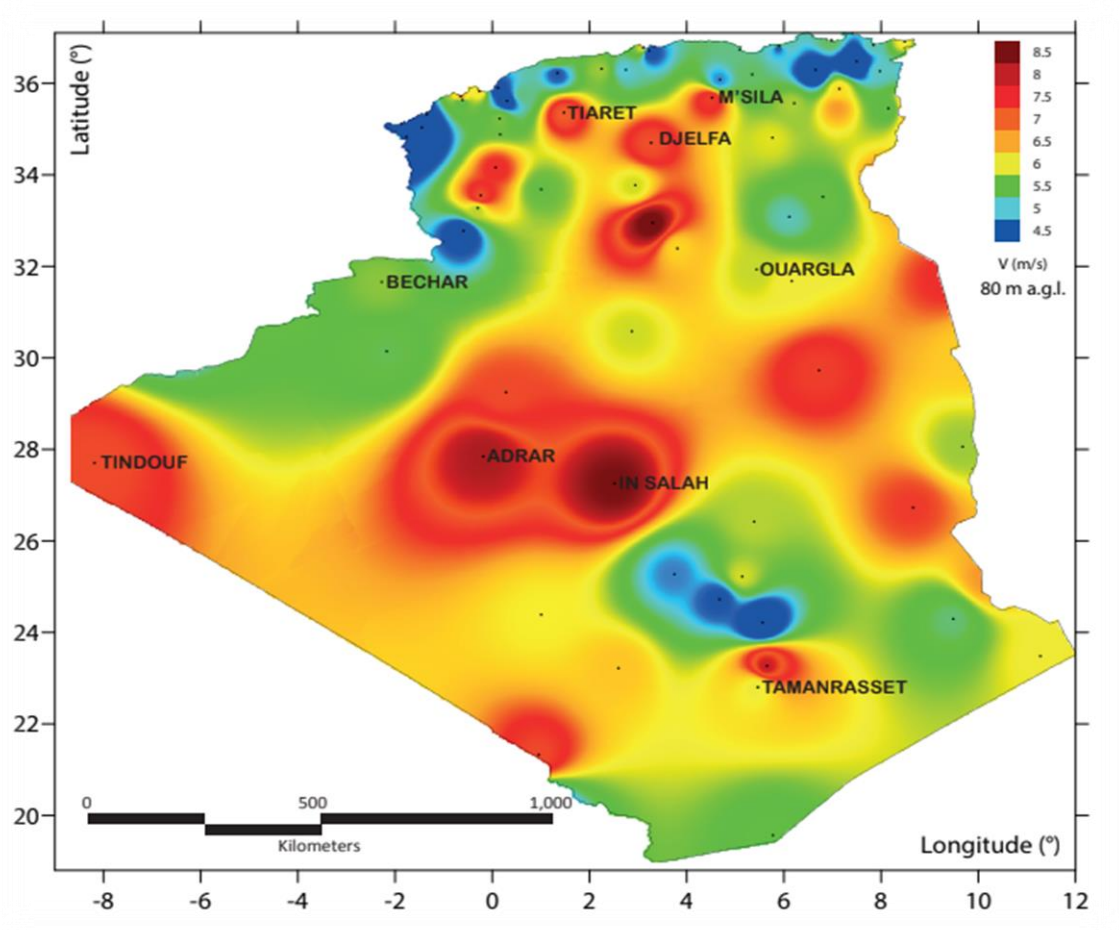

Figure I.6: Average speed mapping the wind [19].

The Algerian government aims to reach a wind energy capacity of 5,000 megawatts by 2030 [21]. The country's first wind farm is being built at Adrar with an installed capacity of 10MW, funded substantially by the state utility Sonelgaz [18].

In terms of offshore wind potential, Algeria has a technical potential of less than 1 GW for fixed (water depth < 50m) and 18 GW for floating (water depth < 1000m) offshore wind within 200 kilometers of the shoreline. This potential is estimated based on the Global Wind Atlas (version 3.0) [23]. Overall, Algeria's wind energy potential is promising and could play a significant role in the country's transition to renewable energy sources.

I. 3.2.4.3. Geothermal potential

Algeria is considered one of the countries in North Africa with the most potential for geothermal energy exploitation. The National Agency for Renewable Energies and Energy Efficiency (CEREFE) has identified 240-280 geothermal sources across the country, believing there is great potential to use this energy in Algeria's energy future [24].

The Algerian government has launched an ambitious Renewable Energy and Energy Efficiency Program, which includes the development and expansion of renewable resources such as biomass. This program aims to generate 22,000 MW of power from renewable sources between 2011 and 2030 [18].

In conclusion, Algeria's biomass energy potential is promising and could play a significant role in the country's transition to renewable energy sources. However, the development of the bioenergy sector in Algeria requires a thorough assessment of national biomass potential [24].

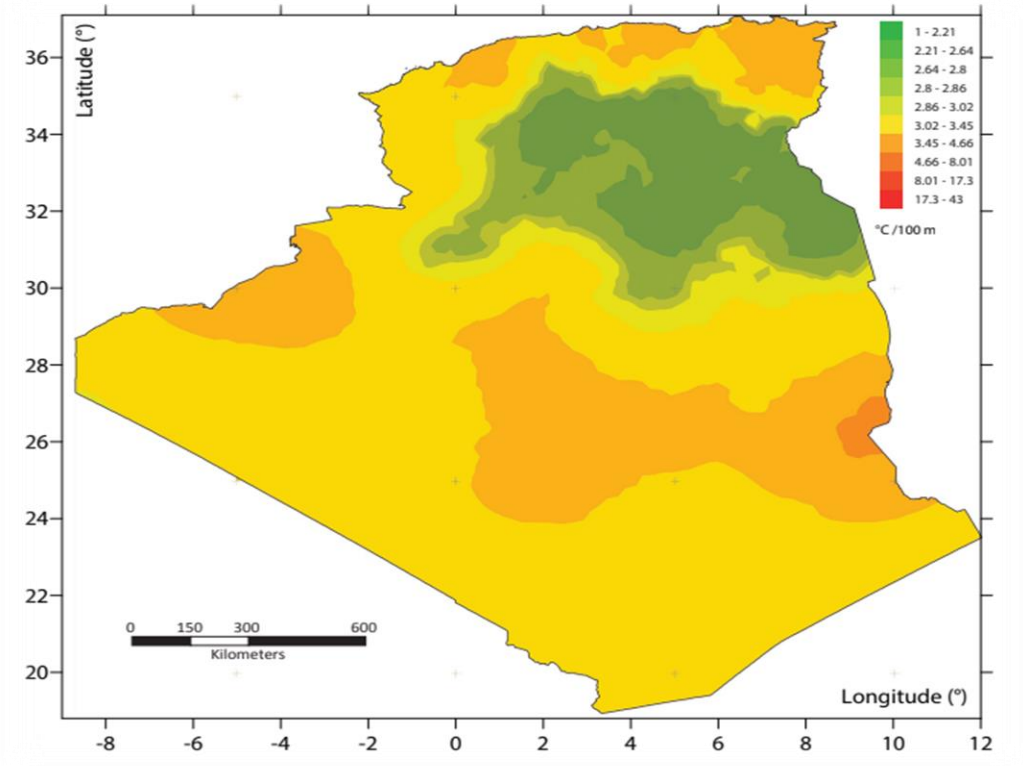

Figure I.7: Geothermal gradient map [19].

I.3.2.4.4. Biomass potential

Algeria has great potential for biomass energy, where the country's biomass energy mainly comes from solid waste, date palm waste, crop waste, and forest residues. Solid waste is an excellent source of biomass energy in the country, with data indicating that annual municipal waste production exceeds 10 million tons.

The Algerian government has launched an ambitious Renewable Energy and Energy Efficiency Program, which includes the development and expansion of renewable resources such as biomass. This program aims to generate 22,000 MW of power from renewable sources between 2011 and 2030 [17].

Table I.7: Sustainable bioenergy resources in Algeria [18].

Resources	**Annual biogas potential (millions of m^3)**	**Power generation potential (GWh)**
Urban wastes:		
- Organic fraction of household wastes	974	1646
- Sewage from wastewater treatment plants	22.91	38.72
Waste olive industry:	-	215.5
- Olive Pomace	10.5	17.74
- Vegetable waters	2.35	3.97
Whey from the dairy industry		
Total	1009.76	1921.93

The table reflects the importance and diversity of bioenergy potentials in Algeria, where it is possible to achieve electricity production exceeding 1900 gigawatts through the utilization of energy recovery resources from waste. Considering that the annual electricity consumption per capita in Algeria was approximately 1236 kilowatt-hours (kWh) in 2016, the International Energy Agency (IEA) indicates that the available potential can meet the electricity needs of over one and a half million people.

In conclusion, Algeria's biomass energy potential is promising and could play a significant role in the country's transition to renewable energy sources. However, the development of the bioenergy sector in Algeria requires a thorough assessment of national biomass potential.

I.2.2.4.5. Hydropower potential

The hydropower potential in Algeria is estimated at 18 billion m^3/year, including 12.5 billion m^3/year in the northern regions and 5.5 billion m^3/year in the Sahara regions [25].
Algeria has launched an ambitious program to develop renewable energy,
including hydropower, to diversify its energy sources and preserve its fossil resources. The program aims to install 22,000 MW of renewable energy by 2030, including 400 MW from cogeneration [26]. Several hydropower projects have been carried out or are being carried out in different ways in the country.

I.3.2.5. Conventional energy sources

Conventional potential in Algeria refers to energy resources derived from fossil fuels, such as oil, natural gas, and coal. Algeria is country rich in hydrocarbons, which represent the country's main source of income and its trade balance. According to the International Energy Agency (IEA), Algeria has the 10th largest proven natural gas reserves in the world, with 4.5 trillion m^3 in 2019, and the 16th largest proven oil reserves, with 12.2 billion barrels in 2019.

Algeria is also a major exporter of natural gas, particularly to Europe, via pipelines and LNG ships [27].

However, the conventional potential in Algeria presents challenges and limits. On the one hand, the production and consumption of hydrocarbons have negative impacts on the environment, contributing to greenhouse gas emissions and climate change. Algeria is the third largest emitter of CO2 in Africa, with 150.7 million tonnes in 2019 [28].

On the other hand, hydrocarbon resources are limited and non-renewable, and their exploitation requires significant investments and advanced technologies. Algeria is facing a decline in its oil and gas production, due to the aging of existing fields, the lack of exploration and development of new fields, and competition from other producers. In addition, the Algerian economy's over-dependence on hydrocarbons makes it vulnerable to fluctuations in prices and demand on the international market.

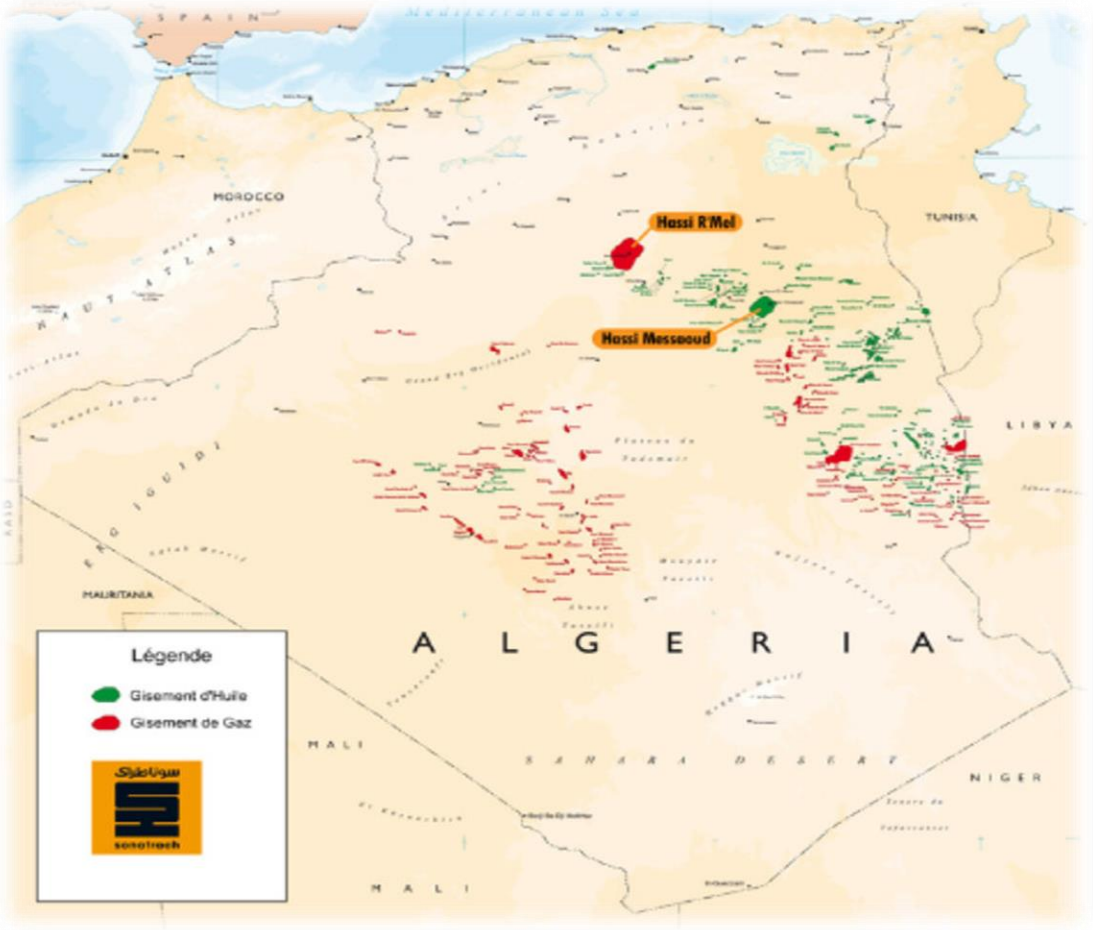

Figure I.8: Map of hydrocarbon fields in Algeria [29].

I.3.2.5.1. Petroleum

Petroleum is a major source of energy and revenue for Algeria. According to the International Energy Agency (IEA), Algeria has the 16th largest proven crude oil reserves in the world, with 12.2 billion barrels as of 2021 [30]. Algeria also produces about 1.4 million barrels of crude oil per day, making it the third-largest oil producer in Africa after Nigeria and Angola [31].

Algeria's oil production is mainly concentrated in the Hassi Messaoud and Berkine basins in the eastern part of the country. Algeria's oil sector faces some challenges due to the global energy transition and the volatile oil market. The country is highly dependent on oil revenues, which account for nearly 25 % of its GDP. However, the oil demand is expected to decline in the coming years as the world shifts to cleaner and renewable sources of energy. Algeria's oil reserves are also costlier and carbon-intensive to produce than those of other regions [31].

Therefore, Algeria needs to diversify its economy, improve its energy efficiency, and invest in new technologies and infrastructure to remain competitive and resilient in the new energy landscape.

I.3.2.5.2. Gas Natural

Algeria is a major producer and exporter of gas and provides a significant share of Europe's energy needs. It has one of the largest proven natural gas reserves globally, with about 2.3 trillion cubic meters as of 2020 [20]. Which is among the largest worldwide. It also has a large potential for shale gas, estimated at 20,000 billion cubic meters [32], but this is not yet developed or exploited.

Algeria's natural gas production was around 85 billion standard cubic meters in 2020, which was mainly used for domestic consumption and power generation, or exported to Europe and other regions. Algeria's natural gas exports were valued at $4.7 billion in 2021, making it a significant source of income for the country.

However, Algeria faces some challenges in maintaining and increasing its natural gas production and exports, such as declining fields, rising domestic demand, insufficient investment, regulatory uncertainty, and geopolitical risks. Algeria needs to reform its energy sector, attract more foreign partners, and diversify its export markets to ensure its long-term natural gas potential [32,33].

I.3.2.5.3. Shale gas

Shale gas is a type of natural gas that is found in layered rocks such as shale. Shale gas is a potential source of clean and renewable energy, but it requires advanced and costly techniques to extract and transport it [20].

Algeria has the third largest technically recoverable shale gas reserves in the world, which are estimated at 707 trillion cubic feet Most of these reserves are located in the southeast of the country [34], where there is also the largest groundwater storage in the Algerian desert. Algeria has seven (7) basins containing shale gas (Fig I.9). These basins are Mouydir, Ahnet, Berkine–Ghadames, Timimoun, Reggane, and Tindouf. Which are estimated 19,800 billion m^3 [29]. Exploiting shale gas in Algeria faces several challenges and problems, such as the high consumption of water and chemicals in the drilling and hydraulic fracturing process, which may lead to the pollution of groundwater and the surrounding environment [33].

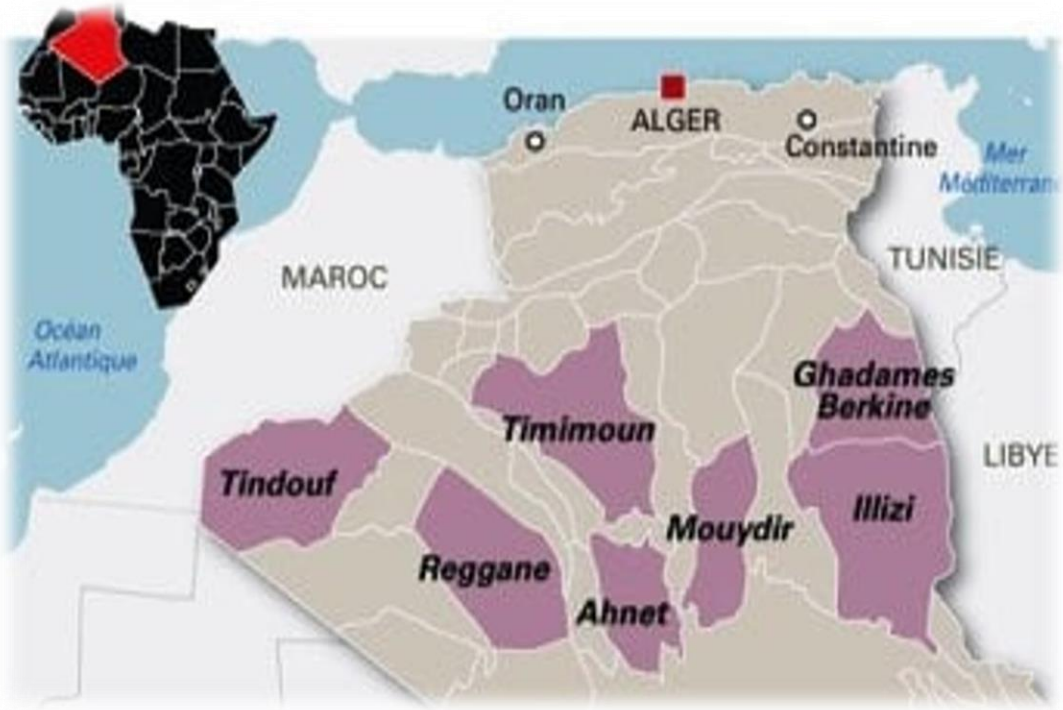

Figure I.9: seven identified shale gas basins in Algeria [12].

I.3.2.5.4. Uranium

Uranium is a radioactive element that can be used for nuclear power generation and other applications. Algeria has some uranium resources, mainly in the south of the country, but they are not very large or well-explored. According to the 2022 edition of the Red Book [35], Algeria has reasonably assured conventional resources of 26,000 tonnes of uranium (tU) at a cost of less than $260 per kilogram of uranium (kg). This is enough to fuel two 1000-megawatt nuclear power plants for 60 years [36].

Algeria has two nuclear research reactors, but no uranium enrichment or fuel fabrication facilities. It also lacks the necessary infrastructure, human resources, and legal framework to develop a nuclear power program. Algeria plans to build its first nuclear power plant by 2025, with the help of foreign partners, to diversify its energy sources and meet its growing electricity demand. However, it still faces many challenges, such as selecting a suitable site, ensuring safety and security, and managing radioactive waste.

I.3.2.5.5. Coal

The coal potential in Algeria is very low, compared to other fossil fuels such as natural gas and oil. Algeria has no domestic coal production and relies on imports to meet its small coal demand. The coal reserves in Algeria are estimated to be 65 million tons, which is very low compared to other countries. Algeria ranks 63rd in the world for coal reserves and accounts for about 0% of the global total. Algeria's coal consumption is also very low, as it relies mainly on gas and oil for power generation [37].

Algeria has set ambitious renewable energy targets, aiming to reach a clean energy capacity of 22,000 megawatts by 2030.

I.3.2.6. Electricity production in Algeria

Algeria is one of the largest energy producers in Africa, with a well-established oil and gas industry, the country relies heavily on fossil fuels—such as natural gas and oil, which contribute 64.84% and 34.63%, respectively—for electricity generation. Algeria showed substantial growth in the production of gas, and oil from the year 2000 to 2018, contributing to a 33.3% increase in the population. Although 28% of Algeria's population is located in rural areas, 100% of households in the country have access to electricity [17].

According to the International Energy Agency (IEA), Algeria's total primary energy production in 2019 was 143.3 million tonnes of oil equivalent (Mtoe), making it the third-largest energy producer in Africa after Nigeria and Egypt [38].

Electricity production rose to 76.4 TWh in 2018 from 76.0 TWh in 2017, proportional to the population growth of almost 1 million people. The load demand increased by 7.4% from 2007 to 2017. The country's population and energy consumption profile are shown in (Fig I.10). By 2030, generation is expected to rise to approximately 150 TWh, with an additional 5.2% increment each year [17].

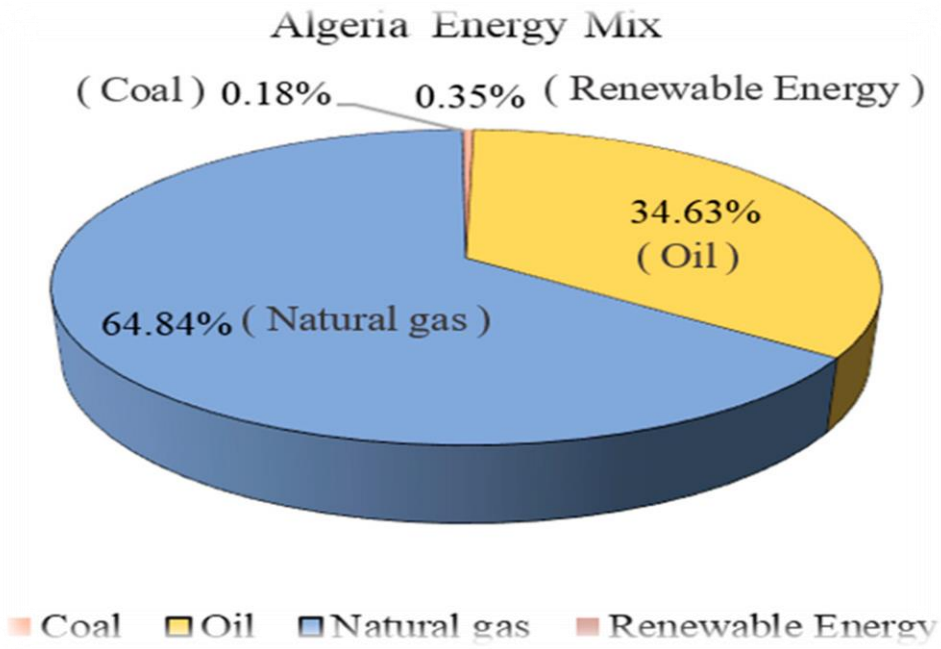

Figure I.10: Algeria energy mix 2007-2017[17].

Algeria has a relatively small share of renewable energy in its electricity production, but it has set ambitious targets to increase it by 2030, in 2015, Algeria had a total installed renewable

power generation capacity of 533 MW, with solar accounting for 295 MW, hydro for 228 MW, and wind for 10 MW [39].

In that year, the country revealed its intention to achieve approximately 22 GW of renewable energy capacity by 2030. This will consist of 1 GW of bio-power from waste, 13.5 GW from solar PV, 2 GW from CSP, 15 MW from geothermal, 400 MW of cogeneration, and 5 GW from wind energy. By 2030, it is expected to produce a total of 22.000 MW by using RE, with 12.000 MW devoted to the national market, and 10.000 MW to exports [40,41]. Producing this quantity of RE would result in saving over 300 billion m3 of natural gas, which is eight times the national consumption in 2014. This would also lead to a reduction of 348 MtCO2 equivalents in CO2 emissions [42]. The main aim of the RE program is to reach a share of about 27% of RE in total electricity production by 2030.

I.4. Conclusion

The energy situation in the world and Algeria is a significant topic. Algeria has diverse geology and is rich in non-conventional energy sources, such as solar and wind power. When it comes to electricity production, Algeria has been making strides, but there's still room for growth. Renewable energy plays a crucial role in the global energy transition, and it refers to energy sources that can be replenished naturally, like solar, wind, and hydro power. By harnessing these sources, we can produce electricity in a more sustainable and environmentally friendly way.

Chapter II

Hybrid Energy System

II.1. Introduction

Hybrid energy systems (HES) combine multiple energy sources to enhance efficiency and reliability. Main components include renewable sources like solar panels, wind turbines, alongside conventional generators and energy storage systems. Architectures vary from DC-only, AC-only, to hybrid AC/DC setups. Sizing HES involves software tools or traditional methods to optimize component capacities. Harmony Search Algorithm (HSA) is a metaheuristic technique used for optimizing HES configurations efficiently. This is the main topic that will be covered in this chapter.

II.2. Hybrid systems

A hybrid power system combines two or more energy sources, typically renewable ones, to generate electricity, heat, or cooling. Such systems can offer increased efficiency, reliability, and environmental benefits compared to a single energy source. Examples of dual power systems include solar and wind energy, hydro and solar energy, diesel and battery, and cogeneration.

II.2.1. Main components of a hybrid energy system:

Photovoltaic solar power, wind power, and diesel generators are often used in SEH. These may also include other sources of energy such as hydraulic, tidal, geothermal energy or the energy contained in hydrogen (fuel cells). Converters, loads, load shedding, and form energy management systems can also be part of an SEH. Batteries are usually used for energy storage.

But there are other options such as inertial storage (flywheel) and hydrogen storage. A description of the typical components of SEH is given below [43].

- **Hybrid energy sources:** There are two main categories of hybrid system sources available:

- Sources of renewable energy: These are the main sources of power in a hybrid energy system and may consist of solar panels, wind turbines, hydroelectric generators, or biomass systems.
- Emergency power source: This element supplies extra power in situations where renewable energy sources are unable to generate sufficient electricity to fulfill the demand. Typical emergency power sources comprise diesel generators or battery storage systems.

- **Energy storage system:** This critical component is responsible for storing surplus energy produced by renewable sources to be utilized during periods of low or no renewable energy generation.
- **Power conditioning unit:** An essential part of the system, this unit transforms the electricity generated by renewable sources into a suitable form for consumption by the various loads within the system.
- **Static converters:** Static converters are devices that transform electric power from one form to another without any moving components. They find extensive applications in power supplies, motor controls, renewable energy setups, and

electric vehicles. These converters can be categorized into four primary types based on the input and output power variations:

- AC to DC converters, also referred to as rectifiers, convert alternating current (AC) to direct current (DC). They are essential for providing DC power to electronic devices, charging batteries, and driving DC motors. Rectifiers are further classified into diode rectifiers and phase-controlled rectifiers.
- DC to DC converters, known as choppers, change DC power from one voltage level to another. They play a crucial role in regulating the output voltage of DC sources like batteries, solar panels, and fuel cells. Choppers are segmented into step-down converters, step-up converters, and buck-boost converters.
- DC to AC converters, or inverters, convert DC power into AC power. They are pivotal in supplying AC power to loads such as induction motors, lighting systems, and household appliances. Inverters can also facilitate the connection of DC sources to the AC grid and are further categorized into voltage-source inverters and current-source inverters.
- AC to AC converters, including cycloconverters and AC voltage controllers, alter AC power from one frequency or voltage level to another. They are instrumental in managing the speed and torque of AC motors like synchronous and induction motors. Cycloconverters and AC voltage controllers can be further segmented into single-phase and three-phase converters.

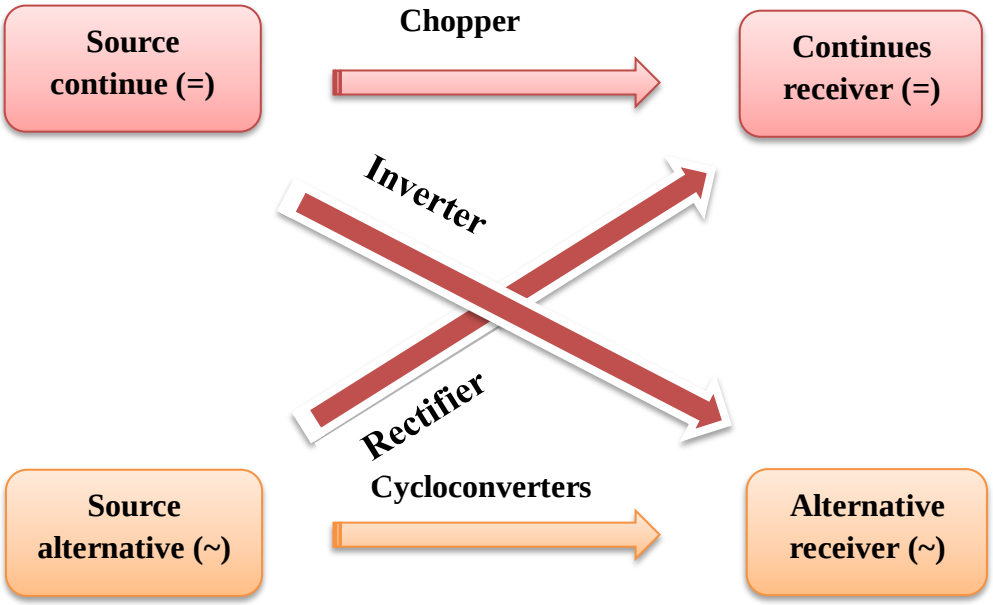

Figure II.1: Sources and loads provided by various static converters.

- **Loads:**

- Alternating Current (AC) or Direct Current (DC): Load components with purely resistive elements in them can be satisfactorily powered using DC. This means that there is no necessity for the use of an inverter. Resistive loads however tend to use a significant amount more power so their use is not recommended for remote area power supply systems. To run most appliances, it is often simpler to use an inverter to produce AC and power the appliance circuits with that.
- Waveform: In most cases a modified square wave current is appropriate, but if there are to be appliances with high surge currents a sine wave inverter may be a better option.
- Interference: Some electrical equipment (radios, TVs, computers) may be affected by interference from /. appliances such as microwave ovens and may not operate as efficiently.

- **Supervision of hybrid system**

Supervision of a hybrid system involves monitoring and controlling the operation of the system to ensure optimal performance and efficiency. This typically involves collecting data from various sensors and components within the system, analyzing this data to detect any anomalies or issues, and taking corrective actions as needed.

Some key aspects of supervising a hybrid system include:

- Monitoring energy consumption involves tracking both conventional and alternative energy sources to ensure efficient operation. Fault detection and diagnostics, detecting

any faults or malfunctions in the system components, and diagnosing the root cause of the issue to prevent further damage.

- System optimization, adjusting the operation of the system based on real-time data to optimize performance and maximize energy efficiency.
- Safety monitoring, ensuring that the system operates safely and within specified limits to prevent accidents or damage to equipment.

II.2.2 Architectures of Hybrid Energy System:

Having multiple power sources in a hybrid system is crucial for reliability. Different power sources require specific connection architectures using converters and buses to supply loads. Various architectures combine energy sources effectively. Energy storage units use bidirectional converters to store and deliver energy when needed. Objectives include efficient energy flow, simplicity, reduced losses, reliability, and cost-effectiveness [44].

II.2.2.1. Continuous bus architecture (DC):

The paragraph describes a coupling DC bus architecture for a hybrid system where different energy sources are connected to a single DC bus line. AC resources are linked to the DC bus through a rectifier, while DC energy sources are connected directly or via a DC/DC converter. A bidirectional converter can stabilize power supply from the battery bank. Power from each source is centralized on the DC bus and converted to either DC or AC energy for end users using a single DC/AC inverter. The AC bus powers AC loads and can connect to the utility grid. However, drawbacks include reliance on a single inverter for AC loads, risking power loss if it malfunctions, necessitating a robust control scheme for efficient power distribution [44].

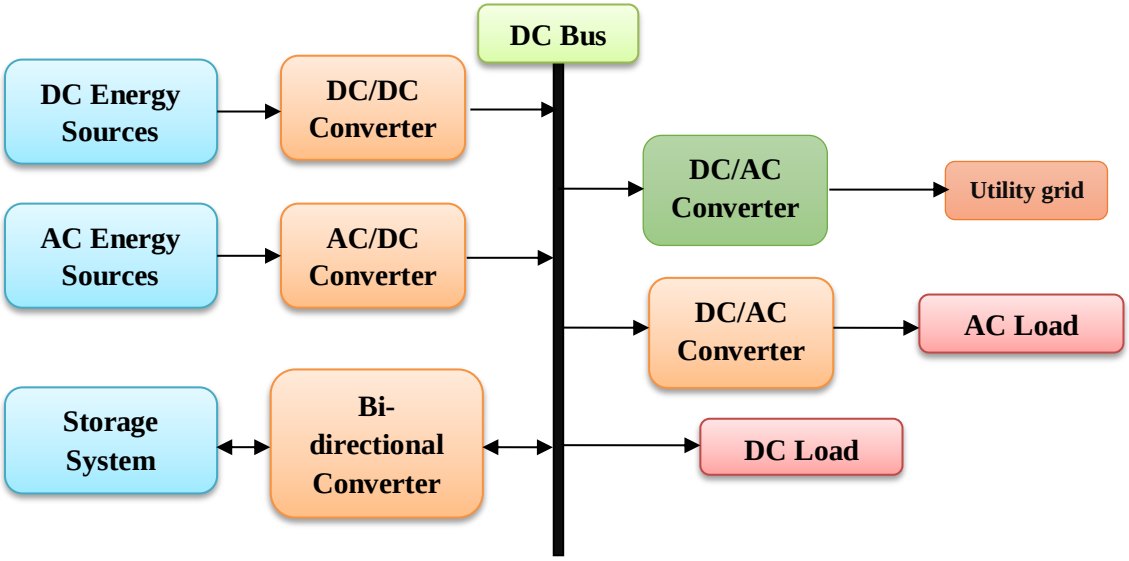

Figure II.2: DC bus hybrid system architecture [44].

II.2.2.2. Alternating bus architecture (AC):

In the coupling of AC bus architecture, all sources of the hybrid system are connected to the AC load, as shown in Figure (II.2). This architecture shows better performance contrasted with the DC architecture, where the problem of synchronizing each converter with its source can be overcome, therefore it can be fed the loads autonomously and at the same time with the other converters, that it provides flexibility for the sources energy to satisfy the needs of the load. In the event of low demand rates, some sources are disconnected leaving a source capable of covering the load consumption rates. However, during acute load requirements i.e. peak hours, the sources of the hybrid system with battery bank work in parallel to fulfill the load needs. The embodiment of this architecture is comparatively considered complex due to the synchronization of the result voltages at the AC bus with the load voltages [44].

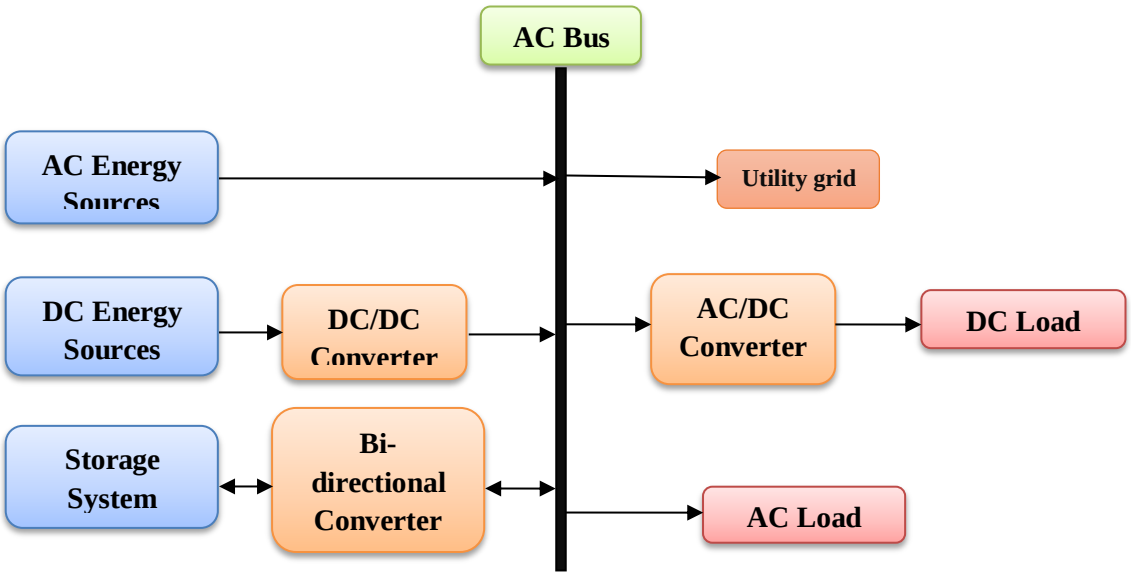

Figure II.3: AC bus hybrid system architecture [44].

II.2.2.3. Mixed architecture with Continuous/Alternating bus (DC/AC):

The coupling DC/AC bus hybrid architecture contains AC and DC buses as shown in Figure I.3. In which, the different sources of the whole system can be associated with the DC or AC bus with or without converters. The interconnection between the two buses can be achieved through bidirectional converters. This configuration can integrate some energy sources directly without the need for converters. Therefore, it provides higher efficiency and low cost [44].

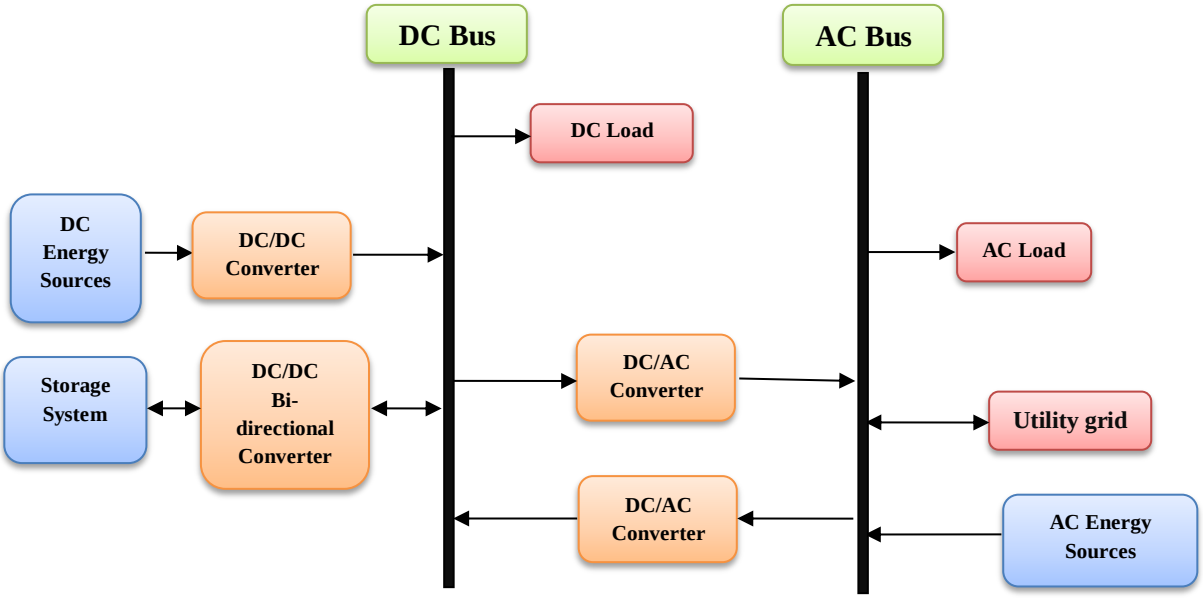

Figure II.4: DC/AC bus hybrid system architecture [44].

In AC bus architecture, all hybrid system sources connect to the AC load, offering better performance than DC architecture. It allows autonomous feeding of loads and flexibility for energy sources to meet load demands. Sources can be disconnected during low demand and work in parallel during peak hours. However, synchronizing voltages at the AC bus with load voltages makes this architecture complex.

II.2.3. Sizing of hybrid energy systems (HES):

Sizing of the hybrid system is an important step in defining the capacity of the generators. Without appropriate sizing, there is a risk of under-sizing or over-sizing the system. The most difficulties encountered are the evaluation of real load and step time to accurately consider fluctuations. However, most researchers take average hours, days, or months as data samples.

There are two categories of sizing methods; the first one is by using software and the second one is by using traditional methods (Fig II.5).

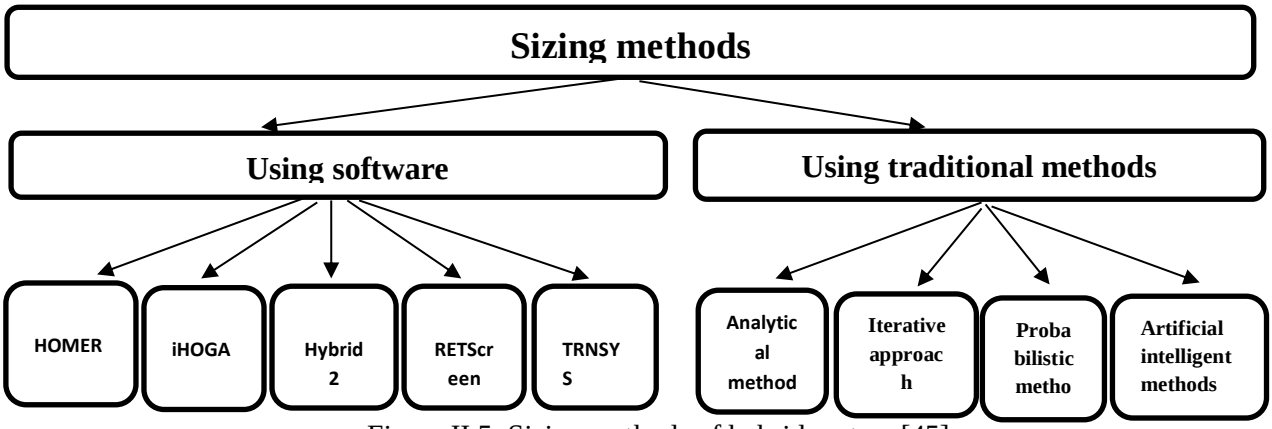

Figure II.5: Sizing methods of hybrid system [45].

II.2.3.1. Sizing hybrid energy system using software:

Many commercial applications are available for sizing hybrid systems, and most of these applications use Windows as a computer platform with the programming language Visual C++ like RET Screen, iHOGA (Hybrid Optimization by Genetic Algorithm), INSEL (Integrated Simulation Environment Language), HOMER (Hybrid Optimization Model for Electric Renewable) and other software [45].

II.2.3.1.1. software tools for unit sizing of hybrid energy systems:

Table II.1: Summary of available software tools for unit sizing of hybrid energy systems [46].

Software tools	Input	Output
1. HOMER	• Load demand • Resource input • Component details including capital, maintenance, and replacement cost • System control	• Optimal unit sizing • Cost of energy, net present cost • Fraction of renewable energy
2. HYBRID2	• Load demand • Resources input • Initial investment and O&M Cost of system components • Components details	• Unit sizing with cost optimization • cost of energy • Emissions in terms of percentage of various greenhouse gases • System payback periods
3. RET Screen	• Load data • Size of Solar Array • Required hydrology and product database • Climate database	• Energy production and savings • Costs • Emission reductions • Financial viability • Sensitivity and risk analysis
4. IHOGA	• Load data • Resources input data • Component and economics details	• Multi-objective optimization • Cost of energy • Life cycle emission • Analysis of buying and selling of energy
5. TRNSYS	• Meteorological data input of resources • Inbuilt models	• Provide the dynamic simulation results of electrical and thermal energy system

II.2.3.1.2. Evolution of different scaling approaches used in a hybrid system:

Table II.2: Evolution of different scaling approaches (professional tools) used in a hybrid system [47].

Commercial Software	*Advantages*	*Limitations*
HOMER	• Create an efficiency graph with the results • Simple to comprehend	• Employs first-order linear equations • Time series data cannot be imported • It's going to take a lot of information to get started • The user is unable to pick relevant system components intuitively
HYBRID2	• A wide range of electrical load possibilities • more detailed Dispatching options • In terms of optimization variables, it is comprehensive, and it necessitates a higher degree of system configuration expertise	• Simulations should take a long time • even though the project was completed successfully, certain simulation flaws were discovered • Only one configuration should be simulated at a time
RET Screen	• The most comprehensive meteorological database • Excel-based software	• Input of data is reduced • Data from time series cannot be imported
IHOGA	• Simulation step time is short • Genetic algorithms are used to carry out the task, which can be mono or multi-objective	• Lack of sensitivity analysis and probability analysis • Daily load limitation (10 kWh) • Only one configuration should be simulated at a time
TRNSYS	• Simulator adaptability • Graphics are quite accurate	• Some generators, such as hydro power, are unable to be simulated • There is no option for optimization

II.2.3.2. Sizing hybrid energy system using traditional methods:

There are four essential traditional sizing methods:

Analytical method; Iterative approach; Probabilistic method; Artificial intelligence methods.

- **Analytical method**

Fast and accurate method for sizing hybrid renewable energy systems. Identifies storage and solar size, iterating to find the lowest cost. Shows solar and storage's increasing role with reduced costs. Used for various hybrid systems, proven effective in case studies.

- **Iterative approach**

The convergence method is common to determine the size of hybrid energy systems. The initial system size is chosen and adjusted iteratively with different optimization algorithms. It is used to improve various types of hybrid systems and has proven its effectiveness in case studies. It is considered a useful tool for designing hybrid energy systems.

- **Probabilistic method**

The probabilistic method for sizing hybrid renewable energy systems uses probability and stats for long-term performance. Based on the convolution technique, assesses system under varying conditions. Provides insights into energy source variability, valuable for designing robust systems. Demonstrated in research and case studies for optimal sizing of hybrid systems.

- **Artificial intelligence methods**

AI methods optimize the sizing of hybrid energy systems. Analysis of AI plans for optimization, likely using machine learning algorithms like genetic algorithms and neural networks. AI adjusts system parameters iteratively for optimal configuration. Growing research area to enhance renewable energy system efficiency. Numerous approaches are reported in the literature such as Genetic Algorithms (GA), Particle Swarm Optimization Technique (PSO), Harmony search algorithm (HSA), Simulated annealing (SA), Ant colony algorithms (ACA), Bacterial Foraging Algorithm (BFO), Artificial bee colony algorithm(ABC), Cuckoo Search (CS).

a) Genetic Algorithms

Genetic algorithms are a type of optimization technique that draws inspiration from the principles of biological evolution. By simulating natural selection and adaptation, genetic

algorithms aim to identify optimal solutions for intricate problems. The main objective when utilizing a genetic algorithm is to determine the most effective combination of system parameters, like component sizes or operating conditions, in order to enhance a specific objective function [48].

When applied to the sizing of hybrid power systems, such as those incorporating photovoltaic, wind, and battery technologies, genetic algorithms can be used to minimize costs, maximize reliability, or achieve a balance between various factors.

The fitness evaluation in GA is typically determined by an objective function that measures the quality of a solution. The fitness value of an individual is calculated using the following equation:

$$Fi = n \sum_{j=1} W_j \times X_{ij}, \quad \textbf{(II.1)}$$

This equation calculates the fitness value as the weighted sum of the decision variables, where the weights reflect the importance or priority of each variable [49].

Fi: represents the fitness value of individual i,

n: is the number of decision variables,

$\mathbf{w_j}$: is the weight associated with decision variable j, and

$\mathbf{x_{ij}}$: is the value of decision variable j for individual i.

b) Particle Swarm Optimization Technique (PSO)

is a metaheuristic global optimization paradigm that has gained prominence in the last two decades, it is particularly useful for solving complex, multidimensional problems that cannot be efficiently addressed using traditional deterministic algorithms [50].

The technique of particle examples (PSO) is a method of global metaheuristic improvement that has gained fame in the past two decades. It is especially used to solve complex and multidimensional problems that cannot be addressed efficiently using traditional identification algorithms.

In PSO, a group of particles (representing potential solutions) move across the search space to find the optimal solution. Each particle adjusts its location based on its own personal experience and adjacent particle experiments. The aim of the algorithm is to reduce or increase the goal function by gradually updating particle sites.

A swarm of particles updates their relative positions from iteration to another, boosting the PSO algorithm to duly perform the search process. To get the optimum solution, each particle moves towards its prior personal best position (**p**best) and the global best position (**g**best) in the swarm [51].

$$\mathbf{p}\text{best}^t = x^*_i \mid f(x^*_i) \quad \min_{k = 1, 2\ldots, t} = (\{f(x^k_i)\}) \qquad \textbf{(II.2)}$$

where $i \in \{1, 2, \ldots, N\}$, and

$$\mathbf{g}\text{best}^t = x^*_i \mid f(x^*_i) \quad \min_{\substack{i = 1, 2\ldots, N \\ k = 1, 2\ldots, t}} = (\{f(x^k_i)\}); \qquad \textbf{(II.3)}$$

where **i** denotes particle's index, **t** is the current iteration's number **f** is the objective function to be optimized (minimized), **x** is the position vector (or a potential solution), and **N** is the total number of particles in the swarm

The following equations describe the velocity and position update mechanisms in a standard PSO algorithm [50]:

$$V_{ij}(t+1) = \omega \times V_{ij}(t) + r_1(t) \times C_1 \times (pbest_{ij}(t) - X_{ij}(t)) + r_2(t) \times C_2 \times (gbest(t) - X_{ij}(t)) \qquad \textbf{(II.4)}$$

$$Xij(t+1) = X_{ij}(t) + V_{ij}(t+1) \qquad \textbf{(II.5)}$$

$\mathbf{r_1}$ and $\mathbf{r_2}$ are independent and identically distributed random numbers whereas $\mathbf{C_1}$ and $\mathbf{C_2}$ are the cognition and social acceleration coefficients. $\mathbf{X_{ij}}$, $\mathbf{V_{ij}}$ are position coordinates and velocity of the $\mathbf{i_{th}}$ agent in the $\mathbf{j_{th}}$ dimension.

c) Harmony search algorithm (HSA)

The Harmony Search Algorithm (HSA) is an optimization technique inspired by music improvisation processes is a kind of population-based algorithm. It aims to find optimal solutions within energy systems, including the sizing of hybrid renewable energy systems (HRES).

The primary goal is to optimize the sizing of components within an HRES. This optimization process aims to minimize the levelized cost of energy, overall system cost, or other relevant metrics while adhering to design and operational constraints.

The improvisation of music players inspired the HS algorithm, and its main steps are as follows [52]:

- In the first step, the HS specifies the static parameter values bandwidth (BW), pitch adjustment rate (PAR), harmony memory acceptance rate (HMCR), and harmony memory size (HMS)
- In the second phase the algorithm will create a new population randomly inside the HM,

$$X'_j = LB + R5 * (UB - LB) \quad \textbf{(II.6)}$$

- In the third phase, the algorithm will improvise the population inside the HM, based on its parameters (BW, PAR, and HMCR). Through this phase the algorithm will have to choices based on HMCR as follow:

If (R1>HMCR), a stochastic value will be processed in the next equation (R1is a stochastic value between 0~1):

$$X'_j = LB + rand * (UB - LB) \quad \textbf{(II.7)}$$

If (R2<HMCR), the algorithm will pick a random HM, and if (R2<=PAR) the value of the chosen HM will be tuned as follows:

$$X'_j = X'_j + R4 \pm bw \quad \textbf{(II.8)}$$

- In the third phase, the new improvised value x'_j will replace the worst one in the HM, if it has a superior objective function value
- Finally, the improvisation process of the HS algorithm will end once the algorithm reaches a stopping cause such as the highest number of iterations.

d) Ant colony algorithms (ACA)

ACO is a metaheuristic optimization algorithm inspired by the foraging behavior of ants. It mimics how ants find the shortest path between their nest and food sources. ACO aims to find optimal solutions by iteratively constructing paths based on pheromone trails left by virtual ants.

ACO is mainly used to solve the traveling salesman problem (TSP), which is a famous problem in the mathematics field. Each ant in the node i moves to the next node j (selected among the unvisited cities) according to a certain probability, so as to obtain the minimum distance from start node to the destination. The probability is calculated according to the pheromone [53]:

$$p^{k_{ij}} = \frac{[\tau ij(t)]\alpha \times [\eta ij(t)]\beta}{\sum s \in Jk\ (i)[\tau is(t)]\alpha \times [\eta is(t)]\beta} \quad \textbf{(II.9)}$$

where $\tau_{ij}(t)$ is the pheromone between **i** and **j** at time **t**, $\eta_{ij}(t)$ is the heuristic factor and **α** and **β** are the coefficients, which stand for the importance degree of **τ** and **η**, respectively. $J_k(i)$ is the set consisting of the cities that ant **k** could select.

e) Bacterial Foraging Algorithm (BFO)

BFO is a metaheuristic optimization algorithm inspired by the foraging activities of Escherichia coli (E. coli) bacteria.

BFO aims to find optimal solutions by simulating the behavior of bacteria as they search for nutrients.

The statistic of algorithm is to allow the cell to swarm stochastically and collectively toward optimal solution. To achieve this three consecutive steps are performed [54]:

- 'Chemotaxis' length of life time of bacteria is measured by the number of chemotactic steps. Where the cost (fitness) J_i of bacteria is calculated by the proximity to other bacteria new position θi after a tumble along the manipulated cost surface one at a time by adding step size C_i in the temple direction lie between [-1,1]. Random direction vector Δ_i is generated to represent the tumble;
- 'Reproduction' where only those cells that performed well over their lifetime, may contribute to the next generation;
- 'Elimination-dispersal' where cells are discarded and new random samples are inserted with a low probability. Detail work flow of BFA is shown in Fig 3.

$$J_i\,[j, k, l] = J_i\,[j, k, l] + J_{cc}\,(\theta_i\,[j, k, l], PoP\,[j, k, l]) \quad \textbf{(II.10)}$$

$$\theta_i\,[j, k, l] = \theta_i\,[j - 1, k, l] + C_i \frac{\Delta i}{\sqrt{\Delta\tau\ i\ \Delta i}} \quad \textbf{(II.11)}$$

In order to obtain the time varying objective, J_{cc} value of objective function is added in the actual objective function.

f) Artificial bee colony algorithm(ABC)

The Artificial Bee Colony (ABC) algorithm is a nature-inspired metaheuristic optimization technique. It simulates the foraging behavior of honeybees in a colony. ABC is inspired by the behavior of real honeybee colonies, it mimics the way bees explore their environment,

communicate, and find food sources. The algorithm aims to find optimal solutions by imitating the search process of bees.

Using the analogy between emergent intelligence in foraging of bees and the ABC algorithm, the units of the basic ABC algorithm can be explained as follows [55]:

- 'Initialization' The ABC algorithm randomly generates Ns numbers of initial feasible solutions Xi, generated as:

$$X_{ij} = X_{ij\ min} + rand * (X_{ij\ max} - X_{ij\ min}) \quad \textbf{(II.12)}$$

where j = 1, 2…, D; $\mathbf{x_{ij}}$ is the j_{th} dimension parameter of a feasible solution Xi; $\mathbf{x_{ij\ max}}$, $\mathbf{x_{ij\ min}}$ are the upper and lower bounds for the dimension j, respectively; **rand** is random number between 0 and 1.

- 'the employed bee phase' In the employed bee phase, the algorithm randomly selects a dimension *j* and a feasible solution X_k, then searches for a new candidate solution X'_i within the neighborhood of the associated feasible solution X_i. The search process is described by the following equation:

$$X'_{ij} = X_{ij} + R_{ij} * (X_{ij} - X_{kj}) \quad \textbf{(II.13)}$$

where j∈ {1, 2…, D}, k∈ {1, 2…, Ne} are randomly generated and k ≠ i; $\mathbf{x'_{ij}}$ is the j_{th} dimension parameter of candidate solution X'_i ; $\mathbf{x_{kj}}$ is the jth dimension parameter of the feasible solution X_k; R_{ij} is random number between −1 and 1.

The fitness values of the feasible solutions are calculated by the following expression:

$$fit = \frac{1}{1+fi} \quad \textbf{(II.14)}$$

where $\mathbf{f_i}$ is the objective function value of feasible solution X_i; and **fit** is the fitness value of feasible solution X_i.

After calculating fitness values, X'_i and X_i are chosen using the greedy selection mechanism. A better feasible solution and a lower objective function value are linked to a higher fitness value.

- 'Onlooker Bee Phase' After all employed bees complete the search processes, each onlooker bee selects a feasible solution depending on the probability value Pi to search

for a new candidate solution using Equation (II.13), and records the better solution by the greedy selection mechanism. Pi is calculated by the following expression:

$$Pi = \frac{fit}{\sum_{i=1}^{Ne} fit} \quad \textbf{(II.15)}$$

- 'Scout Bee Phase' If a feasible solution cannot be improved within a predetermined number of cycles, it indicates that the fitness value of the solution has reached a local optimum. In such cases, the solution is abandoned, and a scout bee generates a new solution without any guidance, following Equation (II.12).

g) Cuckoo Search (CS).

The Cuckoo Search (CS) algorithm is a nature-inspired optimization technique based on the behavior of cuckoo birds. CS is inspired by the brood parasitism behavior of cuckoo birds. Cuckoos lay their eggs in the nests of other bird species, relying on the host birds to raise their chicks. The algorithm aims to find optimal solutions by imitating the search process of cuckoos.

For simplicity in describing our new Cuckoo Search, we now use the following three idealized rules [58]:

- Each cuckoo lays one egg at a time, and dumps it in a randomly chosen nest;
- The best nests with high quality of eggs (solutions) will carry over to the next generations;
- The number of available host nests is fixed, and a host can discover an alien egg with a probability $p_a \in [0, 1]$. In this case, the host bird can either throw the egg away or abandon the nest so as to build a completely new nest in a new location.

When generating new solutions $X^{(t+1)}$ for, say cuckoo i, a Levy flight is performed

$$X_i^{(t+1)} = X_i^{(t)} + \alpha \oplus \text{Levy}(\lambda), \quad \textbf{(II.16)}$$

where $\boldsymbol{\alpha} > 0$ is the step size which should be related to the scales of the problem of interest. In most cases, we can use $\boldsymbol{\alpha} = O(1)$. The product $\oplus$ means entry-wise multiplications. **Levy** flights essentially provide a random walk while their random steps are drawn from a **Levy** distribution for large steps.

$$\text{Levy} \sim u = t^{-\lambda}, (1 < \lambda \leq 3), \quad \textbf{(II.17)}$$

The consecutive jumps or steps of a cuckoo essentially form a random walk process, which follows a power-law step length distribution with a heavy tail. This distribution has an infinite variance and an infinite mean.

II.2.3.2.1. Sizing methodologies and their limitations:

Table II.3: Sizing methodologies and their limitations [46].

SIZING METHODOLOGIES	***INPUT PARAMETERS***	***ENERGY SOURCES***	***LIMITATION***
ANALYTIC METHOD	Hourly or monthly average wind speed and Solar radiation	Systems like solar, wind, Biomass, batteries, etc. are considered, depending on the software tool used such as HOMER, RET-SCREEN, etc.	• Less flexible in designing the system as performance is assessed by the computational models (i.e., commercial software tools and or/numerical approximations of system components)
ITERATIVE APPROACH	Hourly or monthly average wind speed and Solar radiation or Probabilistic approach of sizing of solar and wind systems	Various systems are considered such as solar, wind, batteries, etc.	• Suboptimal solutions are reached as the computation involves linearly changing the decision variables • PV module slope angle and wind turbine installation height are not optimized
PROBABILISTIC METHOD	The probabilistic approach to sizing solar and wind systems	Systems like solar, wind, batteries, etc. are considered	• Unable to represent the dynamic performance of the hybrid energy system
AI METHOD	Hourly wind speed and Solar radiation or monthly average solar and wind energy values or Probabilistic approach of sizing of solar and wind systems	Various systems are considered such as solar, wind, batteries, etc.	• Complexity in designing the system

2.3.2.2. Comparison of various conventional approaches employed in hybrid systems:

Table II.4: Comparison of scaling approaches in hybrid systems [47].

Methods	*Advantages*	*Drawbacks*
ANALYTICAL METHOD	• Quick and simple to use • Time-series data is no longer required	• The degree of flexibility is extremely limited • The optimization procedure can only involve two parameters
ITERATIVE METHOD	• Easy to operate • Eliminate the need for time-series data	• Some critical parameters of higher wind turbines and solar photovoltaic slope angles were overlooked • Typically, this leads to higher computing effort and poorer results
PROBABILISTIC METHOD	• Easy to operate • Time-series data is no longer required	• No way to show the hybrid system's dynamic performance
AI METHODS	• Solve a multi-objective and complex problem • Find the global best system configuration with the least amount of compute	• High complexity

II.3. Conclusion

Hybrid energy systems (HES) are innovative as they blend various energy sources like solar panels, wind turbines, generators, and energy storage to enhance efficiency and reliability. These systems offer flexibility by allowing configurations such as DC-only, AC-only, or a mix of both to cater to diverse energy requirements. Determining the capacity of each component in an HES can be achieved using software tools or traditional methods to ensure seamless integration of renewable sources, generators, and storage. The Harmony Search Algorithm (HSA), drawing inspiration from music, optimizes HES by exploring different settings to discover the most efficient and harmonious system solution. Through the utilization of diverse energy sources and advanced techniques like the HSA, hybrid energy systems present a promising avenue towards a sustainable and dependable energy future with significant positive impacts on both the environment and energy infrastructure.

Chapter III

Methodology of assessing wind and solar energy potential with a case study

III.1. Introduction

This study investigates wind power dynamics using statistical models like Weibull's law, Weibull's hybrid law, and Rayleigh's law to analyze temporal wind speed variations. It includes histogram analysis of occurrence frequency distributions and examines the variation of Weibull parameters. The research focuses on the Ouargla region to match wind speeds with the Adrar region. Additionally, it explores photovoltaic power in Ouargla, utilizing a Photovoltaic Geographical Information System (PVGIS) to assess solar radiation time differences, average monthly temperatures, and PVGIS-5 estimates of solar electricity generation using the specific properties of solar panels in the Al-Hadjira region. Through studying these aspects, we can obtain valuable insights about the potential of wind energy and solar energy in the Ouargla region.

III.2. Geographical Location

The city of Ouargla lies in northeast Algeria and serves as the capital of the wilaya of Ouargla, with an elevation of 128 meters. The agglomeration has 210,175 inhabitants, 133,024 of whom live in Ouargla alone. The city is one of the wealthiest in Algeria, and its wilaya is an economic center of gas and oil reserves, situated in the Hassi Messaoud territory. With 2,887 km², the city has a considerable area. The beauty of its red sand is what makes it famous in the northern Sahara Desert. Ouargla has a warm desert climate. Ouargla is the initial Saharan city to introduce a tram [57].

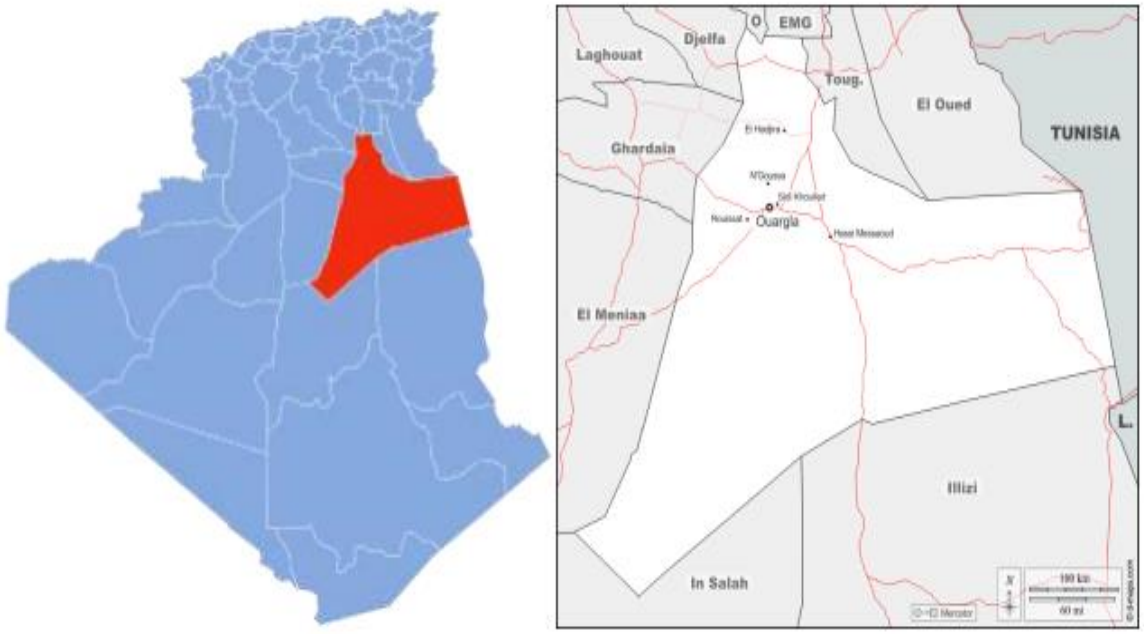

Figure III.1: Geographical boundaries of the Ouargla region [57]

III.3. Study of wind power

III.3.1. Temporal Variation of Wind Speed

To assess the significance of wind at a specific location, it is necessary to calculate the average wind speed over a minimum period of 10 years. This provides an indication of the wind conditions at that location. Additionally, wind patterns fluctuate throughout the day, season, and year. Understanding these variations is crucial for sizing wind energy systems to meet changing energy demands. Daily variations are analyzed hourly, while annual variations are assessed through daily-scale studies. Long-term trends are evaluated over multiple years every year.

III.3.1.1 Daily average variation of wind speed

Daily changes in wind speed are caused by thermal processes associated with solar radiation. Wind speed remains relatively stable at night but gradually increases after sunrise. When observing wind rise, one can see that wind speed and direction fluctuate unexpectedly, the following figure shows ten-year wind speed changes in Ouargla.

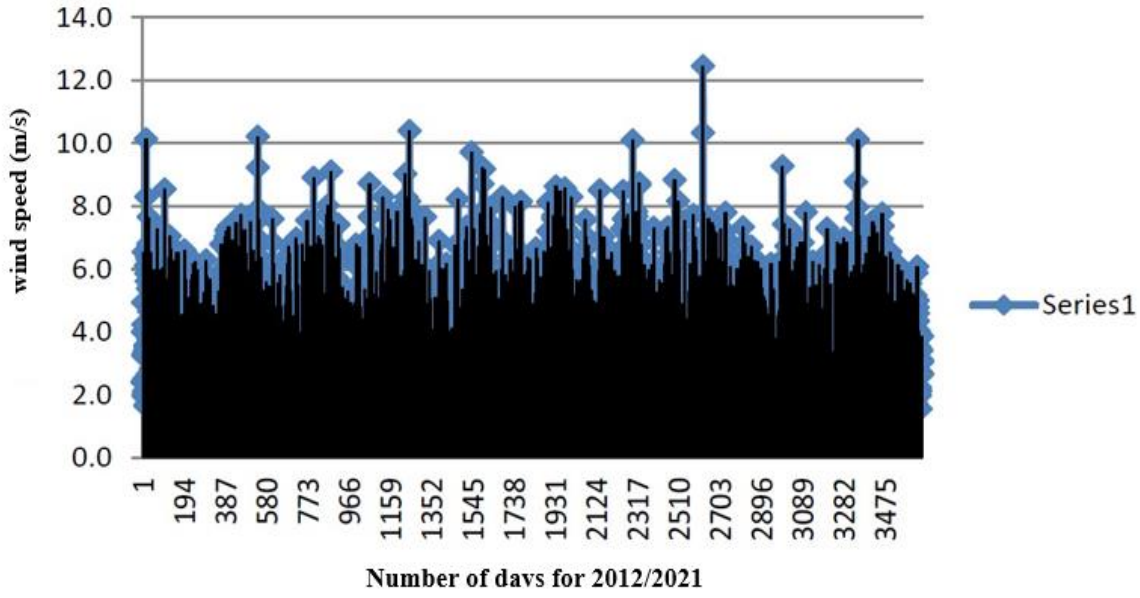

Figure III.2: The graph represents the evolution of wind speed in terms of days for a Multi-year between 2012/2021.

It is noted that the highest wind speed during these years was estimated at 12.4 m/s, and the lowest wind speed was estimated at 1.4 m/s. Most wind speeds ranged from 4.0 m/s to 10.0 m/s.

III.3.1.2 Wind Roses

In the wind rose it can be observed that the speed and direction of the wind vary randomly.

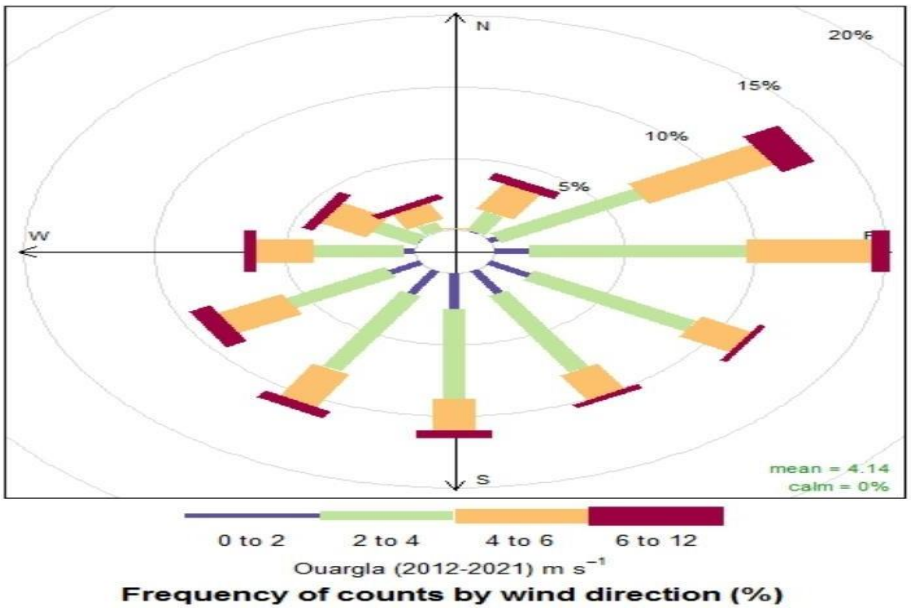

Figure III.3: the wind rose in Ouargla

III.3.2. Statistic study

The wind potential is calculated from the mean velocity Distributions. As the distributions are not always available, we have gotten into the habit of modeling the distributions using the following models: Weibull's law, Weibull's hybrid law, and Rayleigh's law.

III.3.2.1. Weibull distribution

The most widely used model for the variation of wind speeds is the Weibull distribution law Its probability density is as follows [60]:

$$F(v) = (\frac{k}{c})(\frac{k}{v})^{k-1}\exp(-(\frac{v}{c})^{k}) \quad \textbf{(III.1)}$$

By equating frequencies to probabilities, the probability density F(v) represents the frequency distribution of the measured velocities.

k and C are parameters commonly referred to as Weibull parameters. Parameter k (shape factor) is dimensionless and characterizes the shape of the frequency distribution while C determines the wind quality (scale factor). The latter has the dimension of speed.

The determination of these parameters allows the knowledge of the wind distribution for a given site. The treatment can be done directly or through the frequencies by classes by considering the averages.

The probability density F(v) represents the frequency distribution of the measured velocities.

The corresponding cumulative distribution function of Weibull F(v) is [60]:

$$\mathrm{F(v)} = \int f(v)dv = 1 - \mathrm{e}^{-\left(\frac{\mathrm{v}}{\mathrm{c}}\right)^{\mathrm{k}}} \qquad \textbf{(III.2)}$$

III.3.2.2. Rayleigh distribution

The Rayleigh distribution is a special case of the Weibull distribution for the case where the form factor k equals 2.

Its probability density is given by:

$$\mathrm{F}(v) \equiv 2\left(\frac{\mathrm{v}}{\mathrm{c}^2}\right)\exp\left(-\left(\frac{\mathrm{v}^2}{\mathrm{c}}\right)\right) \qquad \textbf{(III.3)}$$

However, the classical Weibull distribution (function of two parameters) is the most indicated. The use of these two parameters allows the evaluation of a large number of properties of the distribution, hence a better characterization of the sites [59].

III.3.2.3. Weibull Hybrid Distribution

The Weibull hybrid distribution is used when the recorded calm wind frequency at a given site is greater than or equal to 15%. Indeed, this proportion cannot be overlooked and must be taken into account when characterizing a site from a potential wind perspective.

a) Methods for determining Weibull parameters

Several methods are used to determine the parameters of Weibull c and k from wind statistics (justus et al. 1978). The least-squares method and the one using the standard deviation of velocity variation and mean velocity [60], the mean velocity method and the wind variability, and the maximum likelihood method.

b) Least squares method

This method is often used to determine the parameters of Weibull c and k by discretizing the function f(V) in frequencies f1, f2…. fn in cumulative frequencies

p1 = f1, p2 = p1 + f2, ……, pn = pn 1 + fn. taking the logarithms, namely

xi = ln(Vi) and yi = ln [ln (1 ft)], we obtain a line y = ax + b whose coefficients are adjusted by linear regression. Parameters c and k.

$$k = b \quad \textbf{(III.4)}$$

$$c = \exp(-\frac{a}{b}) \quad \textbf{(III.5)}$$

c) Adjustment methods

The characteristics of the wind will determine the amount of energy that can be extracted from the wind field. To know the properties of a site, measurements of the wind speed and its direction, over a long time, are necessary (one to ten years). However, previous wind studies have shown that the most important feature is the Weibull statistical distribution.

It has proven to be the most suitable for use in wind turbines. Typically, the form factor characterizes the symmetry of the distribution. The estimation of the two parameters k and c of the Weibull law makes it possible to characterize the statistical distribution of wind speeds over a given period, and consequently to estimate wind energy production.

There are several methods for determining the k and c coefficients of the Weibull distribution adjusted to raw wind speed data taken over a given period.

Below are the methods most used for this purpose.

d) Mean speed and standard deviation method

The mean velocity and standard deviation method also called the moment method was proposed by Justus and all [61].

If mean velocity v and standard deviation σ are known, form factor k and scale factor c are determined by equations [62].

$$\mathrm{k} = \left(\frac{\sigma}{\bar{v}}\right)^{-1,086} \quad \textbf{(III.6)}$$

La facture d'helle est alors d :

$$C = \frac{\bar{v}}{\Gamma\left(1+\frac{1}{k}\right)} \quad \textbf{(III.7)}$$

Where:

Γ: the Gamma function given by equation (III.6)

$\bar{v}$: the mean wind speed expressed by the relation (III.7)

σ: the standard deviation of the wind speed distribution estimated by the relationship

$$\sigma = \frac{1}{N-1}\Sigma_{I+1}^{N}(v_i - \bar{v})f(v_i) \quad \textbf{(III.8)}$$

e) Energy factor method

This is a recent method suggested by Akdag Ali (2009). It is related to the mean values of wind speed data. It is a simple formulation method, easy to execute, and requires less calculation. The method is defined by the following equations [60].

$$E_{pF} = \frac{\nabla^3}{\nabla^3} = \frac{\Gamma\left(1+\frac{3}{k}\right)}{\Gamma^3\left(1+\frac{1}{k}\right)} \quad \textbf{(III.9)}$$

$$k = 1 + \frac{3.69}{E_{PF}^3} \quad \textbf{(III.10)}$$

$$C = \frac{\nabla}{\Gamma\left(1+\frac{1}{k}\right)} \quad \textbf{(III.11)}$$

The wind energy factor (EPF) is expressed as the ratio of the mean value of the wind speed to the mean wind speed at power three, according to the next relationship [63].

$$E_{pF} = \frac{\nabla^3}{\nabla^3} = \frac{\frac{1}{N}\Sigma_{i=3}^{N} vi^3}{\left(\frac{1}{N}\Sigma_{i=1}^{N} vi^3\right)} \quad \textbf{(III.12)}$$

f) Graphical method

The graphical method also called the least square method is the simplest method. It is based on the cumulative function of Weibull, transforming it into the following form [64].

$$\ln[-\ln(1 - F(V))] = K\ln(c) - K\ln(c) \quad \textbf{(III.13)}$$

$$x = \ln(v) \quad \textbf{(III.14)}$$

By identification, it is found that:

K=a

$$c = \exp\left[-\frac{b}{a}\right]$$

This method has two disadvantages:

- It is not applicable if zero speed ((v) = 0 is undetermined).

- The value of y corresponding to the maximum value of the wind speed is indeterminate because

$$\ln\left(1 - F(Vmax)\right) = \ln(0)$$

In order to eliminate these determinations, only the number of non-zero wind speeds and neglecting the probability of having $V = Vmax$

g) Maximum Likelihood Method (MLM)

The maximum likelihood method is an iterative method used to determine the form parameter k. Its value is defined using the following formula [64]:

$$k = \left(\frac{\sum_{i=1}^{N} v_i^k \mathrm{Ln}(v_i)}{\sum_{i=1}^{N} v_i^k} - \frac{\Sigma_{i=1}^{N} \mathrm{Ln}(v_i)}{N} \right)^{-1} \quad \textbf{(III.15)}$$

with:

Vi: The observed non-zero wind speed;

N: Number of non-zero wind velocity data.

K: Shape parameter to be determined by iterative calculation taking an initial value of k =2

Then the value of the scale parameter c is determined using the following formula:

$$C = \left(\frac{\sum_{i=1}^{N} V_i^k}{N} \right)^{\frac{1}{k}} \quad \textbf{(III.16)}$$

h) Modified Maximum Likelihood Method (MEL)

When wind speed data are available in frequency form, a variant of the MLM method can be used. This method is called the Modified Maximum Likelihood Method (MEL). The principle of this method is the mêmeet it is based on the following relations [64]:

$$k = \left(\frac{\sum_{i=1}^{N} v_i^k \mathrm{Ln}(vi)f(vi)}{\sum_{i=1}^{N} v_i^k f(vi)} - \frac{\Sigma_{i=1}^{N} \mathrm{Ln}(v_i)f(vi)}{f(v\geq 0)} \right)^{-1} \quad \textbf{(III.17)}$$

$$C = \left(\frac{1}{f(v\geq 0)} \sum_{i=1}^{N} \left(v_i^k f(v_i)\right)\right)^{\frac{1}{k}} \quad \textbf{(III.18)}$$

k is the shape parameter to be determined by iterative calculation by taking an initial value of k =2

vi is the observed wind speed;

(v 0) = 1, is the probability that the wind speed is equal to or greater than zero;

(vi) is the probability of having wind speed vi.

III.3.2.4. Vertical extrapolation of Weibull parameters

a) Justus and Mikhail Extrapolation Model

In 1976, Justus and Mikhail proposed the following extrapolation formulas for an initial elevation reference of 10 m [64].

$$\frac{Z_2}{Z_1} = \frac{1-0{,}0881 * \ln\left(\frac{Z_1}{10}\right)}{1-0{,}088 * \ln\left(\frac{Z_2}{10}\right)} \quad \textbf{(III.19)}$$

and:

$$\frac{C_1}{C_2} = \left(\frac{Z_2}{Z_1}\right)^m \quad \textbf{(III.20)}$$

With:

$$m = \left(\frac{0.37-0{,}881 \ln(C)}{1-0{,}0881 \ln\left(\frac{Z}{10}\right)}\right) \quad \textbf{(III.21)}$$

b) Poje Modified Justus Extrapolation Model

Taken over by Poje, Justus changed in 1978, the expression extrapolation of parameters

Weibull by introducing the roughness of the soil, such as [65]:

$$\frac{k_2}{k_1} = \left(\frac{1}{1-0{,}0881 \ln\left(\frac{z_2}{z_1}\right)} \right) \quad \textbf{(III.22)}$$

and:

$$\left(\frac{C_2}{C_1}\right) = \left(\frac{z_2}{z_1}\right)^m \quad \textbf{(III.23)}$$

With:

$$m = \frac{1}{\ln\left(\frac{z_g}{z_0}\right)} - 0{,}0881 \ln\left(\frac{C_1}{6}\right) \quad \textbf{(III.24)}$$

Tablel III.1: Arithmetic, Weibull, Hybrid-Weibull, Rayleigh equations for calculating average wind speed

Distributions	$\bar{V}$	$\bar{V}^3$	σ	σ^2
Arithmetic	$\sum_{i=1}^{n} f_i v_i$	$\sum_{i=1}^{n} f_i {v_i}^3$	$\frac{1}{n}\sum_{i=1}^{n} f_i(v_i - \bar{v}_i)$	$\frac{1}{n}\sum_{i=1}^{n} f_i(v_i - \bar{v}_i)^2$
Weibull	$C\Gamma\left(1+\frac{1}{k}\right)$	$C\Gamma^3\left(1+\frac{3}{k}\right)$	$\sqrt{C^2\left[\Gamma\left(1+\frac{2}{k}\right) - \Gamma^2\left(1+\frac{1}{k}\right)\right]}$	$C^2\left[\Gamma\left(1+\frac{2}{k}\right) - \Gamma^2\left(1+\frac{1}{k}\right)\right]$
Hybrid Weibull	$(1-ff_0)C\Gamma\left(1+\frac{1}{k}\right)$	$(1-ff_0)C^3\Gamma\left(1+\frac{3}{k}\right)$	$\sqrt{(1-ff_0)C^2[\Gamma - \Gamma^2\left(1+\frac{1}{k}\right)]}$	$(1-ff_0)C^2[\Gamma - \Gamma^2\left(1+\frac{1}{k}\right)]$
Rayleigh	0.886 C	1.32 C^3	0.4632 C	0.2146 C^2

III.3.3. Histogram of occurrence frequency distributions

Number of classes Nc: $Nc = 3.33\ logN + 1 \Rightarrow Nc = \sqrt{N}$

N: Number of observations

Class interval: $h = \frac{Vmax - Vmin}{Nc}$

Relative frequency:

$$fr = \frac{ni}{N}$$

ni: Number of observations in the class.

N: Total number.

Table III.2: frequency distributions for 10 years.

2012/2021	***Class***	***fa***	***fr***	***f ré***	***fr%***
1	1.4-1.95	12	0.032	0.032	3.2
2	1.95-2.5	29	0.079	0.111	7.9
3	2.5-3.05	37	0.101	0.212	10.1
4	3.05-3.6	61	0.167	0.379	16.7
5	3.6-4.15	40	0.109	0.488	10.9
6	4.15-4.70	70	0.192	0.68	19.2
7	4.70-5.25	35	0.096	0.778	9.6
8	5.25-5.80	31	0.085	0.863	8.5
9	5.80-6.35	16	0.044	0.907	4.4
10	6.35-6.90	10	0.027	0.953	2.7
11	6.90-7.45	9	0.025	0.964	2.5
12	7.45-8	6	0.016	0.97	1.6
13	8-8.55	3	0.008	0.978	0.8
14	8.55-9.1	0	0	0.978	0
15	9.1-9.65	0	0	0.978	0
16	9.65-10.2	0	0	0.978	0
17	10.2-10.75	5	0.014	0.982	1.4
18	10.75-11.3	0	0	0.982	0
19	11.3-11.85	0	0	0.982	0
20	11.85-12.4	1	0.002	0.984	0.2

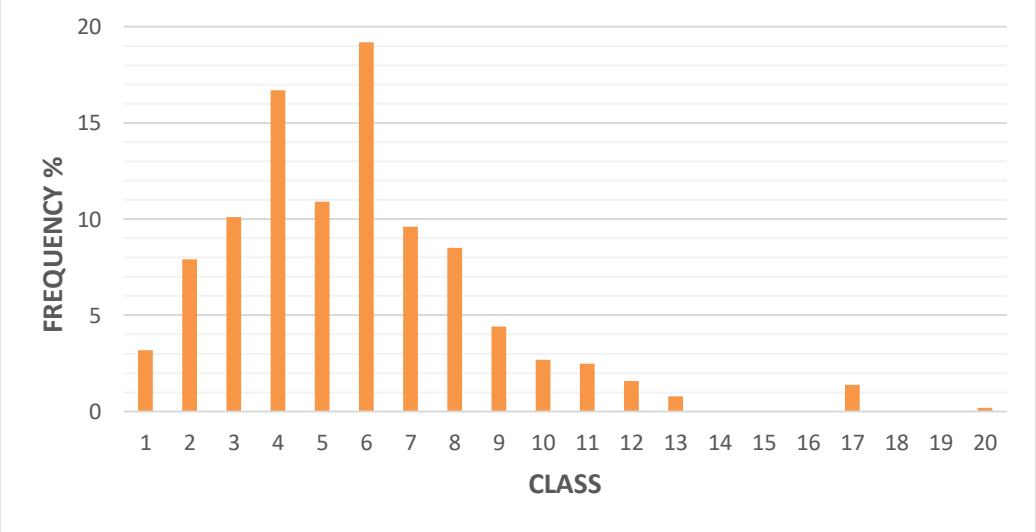

Figure III.4: Histogram of frequency distributions for 10 years.

III.3.4. Variation of Weibull parameters

Table III.3: Find the words y, x and k

bin	NO V	freq	freq %	f(V)	1-f(V)	Ln(1-f(V))	Ln(-Ln(1-f(V)))	Ln(V)
0	0	0	0	0	1	0		
1	16	0.0044	0.4471	0.0044	0.9955	-0.0044	-5.4077	0
2	361	0.1008	10.0894	0.1053	0.8946	-0.1113	-2.1951	0.6931
3	915	0.2557	25.5729	0.3610	0.6389	-0.4480	-0.8029	1.0986
4	950	0.2655	26.5511	0.6266	0.3733	-0.9851	-0.0149	1.3862
5	695	0.1942	19.4242	0.8208	0.1791	-1.7195	0.5420	1.6094
6	405	0.1131	11.3191	0.9340	0.0659	-2.7187	1.0001	1.7917
7	156	0.0435	4.3599	0.9776	0.0223	-3.8005	1.3351	1.9459
8	56	0.0156	1.5651	0.9932	0.0067	-5.0045	1.6103	2.0794
9	17	0.0047	0.4751	0.9980	0.0019	-6.2366	1.8304	2.1972
10	6	0.0016	0.1676	0.9997	0.0002	-8.1825	2.1020	2.3025
13	1	0.0002	0.0279	1	0			

Three statistical methods, including the Weibull distribution, the hybrid Weibull distribution, and the Rayleigh distribution, are utilized to model wind speed distribution. These distributions help determine various wind factors for a site, such as mean wind speed, average cube of wind speed, variance of speed distribution, power factor, and variation index. To fit statistical data and determine Weibull coefficients **k** and **C**, methods like the graphical method of least squares for shape coefficient calculation and the graphical method for scale parameter calculation are commonly used.

$$F(V) = 1 - \exp[-(\frac{V}{C})^K]$$

Convert this exponential equation into a linear equation like this:

$$Ln\,[-Ln\,(-1\mathrm{F(V)})] = \mathrm{k}\,Ln\,(\mathrm{V}) - \mathrm{k}\,Ln\,(\mathrm{C})$$

Let:

$$\mathrm{Xi} = Ln\,(\mathrm{Vi}) \qquad\qquad Y\mathrm{i} = Ln\,[Ln\,(\frac{1}{1-F(V)})]$$

Where i=1, 2, 3……, n

The linear approximation of these data is obtained by the method of least squares, under the form:

$$Y = a + bX$$

$$Ln\,[Ln\,(\frac{1}{1-F(V)})] = k\,Ln\,(Vi)$$

Let: $$Xi = Ln(Vi)$$

$$Yi = Ln\,[Ln\,(\frac{1}{1-F(V)})]$$

Or: $$Y = a + bX$$

Thus, the Weibull parameters are obtained as follows: k = b,

and the scale parameters are $C = e^{-\frac{a}{b}}$

Table III.4: Variation of Weibull parameters C and k.

year	a (intercept)	K = b	C = e (-a/b)
2012	-4.460433665	3.189837421	4.048418589
2013	-3.93969883	2.669461577	4.374710062
2014	-3.971759554	2.766928604	4.201492587
2015	-3.601320703	2.516087022	4.184210445
2016	-3.93002597	2.676325021	4.342460908
2017	-3.979983498	2.700410323	4.365985688
2018	-3.46407575	2.422407117	4.178757105
2019	-3.560719344	2.477519646	4.208942153
2020	-3.798386618	2.747533769	3.984737002
2021	-4.133033106	2.81733558	4.336209776
2012/2021	**-3.756547422**	**2.596324755**	**4.249796779**

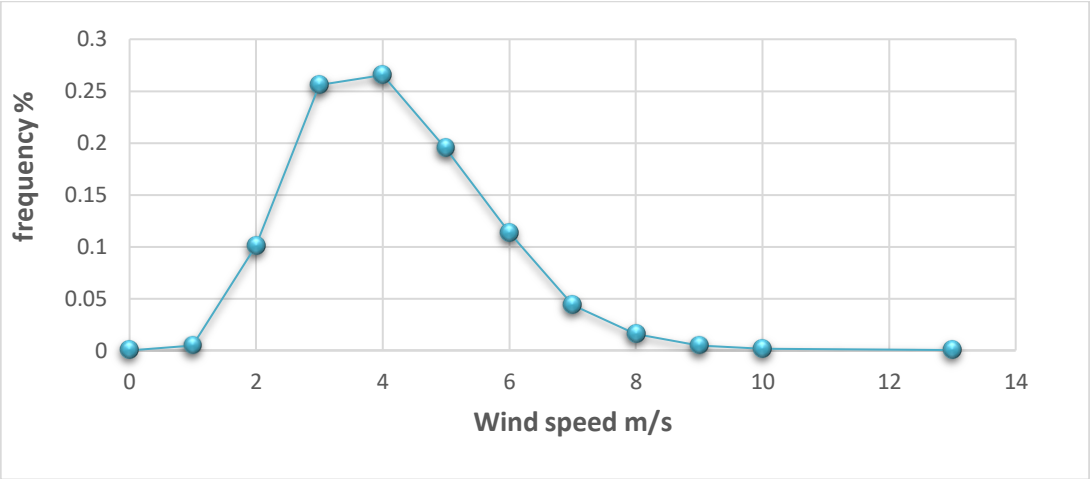

Figure III.5: Daily variation of the Weibull distribution for 10 years (2012/2021)

The data in the table demonstrates that as the shape parameter k rises, the distribution becomes more concentrated, with winds clustering around a particular value. In contrast, lower values of k result in winds being spread out over a wider range. The scale factor C also plays a crucial role, with higher values indicating strong winds and lower values indicating weaker winds in the area or at that time.

III.3.4.1. Wind parameter

Among the laws presented in the second chapter and Table (III.5), we have calculated the wind parameters, which are listed in the following table:

Table III.5: Wind parameters in Ouargla.

year	$\overline{V}$	$\overline{V}^3$	σ	$\sigma 2$
2012	3.5868	87.5850	1.8752	3.5172
2013	3.8759	110.5151	2.0263	4.1070
2014	3.72252	97.9004	1.9461	3.7882
2015	3.70721	96.6973	1.9381	3.7571
2016	3.84742	108.0890	2.0114	4.0467
2017	3.8682	109.8552	2.0223	4.0906
2018	3.7023	96.3197	1.9356	3.74734
2019	3.7291	98.4221	1.94958	3.8016
2020	3.5304	83.5166	1.8457	3.4074
2021	3.8418	107.6229	2.0085	4.0350
2012/2021	3.7653	101.3160	1.9685	3.8758

III.3.4.2. Wind energy potential

1- Mean incident theoretical wind power

This is what we are looking for, the available energy power. Using the law (III.25), we determine the mean kinetic energy at Ouargla per unit of time and surface.

$$P = \frac{1}{2}\rho\bar{V}^3 \qquad \textbf{(III.25)}$$

Worth knowing that $\rho = 1.25\ m^3kg$

Table III.6: theoretical wind power.

Year	**2012**	**2013**	**2014**	**2015**	**2016**	**2017**	**2018**	**2019**	**2020**	**2021**	**2012/ 2021**
Pthe	54.74	69.07	61.18	60.43	67.55	68.65	60.19	61.51	52.19	67.25	63.32

These results have been converted into graphs which are shown in Figure (III.6):

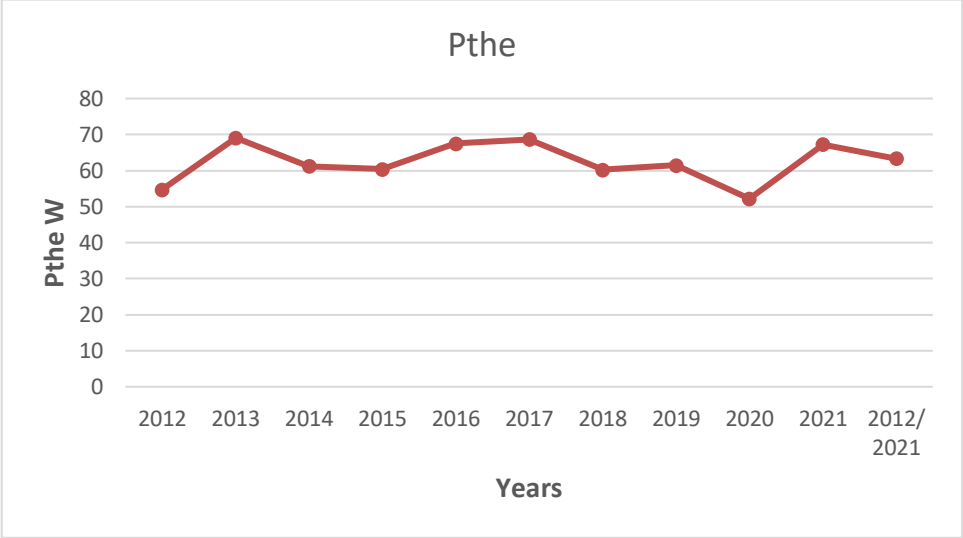

Figure III.6: curve of theoretical wind power for 10 years

In the curve of the theoretical average power, we notice that each year the power differs from another, as it reached its lowest value in 2012 estimated at 54.74 W.

2- The power absorbed by the rotor per unit of surface

The figure below gives us an idea of Betz's theorem:

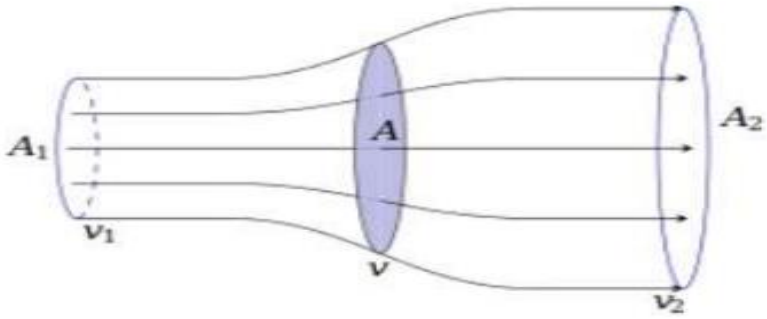

FigureIII.7: Representation of the current tube

Where: V0 > V1 > V2

It means: V2 = V0/ 3 with V1 = (V0 + V2) / 2

Here, the surface A is assumed to be equal to 1 m^2, while the relationship will be:

$$Pabs = V_1^2(V_0 - V_2) \quad \textbf{(III.26)}$$

Table III.7: The result of the values of V1, V2, V0, and Power absorbed

Year	V_0	V_1	V_2	Pabs
2012	3.5864	2.3673	1.1836	16.83565
2013	3.8759	2.5581	1.2790	21.2432
2014	3.72252	2.4568	1.2284	18.8184
2015	3.70721	2.4467	1.22337	18.5872
2016	3.84742	2.5392	1.2696	20.7769
2017	3.8682	2.5530	1.2765	21.1164
2018	3.7023	2.4435	1.2217	18.51463
2019	3.72912	2.4612	1.23061	18.91876
2020	3.53047	2.3301	1.1650	16.05361
2021	3.84188	2.5356	1.26782	20.68734
2012/2021	**3.76531**	**2.4851**	**1.24255**	**19.4750**

These results were converted into graphical curves, which are shown in Figure (III.8)

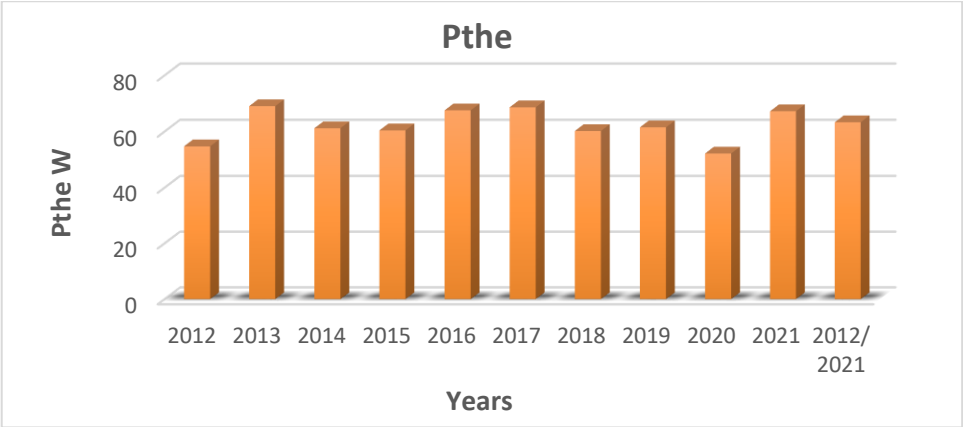

Figure III.8: Power absorbed by the rotor for each year and at 10 years.

The absorbed power reached a maximum value in 2016 estimated at 21.116 W and reached its lowest value in 2020 estimated at 16.053 W.

3- Average maximum recoverable power

The average power during a unit of time and in surface area A depends on the velocities V_0, V_1, and V_2, and can be found with Betz's theorem using the following formula:

$$P = \frac{1}{2} \rho A V_1 (V_0^2 - V_2^2) \quad \textbf{(III.27)}$$

$$P_{max} = \frac{16}{17} P_{the} \quad \textbf{(III.28)}$$

TableIII.8: Pmax and Pthe results

year	Pthé	Pmax
2012	54.74	32.29
2013	69.07	40.75
2014	61.18	36.10
2015	60.43	35.65
2016	67.55	39.85
2017	68.65	40.50
2018	60.19	35.51
2019	61.51	36.29
2020	52.19	30.79
2021	67.26	39.68
2012/2021	63.32	37.36

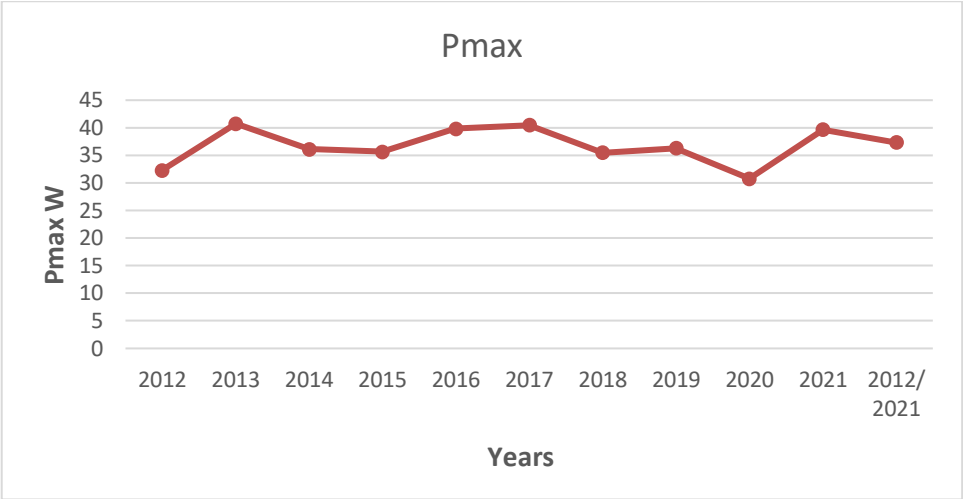

Figure III.9: Average maximum recoverable wind power for each year and over 10 years.

The small discrepancy between the two values of maximum power and theoretical power can be attributed to the estimated maximum power value of 40.75 W in 2013 and the estimated theoretical power of 67.26 W in 2021.

4- Average recoverable energy over one year

The average power recoverable per unit surface area A equal to 1 m2 is given by:

$$Pr = 0.37\ \bar{V}^3 \qquad \textbf{(III.29)}$$

However, the average recoverable energy density, symbolized by $\bar{E}$, expressed as the relation over one year is equal to:

$$\bar{E} = Pr\ \Delta t = 0.37 \text{ x } 24 \text{ x } 365 \text{ x } \bar{V}^3 \text{ [KWh]} \qquad \textbf{(III.30)}$$

TableIII.9: Average cubic hour of wind Average recoverable capacity, recoverable energy

Year	$\bar{V}^3$	Pr	E
2012	87.585	32.40	283880.78
2013	110.515	40.89	358201.65
2014	97.9	36.22	317314.97
2015	96.697	35.77	313415.39
2016	108.089	39.99	350338.21
2017	109.855	40.64	356062.86
2018	96.319	35.63	312191.55
2019	98.422	36.41	319005.83
2020	83.516	30.90	270694.07
2021	107.622	39.82	348827.41
2012/2021	101.316	37.48	328385.71

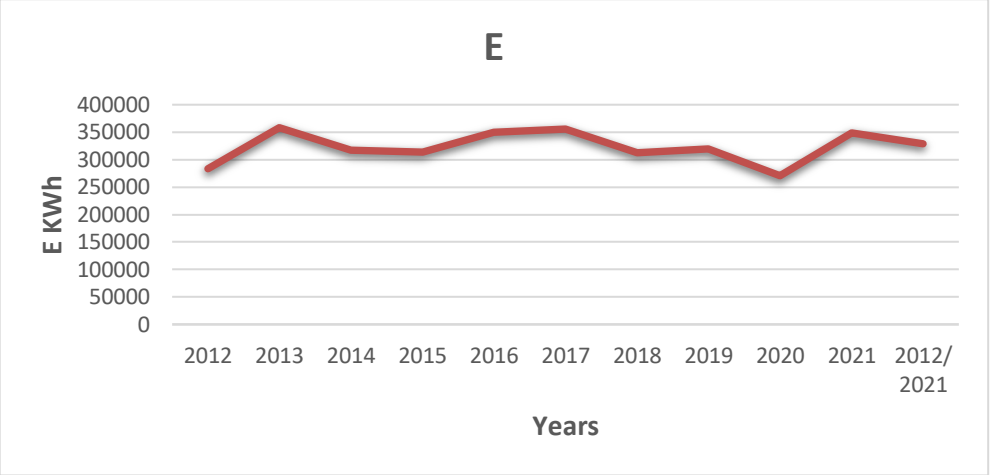

Figure III.10: Average recoverable energy for each year and over 10 years.

Over 10 years, the average recoverable energy was significant, with its peak estimated at 358201.65 Kwh in 2013, and the lowest value estimated at 270694.07 Kwh in 2020.

III.3.5. The geographical location of the selected place

In this study, we calculate the medium wind speed of the Ouargla region, so that this speed is similar to the wind speed of the Adrar region, so we chose a high area at about 173 meters above sea level. Then we calculate the wind speed at 10 meters from the first height plus the turbine height up to 55 meters depending on the turbine height in the Adrar area.

Area coordinates and altitudes:

Study area: 31°52’35” N4°17’18” E height 173m

Figure III.11: picture showing the study areas in the state of Ouargla

III.3.5.1. Weibull parameters for the new height

The Weibull parameters are obtained as follows: k = b,

and the scale parameters are $C = e^{-\frac{a}{b}}$

Table III.10: Variation of Weibull parameters C and k for the new height.

year	K	C
2012	4,2596323	8,18171622
2013	3,5647349	8,67069061
2014	3,6948901	8,41229636
2015	3,3599222	8,38637071
2016	3,5739002	8,62278104
2017	2,6762314	8,6577384
2018	3,2348243	8,37818435
2019	3,3084203	8,42346349
2020	3,6689907	8,0851485
2021	3,7622023	8,613484
2012/2021	3,4670698	8,48461791

III.3.5.2. Wind parameter

Among the laws presented in the second chapter and Table (III.10), we have calculated the wind parameters, which are listed in the following table:

Table III.11: Wind parameters in Ouargla of height 173m.

year	$\overline{V}$	$\overline{V}^3$	σ	σ^2
2012	5,833449321	376,7463497	3,049722038	9,302788
2013	6,219355402	456,5715969	3,251473389	10,57433
2014	6,015137565	413,056497	3,144708488	9,891301
2015	5,994683146	408,8570253	3,134014936	9,824144
2016	6,181442646	448,2727069	3,231652634	10,44581
2017	6,209103656	454,3175314	3,246113785	10,5395
2018	5,988225757	407,5372029	3,130639019	9,802991
2019	6,023950048	414,8746044	3,149315646	9,920304
2020	5,757514245	362,2245062	3,010023249	9,062172
2021	6,17408805	446,6745637	3,227807658	10,42096
2012/2021	6,072231161	424,930255	3,174556968	10,07996

1- Theoretical average of wind energy

That's what you're looking for in the energy available to us; Calculate the average kinetic energy in the private location, within a unit of time and surface, at the expense of speed, found in the house by the following law:

Table III.12: theoretical wind power of height 173m.

Year	**2012**	**2013**	**2014**	**2015**	**2016**	**2017**	**2018**	**2019**	**2020**	**2021**	**2012/ 2021**
Pthe	499,81	605,71	547,98	542,41	594,70	602,72	540,65	550,39	480,54	592,58	563,73

$$P = \frac{1}{2}\rho\bar{V}^3$$

Worth knowing that $\rho = 1.25\ m^3kg$

These results have been converted into graphs which are shown in Histogram (III.12)

The mean theoretical power of a 10-year wind is estimated at 563,7337KW.

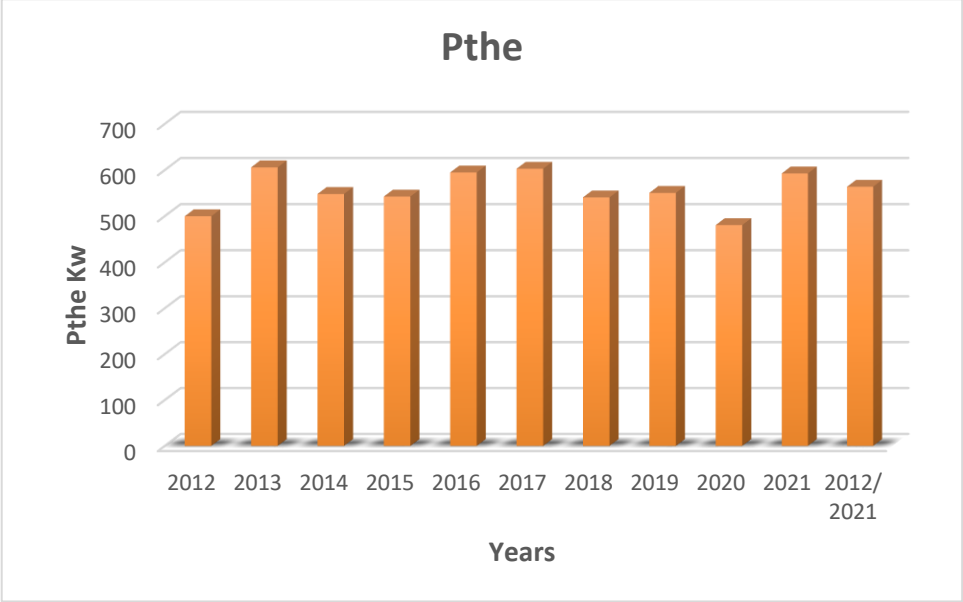

Figure III.12: Histogram of mean incident theoretical wind power for each year and 10 years.

What is remarkable here is that the average theoretical energy (available) in this region is large, reaching about 605,71071KW as its largest value in 2013 and the total energy reached 563,7337KW during the 2012/2021 period.

2- The power absorbed by the rotor per unit area

Here the surface A is assumed equal to 1 [m²], while the relation will be:

$$Pabs = \rho V_1^2 (V_0 - V_2)$$

Table III.13: The result of the values of V1, V2, V0, and Power absorbed of new height

year	V_0	V_1	V_2	P abs
2012	5,83344932	3,88896621	1,944483107	312,118034
2013	6,2193554	4,14623693	2,073118467	378,2497941
2014	6,01513757	4,01009171	2,005045855	342,1994188
2015	5,99468315	3,99645543	1,998227715	338,7203384
2016	6,18144265	4,12096176	2,060480882	371,3745232
2017	6,20910366	4,13940244	2,069701219	376,382399
2018	5,98822576	3,9921505	1,996075252	337,6269223
2019	6,02395005	4,0159667	2,007983349	343,7056422
2020	5,75751425	3,83834283	1,919171415	300,0873159
2021	6,17408805	4,1160587	2,05802935	370,0505311
2012/2021	6,07223116	4,04815411	2,024077054	352,0363134

These results were converted into graphical curves, which are shown in Figure (III.13)

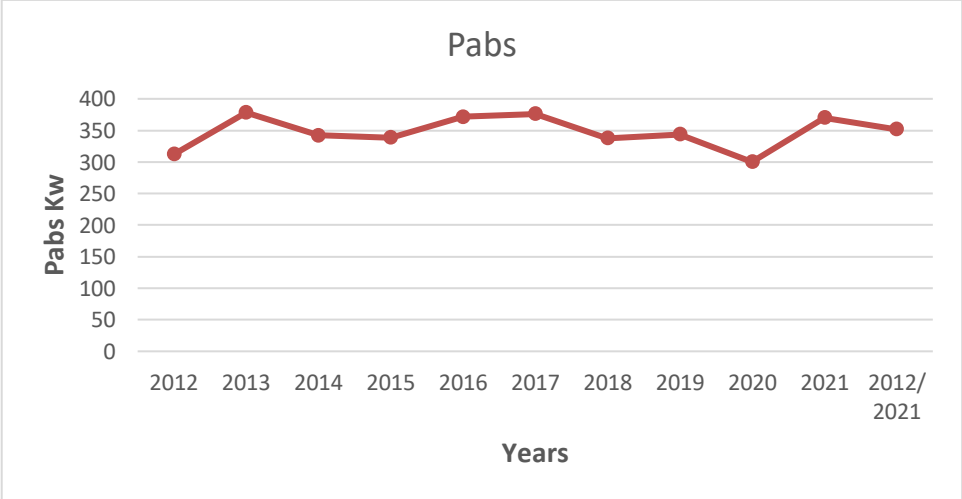

Figure III.13: The result of Power absorbed of 173m height.

3- Average maximum recoverable power

The average power during a unit of time and in the surface A depends on the speeds V0, V1, and V2, on the theorem of Betz finds with us the following law:

$$P = \frac{1}{2} \rho A V_1 (V_0^2 - V_2^2)$$

$$P_{max} = \frac{16}{17} P_{the}$$

16/27 equals 0.59 is the Betz limit

Table III.14: Pmax and Pthe results of the new height

Year	2012	2013	2014	2015	2016	2017	2018	2019	2020	2021	2012/ 2021
Pthe	499,81	605,71	547,98	542,41	594,70	602,72	540,65	550,39	480,54	592,58	563,73
Pmax	296,18	358,93	324,72	321,42	352,41	357,16	320,39	326,15	284,76	351,15	334,064

And we explain the results in this curve for the years:

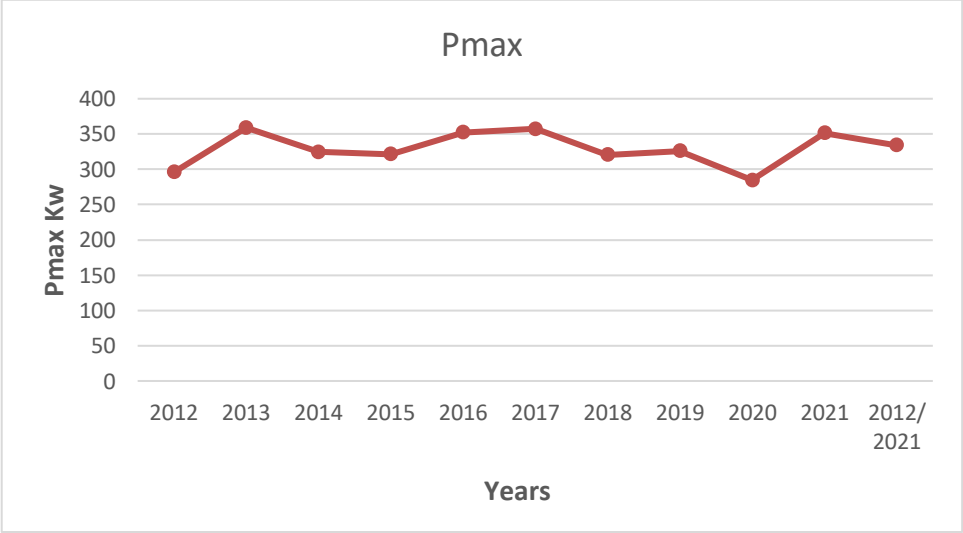

Figure III.14: Average maximum recoverable wind power for each year and over 10 years for height 173m.

The difference between the two maximum power values and the theoretical power is small Because the maximum power value in 2013 is estimated at 358,9396 KW and the theoretical power in 2021 is estimated at 351,159 KW.

4- Average energy recoverable over one year of the new zone

The recoverable average power per unit of area A equal to 1 m^2 is given:

$$Pr = 0.37\ \overline{V}^3$$

However, the average recoverable energy density, symbolized by $\overline{E}$, expressed as the relation over one year is equal to:

$$\overline{E} = Pr\ \Delta t = 0.37 \text{ x } 24 \text{ x } 365 \text{ x } \overline{V}^3\ [KWh/m^2]$$

Table III.15: Average cubic hour of wind Average recoverable capacity, recoverable energy of new height

Year	$\overline{V}^3$	Pr	E
2012	376,7463497	139,3961494	1221110,269
2013	456,5715969	168,9314909	1479839,86
2014	413,056497	152,8309039	1338798,718
2015	408,8570253	151,2770994	1325187,39
2016	448,2727069	165,8609016	1452941,498
2017	454,3175314	168,0974866	1472533,983
2018	407,5372029	150,7887651	1320909,582
2019	414,8746044	153,5036036	1344691,568
2020	362,2245062	134,0230673	1174042,069
2021	446,6745637	165,2695886	1447761,596
2012/2021	424,930255	157,2241944	1377283,943

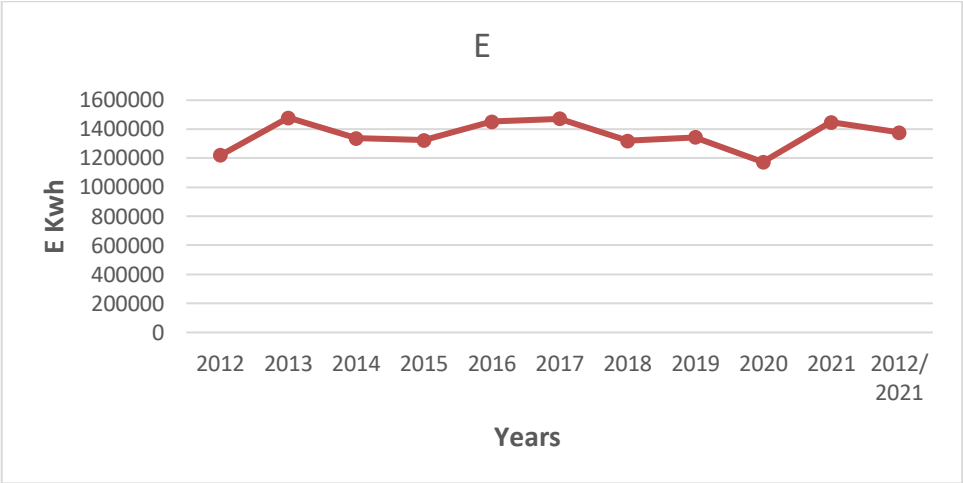

Figure III.15: Average recoverable energy for each year and over 10 years of height 173m.

Over 10 years, the average recoverable energy was significant, with its peak estimated at 1479839,86Kwh in 2013, and the lowest value estimated at 1174042,069Kwh in 2020.

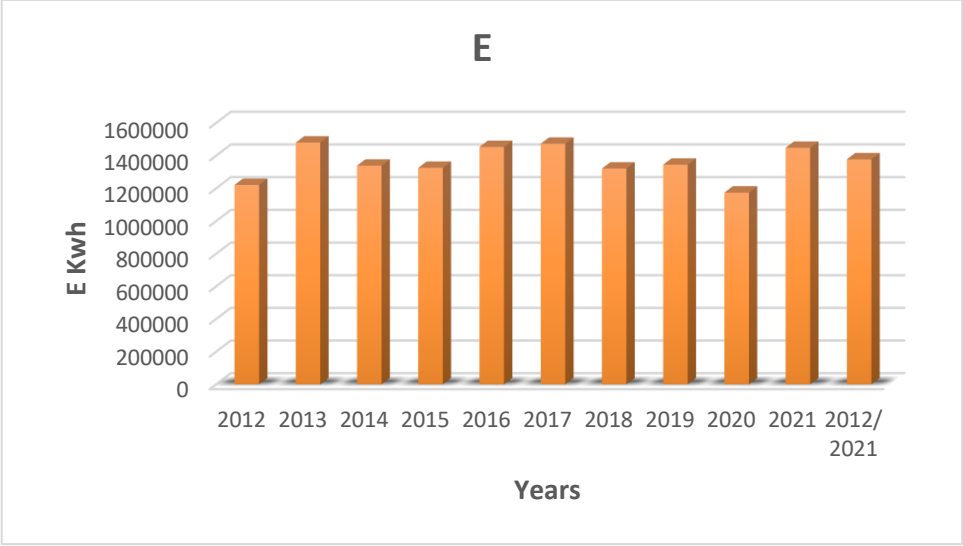

Figure III.16: Average recoverable energy for each year and over 10 years of the new zone.

Over 10 years, the average recoverable energy was significant, with its peak estimated at 1479839,86 Kwh in 2013, and the lowest value estimated at 1174042,069 Kwh in 2020.

5- Useful force for wind turbine

For each wind turbine unit, the factory provides us with three technical criteria for the speed required to operate them, namely:

- **V_D startup speed**

This is the speed at which wind turbines begin to produce power. Below this threshold, there is no power for wind turbines.

- **Nominal Speed Vn**

This is the speed at which wind turbines reach the maximum power production. This threshold remains constant until the cutting speed.

- **The cut-off speed VC**

Wind turbines stop creating electricity at this speed due to automatic blade stoppage for safety reasons. Energy calculation is not affected by speeds exceeding V_C.

$$P = \frac{1}{2}\rho A V\mathrm{n}^3$$

$$\mathrm{V_n} = \begin{cases} 0{,}67\bar{v} \\ 0{,}79\bar{v} \end{cases}$$

Using this data, we can create a table that shows the nominal speeds at the station, as well as the efficiency [0.3 to 0.5] for each year. With this information, we can calculate the average useful wind power:

$$P = \frac{1}{2}\rho V n^3$$

Table III.16: Nominal speed and useful power as a function of machine efficiency [0.3 to 0.5] for each year

Year	$\bar{V}$	Vn	Pu
2012	5,833449	[3,90841_4,60842]	[36,5685_121,586]
2013	6,219355	[4,16697_4,91329]	[44,3166_147,347]
2014	6,015138	[4,03014_4,75196]	[40,0929_133,304]
2015	5,994683	[4,01644_4,7358]	[39,6853_131,949]
2016	6,181443	[4,14157_4,88334]	[43,5111_144,669]
2017	6,209104	[4,1601_4,90519]	[44,0978_146,62]
2018	5,988226	[4,01211_4,7307]	[39,5572_131,523]
2019	6,02395	[4,03605_4,75892]	[40,2693_133,891]
2020	5,757514	[3,85753_4,54844]	[35,1589_116,899]
2021	6,174088	[4,13664_4,87753]	[43,356_144,153]
2012/2021	6,072231	[4,06839_4,79706]	[41,2454_137,136]

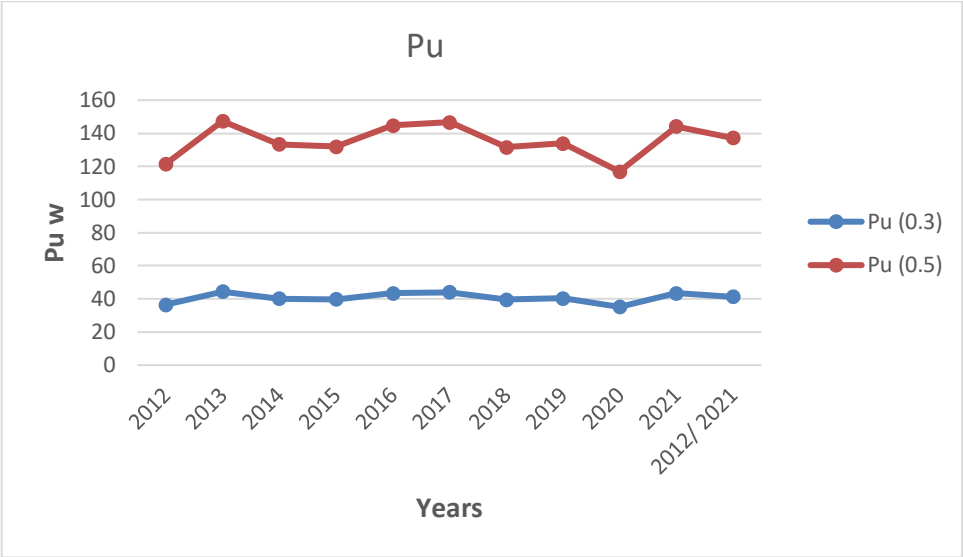

Figure 17: Variation in useful power.

The difference between the two values of the useful powers, the first value is between [36,5685W_44,3166W] and the second is limited to [116,899W to 147,347W], and the average value of the useful power is equal to 41,2454W in the case of machine efficiency is 0,3 and the average value of the useful power is equal to 137,136W in the case efficiency of the machine is 0.5.

III.4. Study of photovoltaic power

In this study we selected the Ouargla area, to complete a solar photovoltaic power plant because it has excellent solar radiation. We also selected the solar panels for the elhdjira area. This is due to the convergence of the climatic features of the two regions. In order to complete this study, we selected the website PHOTOVOLTAIC GEOGRAPHICAL INFORMATION SYSTEM to simulate this station.

III.4.1. Photovoltaic geographical information system (PVGIS)

The European Photovoltaic Geographical Information System (PVGIS) is a free online tool developed by the European Commission's Joint Research Centre. It provides data and information on the solar energy potential for photovoltaic systems across Europe, based on satellite data and meteorological information. PVGIS helps users estimate the electricity production of photovoltaic systems in different locations.

It also provides PVGIS time series for courier, daily or monthly values of solar radiation at the specified location. This information can be used to identify the solar radiation available to design solar energy systems.

PVGIS has a set of data seeking nine climate variables throughout the usual year, which can be used in built energy calculations.

Its Website: http://re.jrc.ec.europa.eu/pvgis/apps4/pvest.php?map=africa&lang=fr

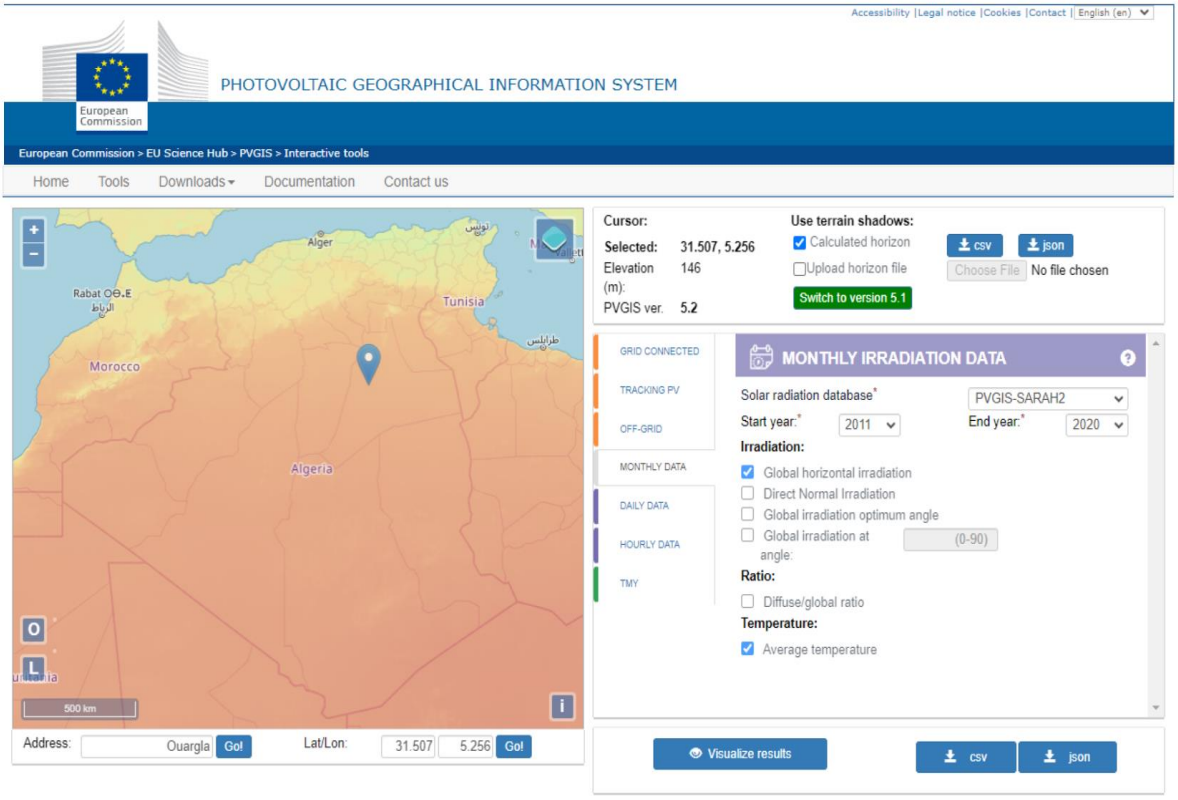

Figure III.18: Photovoltaic geographical information system (PVGIS) website

III.4.2. Solar radiation time difference

Assessing the importance of solar radiation in a given location, it is necessary to calculate the average temperature over a period of at least 10 years. This provides an indication of the heat conditions at that location. In addition, radiation patterns fluctuate throughout the season and year. Understanding these differences is critical to sizing solar energy systems to meet changing energy requirements. Annual differences are analyzed through daily studies.

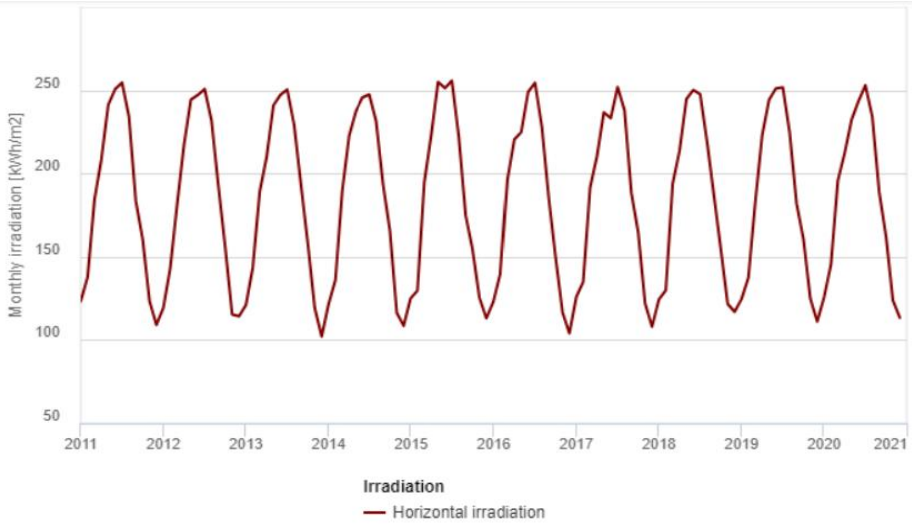

Figure III.19: Curve of Monthly solar irradiation of Ouargla.

The curve represents changes in radiation intensity in the Ouargla region over the course of 10 years from 2011 to 2020, where we note that this area is characterized by high radiation intensity, which makes it have a distinct solar energy. The radiation intensity reached 255kwh/m2 during 2015. The lowest value was recorded during December 2014 at 102kwh/m2.

III.4.3. Average monthly temperature

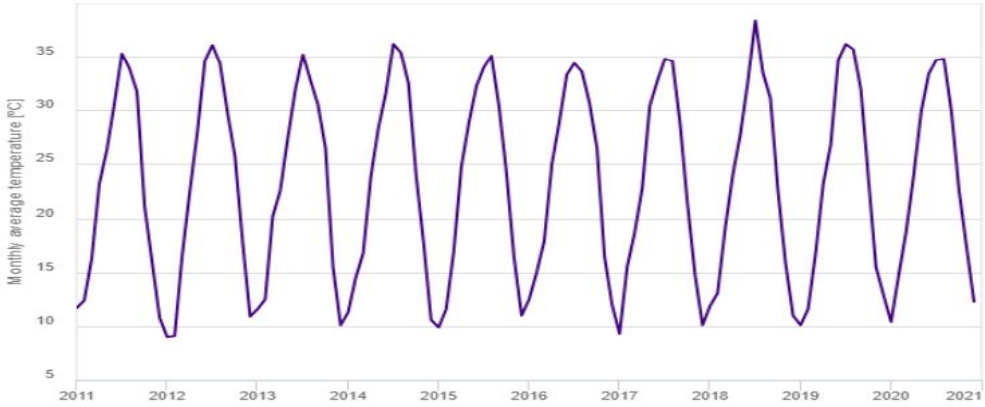

Figure III.20: Curve of Monthly average temperature

The curve represents temperature changes in the Ouargla region over the course of 10 years from 2011 to 2020 where we note that this area is characterized by high heat intensity reaching 38.7 °C as its highest value during 2018 and as the lowest value was recorded in 2012 with a capacity of 9 °C.

III.4.4. PVGIS-5 estimates of solar electricity generation

Solar electricity generation PVGIS-5are estimated based on different inputs such as latitude/longitude, slope angle, photovoltaic technology, in-plane radiation, system size, and

losses. In this case (latitude/longitude: 31.507, 5.256), using a PVGIS-SARAH2 database with crystal silicon photovoltaic technology and 0.25 kWh system depending on the characteristics of the elhdjira region's solar panels Annual power production is estimated at 620.1 kilowatts per hour for one solar panel, equivalent to 74 million kwh for more than 120,000 solar panels with annual irradiation within the aircraft of 3246.94 kwh/m^2.

III.4.4.1. Monthly energy output from tracking PV system

Table (III.17) presents data on monthly electricity production and total global radiation received by the system, in addition to standard deviations of electricity production. Values are given for each month from January to December.

"Ir _ SD" refers to the average monthly electricity production in kilowatt hours, the average monthly global total radiation per m^2 min kilowatt hours/m2, and the standard deviation of the monthly electricity production in kilowatt hours due to year to year-difference.

Data indicate seasonal variability in both electricity production and global radiation received by the system.

The highest monthly average electricity production recorded in July (57.5 Kwh) per plate is equivalent to (6.9 million Kwh) for the plant, while the lowest in December (44.4 Kwh) for a plate is equivalent to (5.32 million Kwh) for the plant.

The highest average monthly total of global radiation was recorded in July (320.7 kWh/m^2), indicating a higher solar potential during that month.

Standard deviations of electricity production vary across months, indicating different levels of variability or consistency in production throughout the year.

In summary, this table represents a dataset showing how monthly electricity production relates to the total global radiation received by the system throughout the year where B was estimated. (74 million Kwh) compared to the elhdjira region's system, where production reached (52 million kWh) This is due to the strength of radiation intensity in the Ouargla region, providing insight into seasonal trends and volatility in power generation.

Table III.17: Monthly energy output from tracking PV system

Month	E	Ir	SD
January	47.8	233.5	4.5
February	47.2	235.1	3.0
March	56.7	289.5	3.0
April	56.6	295.9	2.5
May	56.3	301.2	3.0
June	55.9	305.3	2.6
July	57.5	320.7	1.8
August	55.2	306.6	2.3
September	49.5	267.8	2.1
October	48.4	252.8	3.7
November	44.5	223.2	2.9
December	44.4	215.6	2.9

E: Average monthly electricity production from the defined system [kWh].

Ir: Average monthly sum of global irradiation per square meter received by the modules of the given system [kWh/m²].

SD: Standard deviation of the monthly electricity production due to year-to-year variation [kWh].

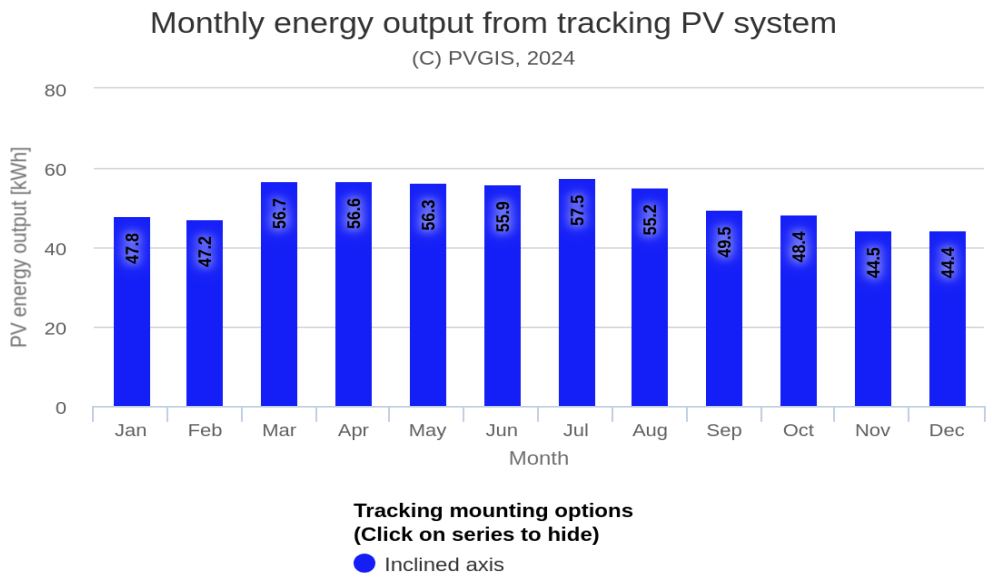

Figure III.21: Diagrams of the monthly energy output from tracking PV system

III.4.4.2. Monthly in-plane irradiation for tracking PV system

Figure (III.22) shows diagrams of the average monthly total of global radiation per m^2 received by kwh/m2 units of this system. Global radiation refers to the total solar radiation received on a horizontal surface, including direct sunlight and widespread radiation.

The chart shows the amount of solar energy received each month throughout the year. Values range from 215.6 kWh/m2 in December to 320.7 kWh/m2 in July, indicating differences in solar availability based on seasonal changes and geographical location.

These values are critical for assessing the potential power generation capacity of solar panels or systems at this site. Higher values indicate greater availability of solar energy, which may affect the efficiency and production of solar energy systems.

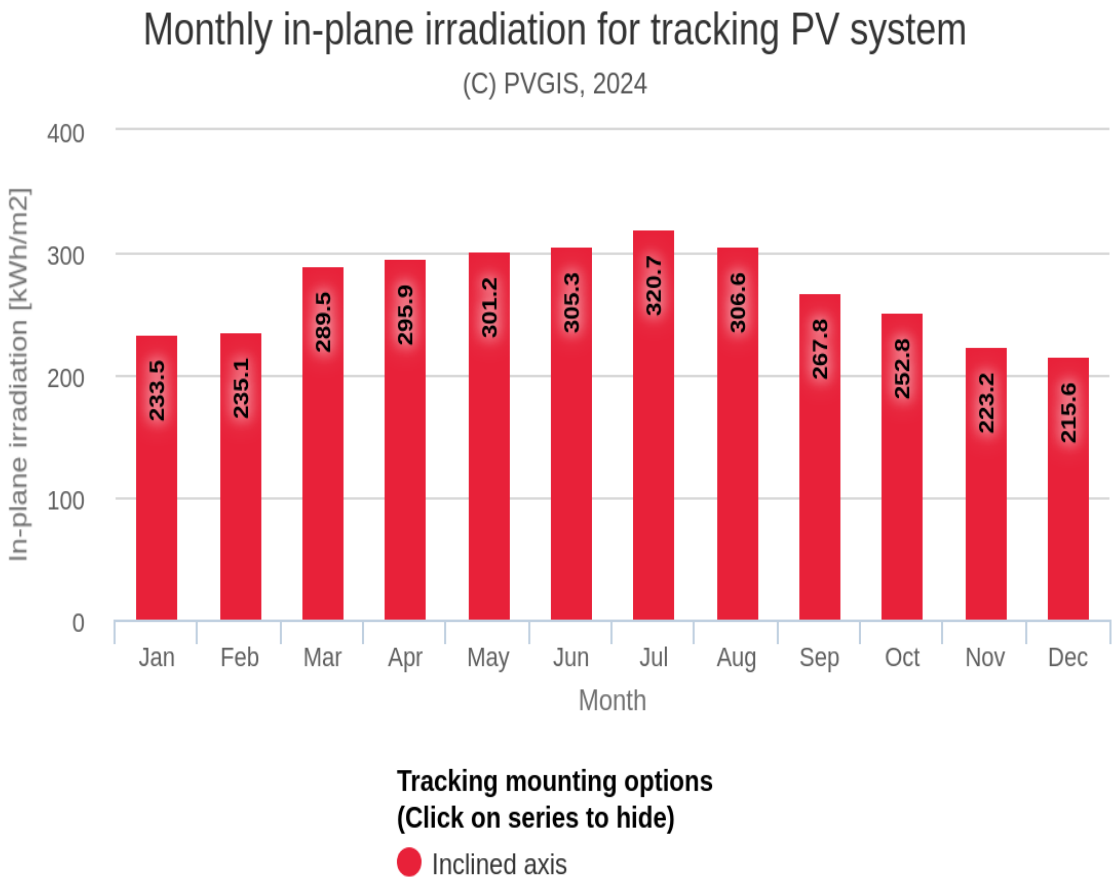

Figure III. 22: diagrams of the average monthly total of global radiation per m2

III.5. Conclusion

Based on the study conducted in the Ouargla region, analyzing wind power dynamics using statistical models like Weibull's law, Weibull's hybrid law, and Rayleigh's law revealed interesting findings. The histogram analysis of occurrence frequency distributions provided insights into the temporal variation of wind speeds. By examining the variation of Weibull parameters, we gained a deeper understanding of wind patterns in the region.

Furthermore, the exploration of photovoltaic power in Ouargla using the Photovoltaic Geographical Information System (PVGIS) allowed us to assess solar radiation time differences and average monthly temperatures. The PVGIS-5 estimates of solar electricity generation, taking into account the specific properties of solar panels in the Al-Hadjira region, provided valuable statistics on solar energy potential.

Chapter IV

Optimization of Hybrid PV/Wind Energy System Using Genetic Algorithm (GA)

IV.1. Meteorological and load data

The proposed method is the optimal size of the hybrid wind PV system for typical farm electrification near the latitude of 31.507° N, longitude 5.256° W, time zone: GMT + 1, Elevation: 173 m. The proposed method requires long-term recorded wind speed and solar radiation data for each day of each month for one year or more, as explained in Chapter III. Figure 5 shows the summary of the typical farm load within 12 months of the year.

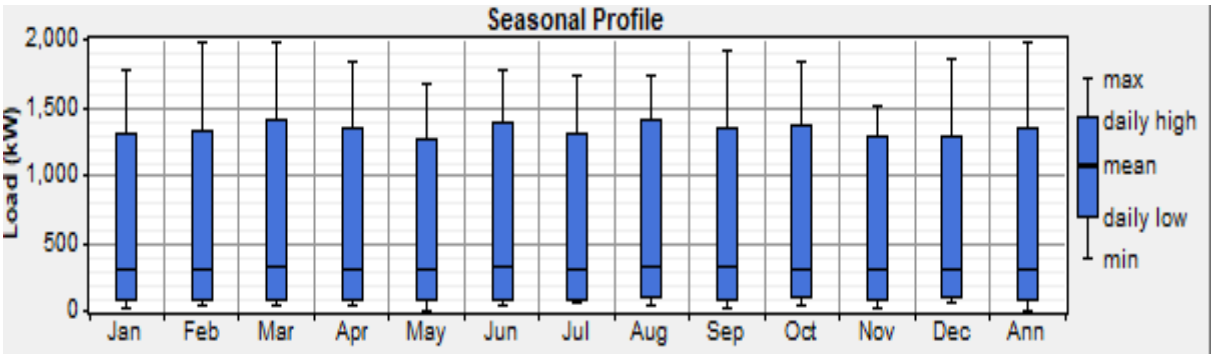

Figure IV.1: Load profile for all months of a typical year

IV.2. Problem formulation

The primary focus in designing the proposed P_{Vwind} hybrid energy system is to optimize the sizing of each participating component to effectively meet the load requirements while being cost-efficient and reliable. Thus, the system components are assessed with two main considerations:

1. Minimizing the total cost (CT) of the system.
2. Ensuring the load is served within specified reliability criteria.

To achieve this, the objective function (CT) is aimed at minimizing the overall cost, which is derived from the summation of several factors: the present worth (PWs) of equipment salvage values, annual operation and maintenance expenses, initial capital investments, and replacement costs of system components. Therefore, the objective function can be defined as [66]:

$$min.\,CT = \sum_{k=1}^{3} I_k + R_{pwk} + OM_{pwk} - S_{pwk} \qquad \textbf{(IV.1)}$$

The index "k" represents the components in the system, including PV (photovoltaic), wind, and batteries. The variables I_k, R_{PWk}, OM_{PWk}, and S_{PWk} represent the capital or initial investment, replacement cost, operation and maintenance costs, and salvage value of each component "k" respectively.

To minimize the objective function CT, certain constraints need to be met to ensure that the load is served according to specific reliability criteria. These constraints are related to the reliability and performance of the system in delivering power to meet the load requirements.

IV.2.1. Basic economic considerations

As indicated by equation (IV.1), we require the present worth (PWs) of certain annual payments and salvage values. Therefore, assuming a project lifespan of N years, an interest rate of r, and an inflation rate of j (reflecting price increases), the PWs can be computed as follows:

IV.2.1.1. Salvage value

If a component currently holds a salvage value of S ($), it is anticipated that the salvage value of the component will be S(1+j) N in N years, assuming the component is utilized starting now.

PW of $S(1+j)^N$ taking the interest rate into consideration, is [66]

$$S_{pw} = \frac{s.(1+j)^N}{(1+r)^N} \quad \textbf{(IV.2)}$$

Les: fac1 = $(1+ j)^N / (1+ r)^N$, then $S_{PWk} = S_k$. fac1, for all components k in the hybrid system.

IV.2.1.2 Operation and Maintenance

If the annual operating and maintenance cost of a component is OM ($/year), it typically increases each year at a rate that may differ from the general inflation rate. Therefore, with an escalation rate es, the operation and maintenance costs at year y will be $OM(1+es)^y$, with a present worth of the annual operating and maintenance cost of a component is OM, it tends to increase each year at a rate that may differ from the general inflation rate. Therefore, with an escalation rate es, the operation and maintenance costs at year y will be $OM(1+es)^y$. and having a PW of [66]:

$$OM(1+es)^y / (1+r)^y \quad \textbf{(IV.3)}$$

The summation of the PWs of all the annual payments are, thus, given by:

$$OM_{pw} = OM \sum_{y=1}^{N} \frac{(1+es)^y}{(1+r)^y} = OM.fac2 \quad \textbf{(IV.4)}$$

Where fac2 represents a geometric progression, and is given by:

$$\text{fac2} = \left(\frac{1+es}{r-es}\right) \cdot \left[1 - \left(\frac{1+es}{r-es}\right)^{N}\right], r \neq es \ , r = es \quad \textbf{(IV.5)}$$

N, Therefore, OM_{PWk} equals OM_k for all components k in the system. It is important to apply the same approach to other PW calculations when analyzing each component.

IV.2.2. Total cost coefficients

IV.2.2.1 The PV array

Given the design variable for the PV array is the total area APV in square meters, this area is limited by available space and budget. The initial investment

$$I_1 = \alpha_{PV}. A_{PV} \quad \textbf{(IV.6)}$$

multiplied by A_{PV}. Assuming the project lifespan aligns with the PV array's lifetime, replacement costs are negligible (R_{PW1}=0). With an annual operation and maintenance cost of α_{OMPV} per square meter per year, the total yearly cost is $OM1 = \alpha_{OMPV}. A_{PV}$.

Consequently, the global present worth of yearly operation and maintenance costs would be calculated.

$$OM_{PW1} = \alpha_{OMPV}. A_{PV}. \text{fac2} \quad \textbf{(IV.7)}$$

The salvage value can be found by multiplying the selling price per square meter SPV by the area APV, and the PW of the selling price would be [66]:

$$S_{PW1} = S_{PV}. A_{PV}. \text{fac1}$$

In summary, the PWs of the PV array costs are:

$$I_1 + R_{PW1} = \alpha_{PV}. A_{PV} = C_1. A_{PV} \quad \textbf{(IV.8)}$$

$$OM_{PW1} = \alpha_{OMPV}. A_{PV}. \text{fac2} = C_2. A_{PV}$$

$$S_{PW1} = S_{PV}. A_{PV}. \text{fac1} = C_3. A_{PV}$$

IV.2.2.2. The wind turbine

The design factor influenced by the wind turbine is the total rotor swept area (Aw) in square meters, limited by space and project budget. If Aw is fixed, designers must allocate it among multiple turbines. Wind turbine lifespan (Lw) is typically shorter than that of a PV array (N), possibly requiring additional purchases before project completion. The number of wind turbine purchases within N years is Xw=N/Lw (rounded up). With αw as the current price in $/m2, the

price at year y would be $\alpha w(1+es)^{y}$ with a present worth (PW) of $\alpha w(1+es)^{y}/(1+r)^{y}$. Therefore, the PW of all initial and replacement wind turbine investments is.

$$I_2 + R_{PW2} = \alpha_w . A_w \sum_{x=1}^{xw} \frac{(1+es)^{(x-1)\cdot L_w}}{(1+r)^{(x-1)\cdot L_w}} \quad \textbf{(IV.9)}$$

Where es represents the escalation rate, r denotes the interest rate, Lw signifies the lifetime of wind turbines, and Xw indicates the frequency of wind turbine purchases. In cases where Xw is set to 1 (i.e., wind turbine lifespan equals or exceeds that of the entire project), RPW2 equals 0 and I2 equals αw. Aw (as turbines are procured once at project onset). Given an annual operation and maintenance cost of α_{OMW} ($/m^2/year), the total yearly operation and maintenance cost would be $OM_2 = \alpha_{OMW}. A_w$. The present worth (PW) of all annual costs would be:

$$OM_{PW2} = \alpha_{OMw} . A_w . fac2 \quad \textbf{(IV.10)}$$

The wind turbine's residual value is expected to decline steadily from αw ($/m^2) to Sw ($/m^2) over its operational lifespan Lw. If the project ends prematurely, the turbines can be sold at a higher value, Spw ($/m^2), exceeding Sw.

$$s_{pw} = \left(\frac{s_w - a_w}{L_w}\right) \cdot Years + a_w \quad \textbf{(IV.11)}$$

The term "years" represents the duration of operation from the installation of the final wind turbine until the project's end. Consequently, the present worth (PW) of all salvage values is determined by:

$$S_{Pw2} = S_w \cdot A_w \sum_{x=1}^{xw-1} \left(\frac{(1+j)^{x\cdot L_w}}{(1+r)^{x\cdot L_w}}\right) + S_{Pw} \cdot A_w \left(\frac{(1+j)^N}{(1_+ r)^N}\right) \quad \textbf{(IV.12)}$$

If the project's lifespan N is a multiple of the wind turbines' lifespan Lw, then Equation (IV.12) can be simplified.:

$$S_{Pw2} = S_w \cdot A_w \sum_{x=1}^{xw} \left(\frac{(1+j)^{x\cdot L_w}}{(1+r)^{x\cdot L_w}}\right) \quad \textbf{(IV.13)}$$

In summary, the PWs of the wind turbine are:

$$I_2 + R_{PW2} = \alpha_w . A_w \sum_{x=1}^{xw} \frac{(1+es)^{(x-1)\cdot L_w}}{(1+r)^{(x-1)\cdot L_w}}$$

$OM_{PW2} = \alpha_{OMw}. A_w. fac2 = C_4. A_W$

$$S_{Pw2} = S_w \cdot A_w \sum_{x=1}^{xw-1} \left(\frac{(1+j)^{x \cdot Lw}}{(1+r)^{x \cdot Lw}}\right) + S_{Pw} \cdot A_w \left(\frac{(1+j)^N}{(1_+ r)^N}\right) = C_6. A_W$$

IV.2.2.3. The storage batteries

The design factor for storage batteries is their capacity (C_b) in kilowatt-hours. Unlike wind turbines, the battery's lifetime (L_b) is expected to be shorter than the project's overall lifespan. Therefore, batteries with capacity C_b need to be bought periodically every L_b. The total present worth (PW) of capital and replacement investments in batteries can be calculated as follows [66]:

$$I_3 + R_{PW3} = \alpha_b. A_b \sum_{x=1}^{xb} \left(\frac{(1+es)^{(x-1)\cdot L_b}}{(1+r)^{(x-1)\cdot L_b}}\right) \quad \textbf{(IV.14)}$$

L_b represents battery lifespan, X_b denotes the frequency of battery purchases over the project's duration (X_b=N/L_b, rounded up), and αb stands for the capital cost in ($/kWh). The batteries' salvage value is considered insignificant. Given an annual operation and maintenance cost of α_{OMb} ($/kWh/year), the total yearly operation and maintenance cost equals $OM3=\alpha_{OMb.} C_b$. The present worth (PW) of all yearly expenses would be:

$OM_{PW3} = \alpha_{OMb}. C_w. fac2$

In summary, the PWs of the battery costs are:

$$I_3 + R_{PW3} = \alpha_b. A_b \sum_{x=1}^{xb} \left(\frac{(1+es)^{(x-1)\cdot L_b}}{(1+r)^{(x-1)\cdot L_b}}\right) = C_7.C_b \quad \textbf{(IV.15)}$$

$OM_{PW2} = \alpha_{OMb}. C_b. fac2 = C_8. A_b,$

$S_{pw} = 0$

IV.3. System modeling

Modeling is a crucial preliminary stage before optimal sizing in any phase. In the suggested PV-wind hybrid system featuring a storage battery, three main components are integrated:

the PV array, the wind turbine generator (WTG), and the battery storage.

IV.3.1. modeling of the PV array

The power output (P_{PV}) of a photovoltaic (PV) array with efficiency η_{PV} and area A_{PV} (m^2), exposed to solar insolation R (kW/m^2) on an inclined surface, can be expressed as.

$$P_{pv} = R.\ A_{PV}.\ \eta_{PV}$$

IV.3.2. Modeling of the WTG

A wind turbine generator (WTG) generates power Pw above the cut-in speed Vci and stops at the cut-out speed Vco. Between the rated wind speed Vr and Vco, it produces rated power Pr. In the range where Vci < V < Vr, the WTG's output power follows the cube law. These equations are utilized to simulate the WTG.

$$P_w = \begin{cases} P_r \cdot \left(\frac{V^3 - V_{ci}^3}{V_r^3 - V_{ci}^3}\right), & V_{ci} \le V \le V_r \\ P_r, & V_r \le V \le V_{co} \\ 0, & V_{co} \le V \text{ or } V \le V_{ci} \end{cases} \qquad \textbf{(IV.17)}$$

Where: $P_r = \frac{1}{2} Cp\ \rho_{air} A_W\ V_r^3$

In the equation provided, Cp represents the power coefficient, ρair is the air density, and Aw stands for the rotor swept area.

IV.3.3. Modeling of the storage battery

At each time t, the battery's charge level (SOC) is influenced by the prior SOC at time t-1 and the energy dynamics between t-1 and t. When the battery is being charged (PB>0), the SOC at time t is determined by the flow of power into the battery:

$$SOC\ (t) = SOC\ (t\text{-}1) + \frac{P_1(t)\ X\ \Delta t}{1000\ X\ C_b} \qquad \textbf{(IV.18)}$$

When Δt represents the simulation time step (fixed at 1 hour) and Cb denotes the total nominal battery capacity in kilowatt-hours, if the battery power exits the battery (PB<0), it indicates discharging. Hence, the current state of charge of the battery at hour t can be defined as:

$$SOC\ (t) = SOC\ (t\text{-}1) + \frac{P_1(t)\ X\ \Delta t}{1000\ X\ C_b} \qquad \textbf{(IV.19)}$$

To prolong the battery life, the battery should not be over-discharged or overcharged. This means that the battery SOC at any hour t must be subject to the following constraints:

$(1 - DODmax) \leq SOC(t) \leq SOCmax$

Where DODmax and SOCmax are the battery's maximum permissible depth of discharge and SOC, respectively.

IV.4. System reliability

First of all, it is assumed, in this work, that the peak power trackers, the battery charger/discharger, and the distribution lines are ideal (i.e., they are lossless). Also, it is assumed that the inverter efficiency ηinv is constant; the battery charge efficiency ηb is set to equal to the manufacturers' round-trip efficiency, and the battery discharging efficiency is set to be 1. The total generated power by the PV array and WTG for hour t, Pg(t), can be expressed as

$$Pg(t) = P_{PV}(t) + P_W(t) \quad \textbf{(IV.20)}$$

It is to be noted that the desired load demand at any hour t, PL ∗ (t), may or may not be satisfied according to the corresponding values of the total generated power Pg(t) and the available battery SOC(t) at that hour. The proposed energy management of the PVwind hybrid system can be summarized as follows:

- If [Pg(t)>PL ∗ (t)/ηinv] and [SOC (t –1) <SOCmax]

then satisfy the load and charge the battery with the surplus power:

[PB(t)= (Pg (t)− PL ∗(t)/ηinv) ηb].

Afterwards, check if: [SOC(t)≥SOCmax] then stop battery charging, set SOC(t)=SOCmax, and dump the surplus power

(PDump(t)=Pg(t) − [PL ∗(t)/ηinv+1000×Cb/Δt×ηb× (SOCmax−SOC(t−1))]).

- If [Pg(t)>PL∗(t)/ηinv] and [SOC(t–1) ≥SOCmax] then stop charging the battery, satisfy the load,

and dump the surplus power [PDump(t)= Pg(t)−PL∗(t)/ηinv].

- If [Pg(t) =PL∗(t)/ηinv] then satisfy the load only.
- If [Pg(t)<PL ∗(t)/ηinv] and [DOD(t–1) <DODmax] then satisfy the load by discharging the battery [using Equation (21)] to cover the deficit in load Power [PB(t)= PL∗(t)/ηinv - Pg(t)]. Afterwards,

check if [DOD(t)≥DODmax] then stop battery discharging, set DOD(t)=DODmax, and calculate

the deficit in load power (Pdeficit(t)=PL∗(t)-[Pg(t)+1000×Cb/Δt×(SOC(t−1) −(1−DODmax))] ηinv.

- If [Pg(t)<PL∗(t)/ηinv] and [DOD(t–1) ≥DODmax] then stop battery discharging and

[Pdeficit(t)= PL∗(t)− Pg(t). ηinv.

As it is assumed, in this work, the simulation step time Δt is equal to 1 h and the generated PV and wind powers are constants during Δt then, the power is numerically equal to the energy within Δt.

The input data for this program consist of mean hourly global insolation on a tilted array R, mean hourly wind speed Vi, and desired load power during the year PL∗. Note, here, that for every configuration of the proposed PV-wind hybrid system, this program simulates the system. Three additional bounds should be imposed on the sizes of the system components.

VI.5. Final form and GA optimization

At this stage, the optimization problem can be written in its final form as follows:

1. Minimize the cost function $C_{T:}$

$$(C_1+C_2-C_3).\ APV+\ (C_4+C_5-C_6).\ A_W\ +\ (C_7+C_8).\ Cb$$

2. Subject to:

$$\begin{aligned} 0 \leq A_{PV} \leq A_{PVmax} \\ 0 \leq Aw \leq A_{w\ max} \\ 0 \leq C_b \leq C_{b\ max} \end{aligned} \qquad \textbf{(IV.21)}$$

To solve the optimization problem mentioned above, we propose using a Genetic Algorithm (GA) with an elitist approach. This means that the best individual from each generation is directly copied to the next generation without any changes. We will utilize the Genetic Algorithm Code in MATLAB to implement this approach.

To use the GA, we need to write an M-file (MATLAB code) that computes the objective function (also known as the fitness function). This M-file should accept a vector (individual) with the same length as the number of independent variables in the objective function and return the corresponding scalar value of the objective function (cost). In this case, the individual consists of three variables: A_{PV}, Aw, and C_b.

The GA follows a flowchart in Figure (IV.2) to find the optimal solution. It starts by randomly selecting individuals from the current population as parents and uses them to produce children for the next generation through selection, crossover, and mutation operations. The population evolves over successive generations towards an optimal solution.

In our implementation, we set the population size to 100 individuals. We use a stochastic uniform function for selection, a scattered crossover function with a crossover probability of 80%, and an adaptive feasible mutation function with a probability rate of 1%. Additionally, we include an elite individual in each generation.

It's important to note that you can directly enter any additional bounds or constraints into the GA code. These bounds will ensure that the variables A_{PV}, Aw, and C_b satisfy the specified constraints during the optimization process.

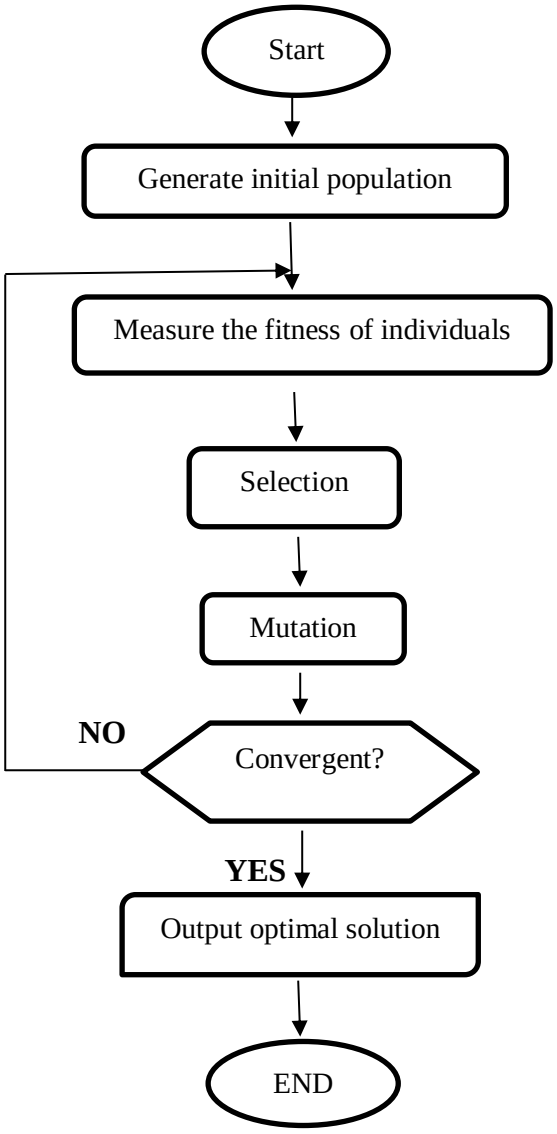

Figure IV.2: Flow-chart of the Genetic Algorithm (GA) [66]

IV.6. Results and Discussion

The formulated optimization problem of the PV-wind hybrid energy system is solved, in this work, by using the GA under MATLAB software, which may provide several potential solutions to the given problem. The choice of the final optimum solution is left to the system's designer.

The specifications and the related maintenance and installation costs of different wind turbines, PV panels, and batteries, which are input to the optimal sizing procedure, are listed in Tables (IV.1-IV.2 - IV.3).

The maintenance cost of each unit per year and the installation cost of each component have been set at 0-1% and 5-10% respectively of the corresponding cost. The lifetime of the Wind Turbine, PV panel is 20 years, and Battery is considered to be 5 years.

Since the tower heights of wind turbines affect the results significantly, a 55-meter-high tower at an elevation of 173m is chosen. The minimization of the system's total cost is achieved by selecting an appropriate system configuration. Table (IV.4), indicates the resulting optimum sizes of the different components included in the hybrid system. The corresponding fitness function optimization (i.e., minimization of the system cost in rupees) along the successive generations of the GA is shown in Figure (IV.1), which indicates that the system is optimized after forty iterations only.

The combination of PV and wind in a hybrid energy system reduces the battery bank and diesel requirements; therefore, the system's total cost is reduced. Table (IV.5) shows the cost that resulted from solving the formulated optimization problem by using the proposed GA-based technique using MATLAB software. Thus, Table (IV.5) indicates that the proposed GA-based technique is the best solution for optimizing this system. and this is because the GA is capable of converging to the global optimum solution instead of converging at a local optimum one.

Table IV.1: PV Array Data

Ppv (w)	250
Life Time of the PV Panel (years)	20
Installation Cost ($./m^2)	6
Operation and Maintenance Cost ($. /yr)	0.58

Table IV.2: Wind Turbine Data

Power Rating (KW)	850
V_r (m/s)	4
V_{ci} (m/s)	16
V_{co} (m/s)	25
Life Time of the WTG (years)	20
Installation Cost ($./m^2)	30.5
Operation and Maintenance Cost ($. /yr.)	8.5

Table IV.3: Battery Specifications

Nominal Capacity (Ah)	260
Voltage (V)	12
DOD (%)	80
Efficiency (%)	80
Life Time of the Battery (years)	5
Installation Cost ($./m^2)	10.21
Operation and Maintenance Cost ($. /yr.)	1.34

Table IV.4: Optimum sizes of the hybrid System.

A_{pv} (m^2)	A_W (m^2)	C_b (KWh)
18.89	2016.32	29.36

Table IV.5: Cost using GA

Technique Cost	**Cost ($)**
Genetic Algorithm (GA)	102,324.54

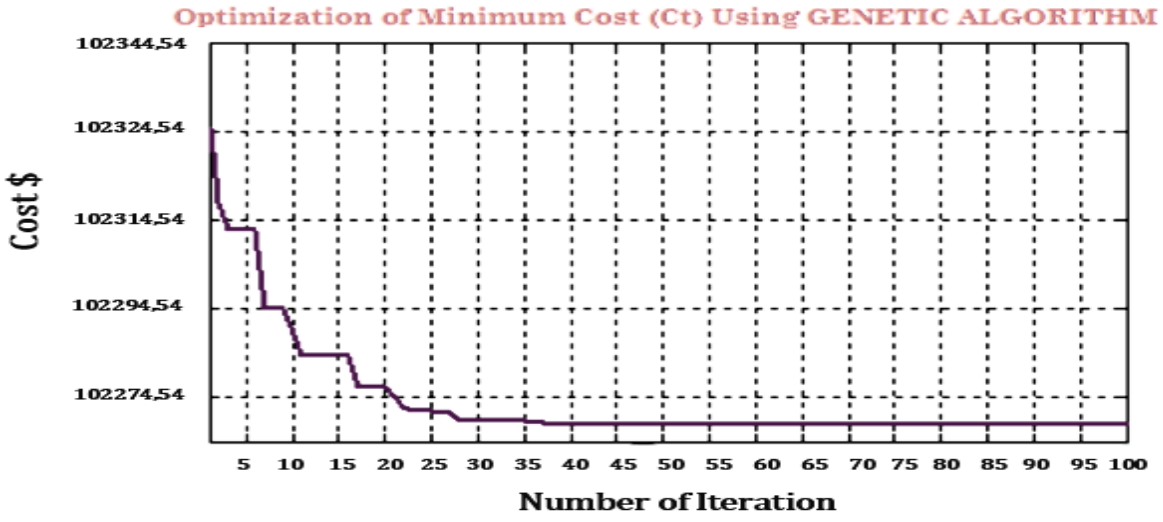

Figure IV.2: Optimization of the Objective function using GA

Figures (IV.3, IV.4, and IV.5) provide a visual representation of the generated solar photovoltaic power, wind power, and the total generated power of the recommended solar photovoltaic-wind hybrid system for each month throughout the year.

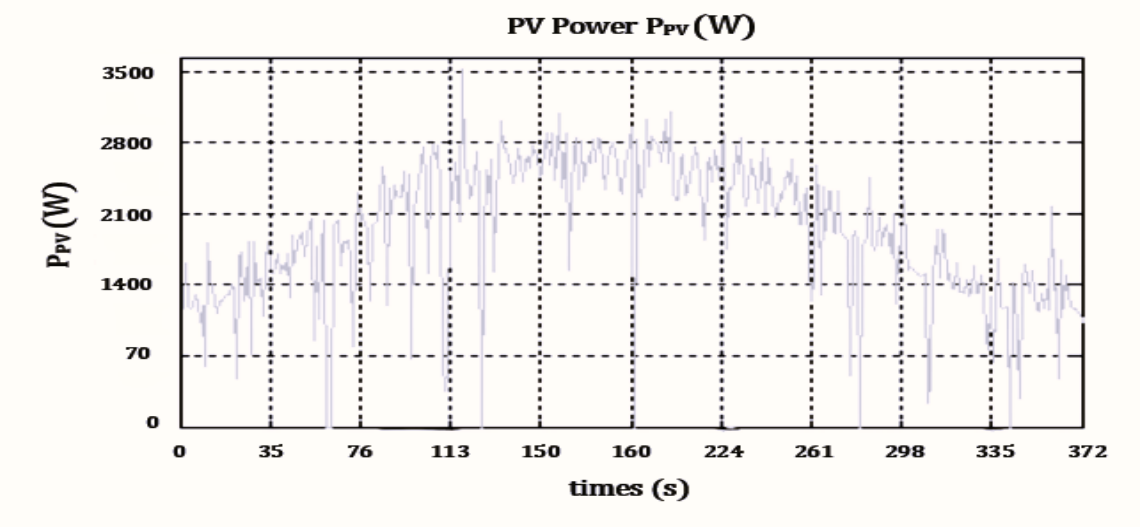

Figure IV.3: PV Power

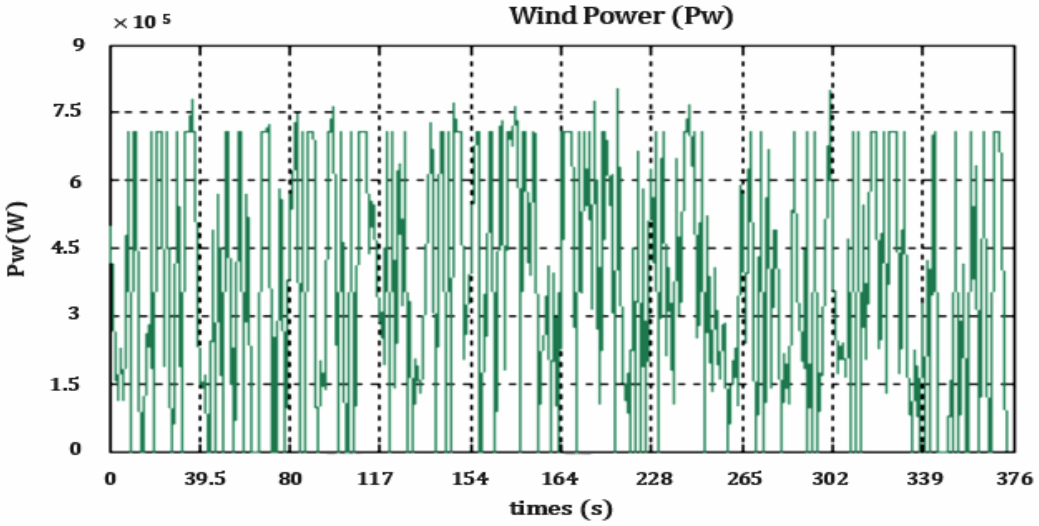

Figure IV.4: Wind Power

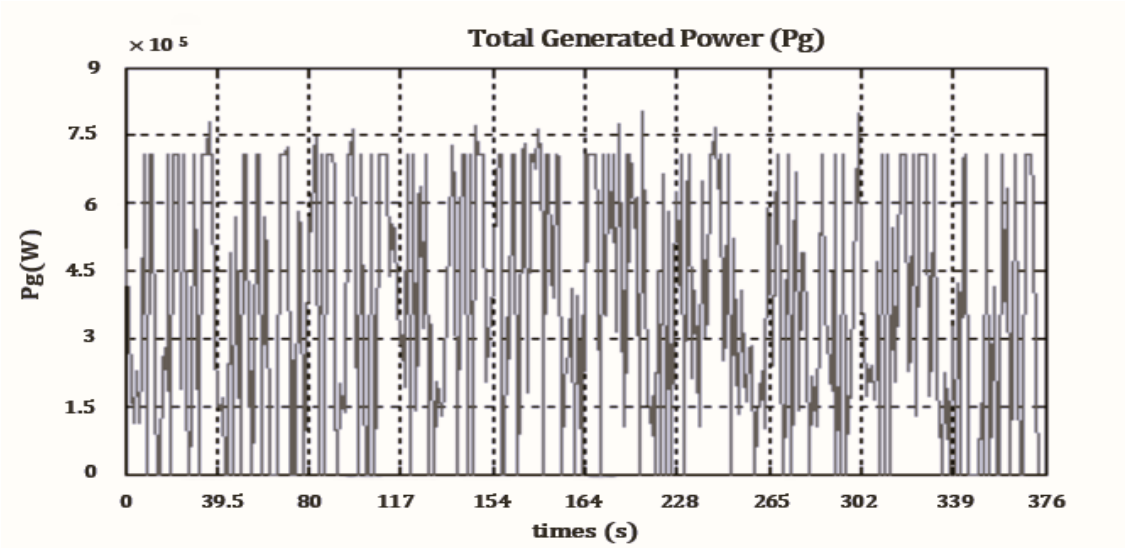

Figure IV.5: Total Generated Power

IV.7. Conclusion

This paper presents a genetic algorithm-based optimization technique for determining the optimal size of a proposed PV-wind hybrid energy system that includes a storage battery. The goal of this work is to minimize the total cost of the system components while ensuring a reliable power supply. The findings show that the genetic algorithm performs well in convergence and that the proposed technique is applicable for sizing the PV-wind hybrid energy system, standalone PV system, or standalone wind system. Moreover, this technique can be adapted to account for changes in insolation, wind speed, load demand, and initial costs of system components. Additionally, the results indicate that PV-wind hybrid energy systems offer the most cost-effective and dependable solution for powering remote areas.

Conclusion General

Conclusion general

At the conclusion of this study, we first carried out an analysis of the irregular speeds obtained from the National Bureau of Meteorology and analyzed the statistics of the region in which the agricultural investor is to be established. We also conducted a statistical analysis of the region's potential of solar and wind energy so that a 250w solar panel was tested so that we got an electric power of 57kwh during the month of Jar this year.

In terms of wind energy, we got 1479839kwh power during 2012 after a ten-year study, using a model of wind turbines with a maximum production capacity of 850kw.

Then we improved the previous models using an AI model and gave us the following results: the cost of accomplishing an electric plant to electrify a peasant investor was $102,324.54 with a production capacity of up to 7.5kwh.

Finally, this type of hybrid system meets the needs of the investor and increases it. From the point of view of the best solution to meet the power of any investor away from the electrical network, we recommend using this hybrid type to produce electricity.

References & Bibliography:

References & Bibliography:

[1] IEA (2021), Global Energy Review 2021, IEA, Paris https://www.iea.org/reports/global-energy-review-2021, Licence: CC BY 4.0.

[2] Ritchie, H., M. Roser, and P. Rosado, Energy. Published online at OurWorldInData. Org, 2020.

[3] IEA. International Energy Agency. Electricity Market Report 2023, https://www.iea.org/.

[4] IEA (2022), World Energy Outlook 2022, IEA, Paris https://www.iea.org/reports/world-energy-outlook-2022, Licence: CC BY 4.0 (report); CC BY NC SA 4.0 (Annex A).

[5] Solar Energy - National Geographic Society. https://www.nationalgeographic.org/encyclopedia/solar-energy/.

[6] Today in Energy - U.S. Energy Information Administration (EIA). https://www.eia.gov/todayinenergy/detail.php?id=50357.

[7] Today in Energy - U.S. Energy Information Administration (EIA). https://www.eia.gov/todayinenergy/detail.php?id=50357.

[8] N. YASSAA. Et al, Algeria Renewable Energy Resource Atlas 1st edition 2019, Centre de Développement des Energies Renouvelables, Mars 2019.

[9] Geothermal Electricity Production Basics | NREL. https://www.nrel.gov/research/re-geo-elec-production.html.

[10] Max Roser (2020) - "The world's energy problem" Published online at OurWorldInData.org.

[11] World Economic Forum- This is the state of world's energy - in charts -Aug 3, 2022.

[12] Z'hour, A., Stratégies d'approvisionnement en énergies fossiles des centrales électriques algériennes Perspectives et développements. Doctoral thesis (2018), Université de Batna 2. 2018.

[13] Khaider, B.K., G. Mohammed, and B. Meriem, Renewable Energy in Algeria Reality and Perspective. J. Inf. Syst. Technol. Manag, 2018. 3(10): p. 1-19.

[14] Hannah Ritchie, Max Roser and Pablo Rosado (2022) - "Energy". Published online at OurWorldInData.org.

[15] CENTRAL INTELLIGENCE AGENCY, The World Factbook: Algeria (2010), https://www.cia.gov/library/ publications/the-world-factbook/index.html.

[16] Harrouz, A., A. Temmam, and M. Abbes, Renewable energy in Algeria and energy management systems. International Journal of Smart Grids, ijSmartGrid, 2018. 2(1): p. 34-39.

[17] Zahraoui, Y., et al., Current status, scenario, and perspective of renewable energy in Algeria: a review. Energies, 2021. 14(9): p. 2354.

[18] Zafar, S., Renewable energy in Algeria. Africa, renewable energy, 2017.

[19] N. YASSAA. Et al, Algeria Renewable Energy Resource Atlas 1st edition 2019, Centre de Développement des Energies Renouvelables, Mars 2019.

[20] S. Galal, Renewable energy in Algeria - statistics & facts | Statista, Dec 21, 2023. https://www.statista.com/topics/10656/renewable-energy-in-algeria/.

[21] Algeria Powers Ahead with Huge Renewable Energy Plans. https://www.ief.org/news/algeria-powers-ahead-with-huge-renewable-energy-plans.

[22] Technical potential for offshore wind in Algeria.https://documents.worldbank.org/curated/en/970971586844506483/pdf/Technical-Potential-for-Offshore-Wind-in-Algeria-Map.pdf.

[23] A. Richter, Algeria identifies strong geothermal potential and explores the contribution to its energy future, 27 Jan 2021.

[24] Akbi, A., et al., An overview of sustainable bioenergy potential in Algeria. Renewable and Sustainable Energy Reviews, 2017. 72: p. 240-245.

[25] Guereueb, M. and A. Ferhat, La Gestion Des Eaux En Algérie : Vers Un Nouveau Paradigme Water Management In Algeria : Towards A New Paradigm. 2021.

[26] MINISTÈRE DE L'ÉNERGIE ET DES MINES : Energies Nouvelles, Renouvelables ET Maitrise de l'Energie.

[27] Bouznit, M., M.d.P. Pablo-Romero, and A. Sánchez-Braza, Measures to promote renewable energy for electricity generation in Algeria. Sustainability, 2020. 12(4): p. 1468.

[28] Michael Hochberg, From Dependence to Diversification: Algeria's Renewable Energy Potential -2022/01/19.

[29] Abada, Z. and M. Bouharkat, Study of management strategy of energy resources in Algeria. Energy Reports, 2018. 4: p. 1-7.

[30] Farid L. Réserves de pétrole : l'Algérie dans le top 20 mondial en 2023.4 janvier 2023 à 21 :14.

[31] Leke, A., P. Gaius-Obaseki, and O. Onyekweli, The future of African oil and gas: Positioning for the energy transition. McKinsey Company. (Online) Available at: https://www. Mckinsey. Com/industries/oil-and-gas/our-insights [Accessed April 28, 2023], 2022.

[32] Ouki, M., Algerian Gas in Transition: Domestic transformation and changing gas export potential. 2019.

[33] Fakir, I., Given capacity constraints, Algeria is no quick fix for Europe's Russian gas concerns. Middle East Institute (MEI), 2022. 8.

[34] Boersma, T., Algeria Field Report, Developing Shale Gas in North Africa (Markaz field report). Brookings Institute https://www. Brookings. edu/blog/markaz/2015/03/24/algeria-field-report-developing-shale-gas-in-north-africa, 2015.

[35] https://www.world-nuclear.org/information-library/country profiles/others/uranium-in-africa.aspx.

[36] https://www.connaissancedesenergies.org/afp/lalgerie-aura-sa-premiere-centrale-nucleaire-en-2025-130519.

[37] Algeria Coal Reserves and Consumption Statistics - World meter. https://www.worldometers.info/coal/algeria-coal/.

[38] Serradj, W., Reality and prospects of fuel demand growth in Algeria-a forward-looking analytical study for the period 2012-2030. 8 .2023 ,مجلة التمويل والاستثمار والتنمية المستدامة(1): p. 024-043.

[39] International Renewable Energy Agency (IRENA). Renewable Energy in the Arab Region. Overview of Developments; IRENA: Abu Dhabi, United Arab Emirates, 2016.

[40] Hill, J. Global Renewable Energy Capacity Increased 167 Gigawatts in 2017, Reached 2179 Gigawatts. CleanTechnica. 2018.

[41] Schröder, M., The discursive construction of Turkey's role for European energy security: a critical geopolitical perspective. University of Cologne: Cologne, Germany, 2017.

[42] Himri, Y., et al., Overview of the Role of Energy Resources in Algeria's Energy Transition. Energies, 2022. 15(13): p. 4731.

[43] Lerouge, C., Recherche & Industrie Photovoltaïque (PV) aux Etats-Unis. SCIENCES PHYSIQUES ETATS-UNIS, Nanoscience, Microélectronique, Matériaux, 2006.

[44] Hamza, B., Etude, modélisation et optimisation d'un système d'énergie hybride PV/Pile à combustible, université msila.

[45] Ammari, C., et al., Sizing, optimization, control and energy management of hybrid renewable energy system—A review. Energy and Built Environment, 2022. 3(4): p. 399-411.

[46] Upadhyay, S. and M. Sharma, A review on configurations, control and sizing methodologies of hybrid energy systems. Renewable and Sustainable Energy Reviews, 2014. 38: p. 47-63.

[47] Khan, A.A., et al., Optimal Sizing, Control, and Management Strategies for Hybrid Renewable Energy Systems: A Comprehensive Review. Energies, 2022. **15**(17): p. 6249.

[48] Makhloufi, S. Comparative study between classical methods and genetic algorithms for sizing remote PV systems. Int J Energy Environ Eng 6, 221–231 (2015).

[49] Elmi, Y.K., M. Şenol, and M. Kuşaf, Optimizing separate and combined grids for cost-effective hybrid renewable energy electrification in Mogadishu, Somalia. AIP Advances, 2024. 14(1).

[50] Sengupta, S., S. Basak, and R.A. Peters, Particle Swarm Optimization: A survey of historical and recent developments with hybridization perspectives. Machine Learning and Knowledge Extraction, 2018. 1(1): p. 157-191.

[51] Gad, A.G. Particle Swarm Optimization Algorithm and Its Applications: A Systematic Review. Arch Computat Methods Eng **29**, 2531–2561 (2022).

[52] Alomoush, A.A., et al., Enhancing three variants of harmony search algorithm for continuous optimization problems. Int. J. Electr. Comput. Eng.(IJECE), 2021. **11**: p. 2343-2349.

[53] Dong, W., Y. Li, and J. Xiang, Optimal sizing of a stand-alone hybrid power system based on battery/hydrogen with an improved ant colony optimization. Energies, 2016. **9**(10): p. 785.

[54] Khalid, A., et al. Demand side management using hybrid bacterial foraging and genetic algorithm optimization techniques. in 2016 10th International Conference on Complex, Intelligent, and Software Intensive Systems (CISIS). 2016. IEEE.

[55] He, X., et al., An improved artificial bee colony algorithm and its application to multi-objective optimal power flow. Energies, 2015. **8**(4): p. 2412-2437.

[56] Yang, X.-S. and S. Deb, Engineering optimisation by cuckoo search. International Journal of Mathematical Modelling and Numerical Optimisation, 2010. **1**(4): p. 330-343.

[57] fr-fr. topographic-map.

[58] Nachida KASBADJI MERZOUK –Thése De Doctorat « Evaluation Du Gisement Energétique Eolien Contribution à La Détermination Profil Vertical De La Vitesse Du Vent En Algerie ».

[59] Chang T.P., Performance comparaison of six numerical methods in estimating Weibull parameters for wind speed energy application. Appl Energy 2011; 88: 272-82.

[60] Saidou Madougou-Thèse << Etude du potentiel éolien du jet nocturne dans la zone sahélienne à partir des observations de radars profileurs de vent >>

[61] Http : //www. lyc-richelieu-rueil.ac-versailles.fr/arch]

[62] Seyit A. Akdag Ali Dinler. A new method to estimate Weibull parameters for wind energy applications. Energy Conversion and Management 50, 2009, 1761-1766.

[63] Tenneekes A., « The logarithmic wind profile » J. of Atmospheric sciences, vol. 30, pp: 234:238, 1973.

[64] Justus C.G. et A. Mikhail, « Height Variation of Wind speed and Wind Distributions Statistics ». Geophysical Research Letters, vol. 3, N° 5, 1976//// Peterson E., « On the Use of Power Laws Estimates of Wind Power Potential » J. of Applied Meteorology, vol. 17, pp 390:394, 1978].

[65] Poje S. et B. Cividini, « Assessment of Wind Energy Potential in Croatia » Solar Energy vol.41 N°6 pp 543 554, 1988.

[66] Ramoji, S.K., B.B. Rath, and D.V. Kumar, Optimization of hybrid PV/wind energy system using genetic algorithm *(GA)*. J Eng Res Appl, 2014. **4**(1): p. 29-37.

Appendices

Appendix 1

1. characteristic of Kabertene central wind turbine

Brand	GAMESA
Type	G52- 850
Total nominal power delivered by the machine (Sum of stator and rotor power)	850kw
Nominal power of stator	812kw
Nominal power rotor	59kw
Nominal voltage	690kw
Maximum short circuit current	± 19.5 kA
Voltage limits in normal operation	10%(Permanent) +20%(0.1 s) -20%(1 s)
Complies with network regulation	P.O.12.3
Nominal Network Working Frequency	50/60 Hz
Frequency range allowed.	±2 Hz (cont) ±4 Hz (5s)
Cos Φ range scalable	0.95 cap./ind.
Generator synchronous speed.	1500 tr/min (F=50 Hz) 1800 tr/min (60 Hz)
Nominal generator speed	1620 tr/min (F=50 Hz) 1944 tr/min (F=60 Hz)
Nominal slip of generator	8%
Speed range with 1,050 triangle connection	1050 – 1900 tr/min
Allowable operating temperature range	- 30 °C/+ 50 °C
Storage and storage temperature range transport	- 40 °C/+ 60 °C
Maximum allowed humidity level during the exploitation	95% (without condensation)
Operating altitude. Standard	< 2 000 m
In section 6 of the G5XDAC.	IP23
In sections 1, 2, 3, 4, and 5 of the G5XDAC.	IP54

Degree of corrosion protection.	C3H
Nominal Network Voltage	690V
Network Side Converter Nominal Current	71 Arms
Network Side Converter Maximum Current	91 Arms
Network Side Converter Minimum Current	59 Arms
Short Circuit Maximum Current	19.5 Arms
Rotor side converter power	59kw
Rotor-rated converter voltage	183V
rotor side converter nominal current	268A
Maximum converter voltage on the Rotor side	608V
rotor side converter maximum current	354A
Maximum slip.	26.6%

2. Caractéristiques électriques des panneaux en silicium poly-cristallin of elhdjira

Brand	YINGLI SOLAR
Type of module	YL245P-29b
Application class	A
Measured power (W)	245
Measured voltage (V)	29.6
Measured current (A)	8.28
Max series fuse (A)	15
Open Circuit Voltage (V)	37.5
Short circuit current (A)	8.83
Max system voltage (V)	1000

Appendix 2

1. Global horizontal irradiation in the Ouargla region

Month	2011	2012	2013	2014	2015	2016	2017	2018	2019	2020
January	123.23	119.32	121.04	121.49	124.94	122.68	125.87	124.37	124.55	125.76
February	137.83	143.08	143.58	136.03	129.72	139.39	134.9	129.84	137.44	145.41
March	184.42	181.21	188.96	189.76	194.81	196.42	191.42	193.87	182.72	195.77
April	208.51	217.18	209.67	222.71	222.89	220.45	210.3	213.63	222.82	212.44
May	241.31	244.28	240.99	237.5	254.98	224.85	236.69	244.66	244.18	232.39
June	250.62	247.09	247.13	245.64	251.22	248.99	233.16	250.12	251.14	243.53
July	254.52	250.75	250.42	247.44	255.74	254.4	251.9	247.6	251.78	252.91
August	234.25	231.82	229.32	231.34	222.46	227.84	238.02	219.01	224.36	234.14
September	183.56	192.44	193.11	193.78	174.88	185.15	188.23	186.62	181.97	189.07
October	160.53	155.42	157.58	165.76	154.47	149.35	164.42	154.37	160.64	162.05
November	123.22	115.38	119.12	116.4	125.51	116.6	121.79	121.61	124.82	123.71
December	109.09	114.3	102.09	108.56	113.07	104.09	107.96	116.99	111.09	113.4

2. The monthly average temperature of Ouargla

Month	2011	2012	2013	2014	2015	2016	2017	2018	2019	2020
January	11.7	9	11.6	11.3	9.9	12.5	9.3	11.9	10.1	10.4
February	12.4	9.1	12.5	14.5	11.6	15	15.5	13.1	11.6	14.7
March	16.3	16.6	20.2	16.8	16.9	17.9	18.7	19.1	16.8	18.8
April	23.2	22.5	22.6	23.8	24.7	24.9	22.8	24	23.2	24
May	26.3	27.9	27.4	28.3	28.8	28.9	30.4	27.7	26.8	29.9
June	30.6	34.6	31.9	31.6	32.2	33.3	32.7	32.6	34.7	33.4
July	35.3	36.1	35.2	36.2	34	34.4	34.8	38.4	36.2	34.7
August	33.9	34.4	32.8	35.4	35.1	33.6	34.6	33.5	35.7	34.8
September	31.7	29.8	30.5	32.5	30.4	30.7	28.9	31.1	31.9	29.9
October	21.2	25.7	26.5	24.1	24.2	26.5	21.4	22.6	23.7	22.7
November	16	17.9	15.5	17.8	16.4	16.5	14.8	15.9	15.5	17.4
December	10.8	10.9	10.1	10.6	11	12	10.1	11	12.9	12.3

Abstract

The Algerian government aims to develop agricultural projects in remote desert lands away from urban areas and electricity networks. In this memo, we met the energy needs of farmer investors by studying how to optimizing the solar/wind hybrid energy system using genetic algorithm (GA) technology, considering economic and environmental factors as well as system reliability to reduce costs and increase efficiency. Matlab software was used to formulate and optimize this problem, and the results showed the effectiveness of the mentioned method when applied to a hybrid system example.

keys words: solar energy, wind energy, hybrid system, optimization, genetic algorithm.

الملخص

تهدف الدولة الجزائرية إلى تنمية المشاريع الزراعية في الأراضي الصحراوية البعيدة عن المناطق الحضارية والشبكات الكهربائية. حيث قمنا في هذه المذكرة بتلبية احتياجات المستثمرين الفلاحيين من الطاقة الكهربائية من خلال دراسة لتحسين نظام الطاقة الشمسية / الرياح الهجين باستخدام تقنية الخوارزمية الجينية(GA) ، مع مراعاة العوامل الاقتصادية والبيئية وموثوقية النظام لتقليل التكاليف وزيادة الكفاءة. تم استخدام برنامج Matlab لصياغة وتحسين هذه المشكلة، وأثبتت النتائج فعالية الطريقة المذكورة عند استخدام مثال على نظام هجين.

الكلمات المفتاحية: الطاقة الشمسية، طاقة الرياح، النظام الهجين، التحسين، الخوارزمية الوراثية.

Résumé

L'État algérien vise à développer des projets agricoles dans des terres désertiques éloignées des zones urbaines et des réseaux électriques. Dans cette note, nous avons répondu aux besoins énergétiques des investisseurs agricoles en étudiant comment améliorer le système énergétique hybride solaire/éolien en utilisant la technologie de l'algorithme génétique (GA), en tenant compte des facteurs économiques et environnementaux ainsi que de la fiabilité du système pour réduire les coûts et augmenter l'efficacité. Le logiciel Matlab a été utilisé pour formuler et optimiser ce problème, et les résultats ont montré l'efficacité de la méthode mentionnée lorsqu'elle est appliquée à un exemple de système hybride.

Mots clés : énergie solaire, énergie éolienne, système hybride, optimisation, algorithme génétique.